UCLouvain

IREC

Controlled growth factor delivery for therapeutic angiogenesis into the heart by cell-based gene expression or fibrin-based protein release

Ludovic Melly

Juillet 2020

Thèse présentée en vue de l'obtention du grade
de docteur en sciences médicales

Secteur des sciences de la santé

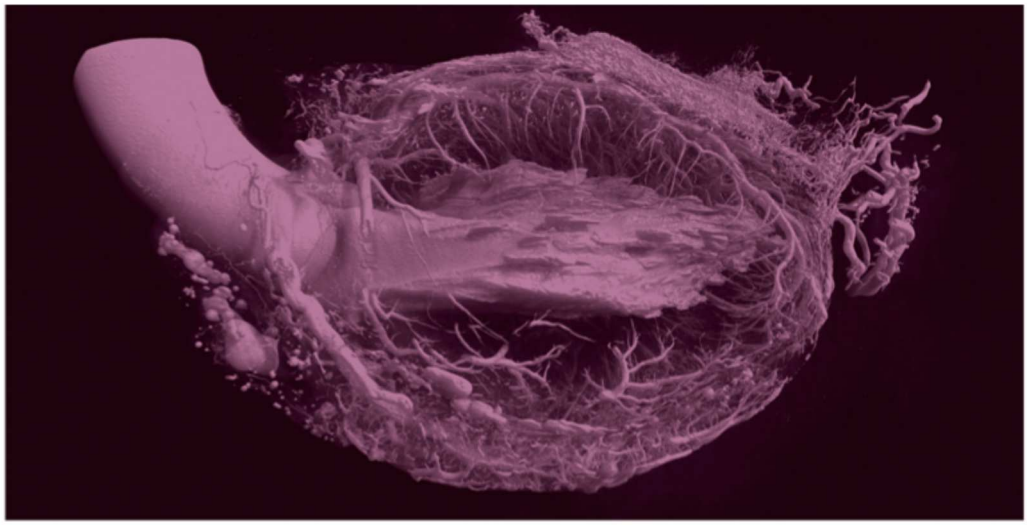

La plus grande découverte scientifique
a été la découverte de l'ignorance.

Du jour où les hommes ont compris
à quel point ils en savaient peu sur le monde,
ils ont eu soudain une excellente raison
de rechercher des connaissances nouvelles,
ce qui a ouvert la voie scientifique du progrès.

Harari YN, Homo Deus, p.233

COMPOSITION OF THE JURY

Pr Dr Alain Poncelet (President)
Cardiac Surgery Department, Cliniques Universitaires Saint-Luc, UCLouvain, Brussels, Belgium

Pr Dr Benoît Rondelet (Promotor)
Cardiac, Vascular and Thoracic Surgery Department, CHU UCL Namur, UCLouvain, Yvoir, Belgium

Pr Dr Isabelle Michaux (Secretary)
Intensive care Department, CHU UCL Namur, UCLouvain, Yvoir, Belgium

Pr Dr Marie-Cécile Nollevaux (UCL Jury Member)
Pathology Department, CHU UCL Namur, UCLouvain, Yvoir, Belgium

Pr Dr Maximillien Gourdin (UCL Jury Member)
Anesthesiology Department, CHU UCL Namur, UCLouvain, Yvoir, Belgium

Pr Dr Pierre Gianello (UCL Jury Member)
Pole of Experimental Surgery (CHEX), Institut de Recherche Expérimentale et Clinique (IREC), UCLouvain, Brussels, Belgium

Pr Dr Andrea Banfi (External Jury Member)
Cell and Gene Therapy, Department of Biomedicine, Basel University Hospital and University of Basel, Basel, Switzerland

Pr Dr Petra Korpisalo (External Jury Member)
Heart Center of Kuopio University Hospital, Kuopio, Finland

Pr Dr Nikolaos Bonaros (External Jury Member)
Cardiac Surgery, Innsbruck Medical University Hospital, Innsbruck, Austria

TABLE OF CONTENTS

INTRODUCTION

DISCUSSION

REFERENCES

LIST OF ABBREVIATIONS

AAV	adeno-associated virus
ACEI	angiotensin converting enzyme inhibitor
ALL	cells expressing heterogeneous (all) levels of VEGF levels
Ang II	angiotensin 2 protein
ANOVA	analysis of variance
Apro	aprotinin
ASC	adipose tissue-derived stem cell
AT-1	angiotensin receptor receptor 1
AV	adenovirus
BAPN	beta-amino-propionitrile
BMSC	bone marrow-derived stem cell
CABG	coronary artery bypass grafting surgery
CAD	coronary artery disease
CCN2	connective tissue growth factor 2
CCS	Canadian cardiovascular society score
CD8	cluster of differentiation 8 (cell surface marker)
CD31	cluster of differentiation 31
CHF	chronic heart failure
CMD	coronary microvascular disease
CPB	cardiopulmonary bypass
CTR	control (cell, hydrogel)
DAPI	4',6-diamidino-2-phenylindole
DES	drug-eluting stents
EF	ejection fraction
EGF	epidermal growth factor
EPC	endothelial progenitor cell
Eph B4	ephrin type-B receptor 4
FACS	fluorescence activated cell sorting
Fib	fibrin
HA	hyaluronic acid
HF	heart failure
HuNu	human nuclei
IBA1	ionized binding adaptor molecule 1
Ig	immunoglobulin
IRES	internal ribosomal entry sequence
Jag1	jagged 1 protein

LAD	left anterior descending coronary artery
MI	myocardial infarction
MMP	matrix metalloproteinase
MRA	mineralocorticoid antagonist
MSC	mesenchymal stem cell
NEM	neuropilin1-expressing monocyte
NG2	neural/glial antigen 2 proteoglycan
OCT	optimal cutting temperature (compound)
PBS	phosphate-buffered saline
PCI	percutaneous coronary intervention
PDGF	platelet-derived growth factor
PDGF-Rα	PDGF receptor alpha
PEG	polyethylene glycol
PlGF	placenta-derived growth factor
α-SMA	alpha-smooth muscle actin
Sema3A	semaphorin3A protein
SPEC	cells expressing a specific homogeneous VEGF level
Trka	tyrosine receptor kinase A
Tie2	tyrosine kinase with Ig and EGF homology domains, Ang1 receptor
TGF-β	transforming growth factor beta
TGFβ-R	transforming growth factor beta receptor
VE-Cad	vascular endothelial cadherin (also known as CD144)
VEGF	vascular endothelial growth factor
VEGF-R	vascular endothelial growth factor receptor
VLD	vessel length density
Vol	volume
VP	VEGF + PDGF
TG	transglutaminase

INTRODUCTION

I. CARDIAC PHYSIOPATHOLOGY AND THERAPIES

A. CARDIAC VASCULARIZATION

The heart is a hollow muscular organ that regulates the distribution of blood to the lung for its oxygenation (pulmonary circulation) and then throughout the whole body to deliver its oxygen (systemic circulation). This system is rhythmed by contractions and dilations called systole and diastole. The heart itself is composed of three layers: an outer envelope, the epicardium, the central thickest contractile layer namely the myocardium and the inner layer inside the heart cavities, the endocardium (Fig. 1).

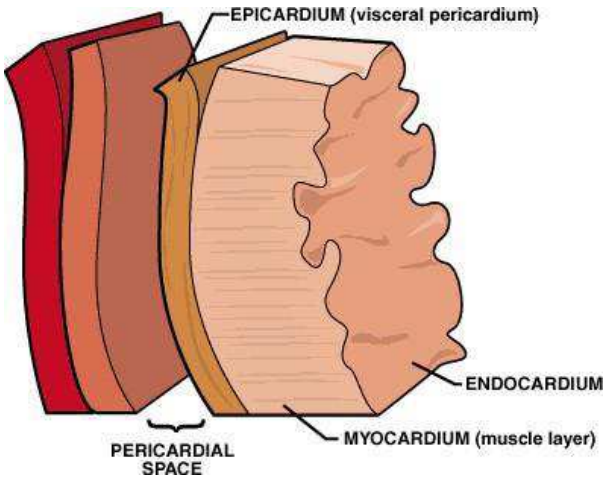

Figure 1. Layers of the heart. *From https://florida.theorangegrove.org/og*

Arteries are strong and stretchy vessels that generally carry oxygenated blood from the heart to the rest of the body, while veins have a thinner wall and carry deoxygenated blood back to the heart. In between, the capillaries connect the smallest arteries and veins and allow the exchange of carbon dioxide, oxygen, water, nutriments and waste.

Specifically, in the heart the arteries are called coronary arteries, which originate from the aortic root on usually two different ostia. The perfusion of the myocardium happens during the diastole. Indeed, in the systolic phase all the coronaries are collapsed because of the pressure exercised on the vessels by the muscle contraction. On the left side of the heart, the left main coronary artery divides then into the left anterior descending artery (LAD) coursing anteriorly towards the apex, and the circumflex artery coursing laterally. The right coronary runs along the right ventricle and eventually terminates into the posterior descending artery and posterior left ventricular artery in case of right dominance. After the capillaries, where the oxygen exchange takes place, the blood collects through three cardiac veins (great/middle/small) into the coronary sinus and returns to the right atrium.

B. ISCHEMIA

Ischemia is caused by inadequate balance between oxygen supply and demand. When happening in the heart, patients suffer from angina if the imbalance remains transient, or they undergo a myocardial infarction (MI) in case a complete occlusion occurs. Angina is described the classic central crushing chest pain radiating to the jaw and the left arm, but it can also be perceived as heaviness, indigestion, nausea and fatigue. It is intensified by, stress, emotion, cold air and exertion, which allows to classify into four categories according to the Canadian Cardiovascular Society (CCS) from no angina with ordinary activity (Class I) to angina already at rest (Class IV).

The vascularization can be divided in two main categories. When the larger vessels are impacted, we refer to the **macro-**circulation. This is the most common cause of ischemic heart disease that is still one of the most frequent causes of death worldwide [1]. The impact of cardiovascular diseases on the health care system is estimated to grow as the population ages. In order to restore that macro-vascularization, revascularization strategies are possible to increase the blood flow distal to a vascular stenosis or occlusion. This can be done by a cardiologist as a percutaneous coronary intervention (PCI) with the implantation of a stent at the place of the stenosis or by a cardiac surgeon as a coronary artery bypass grafting (CABG), which implies to sew new vessels called grafts distal to the lesion.

As another etiology or in addition, the angina can rely on the dysfunction of the **micro**-circulation. The subset of disorders affecting the coronary microcirculation itself is termed coronary microvascular disease (CMD). Consequently, symptomatic patients without identifiable obstructive plaque may still harbor significant nonobstructive coronary atherosclerosis and microvascular ischemia also called coronary syndrome X [2]. Here an adjuvant angiogenic therapy would aim at stimulating the growth of new capillaries in an ischemic tissue in order to increase the micro-vascularization (Fig. 2).

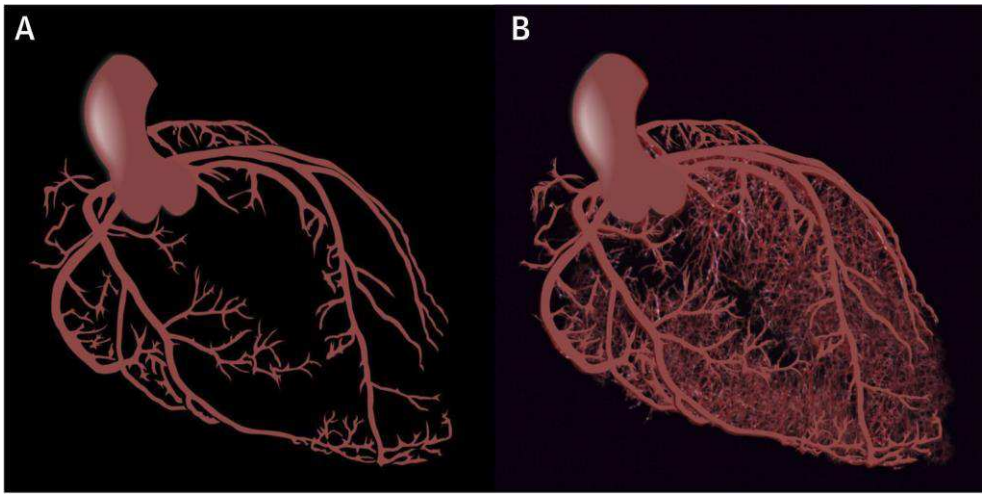

Figure 2. Schematic of (**A**) the epicardial coronary arteries (macrocirculation) and (**B**) the full coronary circulation (both macro- and microcirculation).

From Taqueti VR & Di Carli MF, J Am Coll Cardiol 2018

C. HISTORY OF REVASCULARIZATION STRATEGIES

Coronary revascularization strategies such as percutaneous coronary intervention and (PCI) or coronary artery bypass grafting (CABG) surgery currently provide the best treatment for patients with coronary artery disease. Revascularization procedures mainly aim to improve cardiac function and reduce the risk of myocardial infarction (MI).

CABG is still the most commonly performed cardiac surgery procedure worldwide, representing annual volumes of approximately 200,000 isolated cases [3] in the US and an average incidence rate of 62 per 100,000 inhabitants in western European countries [4]. The journey of CABG has been embraced by many of the pioneers in cardiovascular surgery with both their successes and failures. All those contributions can be conceptually categorized into three distinct eras starting at the beginning of the last century. First, the experimental work performed up to the early 1960's with reports of some laconic but also some impressive early clinical results and the development of the cardiopulmonary bypass (CPB) machine allowing operations within the cardiac cavities. Second, the modern coronary artery surgery has developed on the foundation of testing several grafts and an attempt to standardize them, which has brought along the beginning of evidence-based cardiac surgery. Third, like in other surgeries in the 21st century, the minimal invasive surgery evolves towards enhanced collaboration between conventional surgery and interventional medicine [5]. Indeed, the same surgeries are performed through smaller access (hemi-sternotomy instead of full sternotomy), with the help of video-assistance through mini-thoracotomy or even robotically assisted with the Da Vinci system® (Intuitive Inc.).

In parallel the cardiologists have moved from diagnostic angiograms towards more aggressive interventional catheter-based therapy. Already in 1977 in Zürich, Grüntzig first performed the first PCI as a transluminal balloon angioplasty to dilate a stenosis in the LAD [6]. It took less than 10 years before metallic stents could be successfully folded and inserted into the coronary arteries in order to prevent arterial recoil and restenosis with the first clinical data reported by Sigwart in Geneva [7]. The introduction of bare-metal stents brought into light two major limiting phenomena: in-stent restenosis (with intimal proliferation) and stent thrombosis. Logically, scaffolds capable of delivering drugs emerged quickly thereafter in order to counteract those problems. The first generation of drug-eluting stents (DES) made out of stainless steel and delivering sirolimus (rapamycin) or paclitaxel soon yielded to the second generation of stent materials (e.g., cobalt chromium) with decreased strut thickness reducing mechanical risk factors of incomplete stent apposition but delivering similar drugs (paclitaxel or

sirolimus-derived zotarolimus and everolimus). Nowadays research aims at eliminating the adverse long-term concerns related to the polymer-induced delayed vessel healing by developing bioresorbable stents [8].

CABG surgery and PCI have a storied history ripe with successes and failures of pioneers in the field. Its development has progressed from experimental stages, to the discovery of optimal conduit selection, which was driven by patient-focused evidence, to a current era, in which the method of performing the surgery or the intervention has become the focus. The next era may/should concentrate more on the optimal use of the surgical and interventional resources to provide the least invasive but best long-term treatment. Those borders between cardiac surgeons and interventional cardiologists may be fading in the future.

II. THERAPEUTIC ANGIOGENESIS

Some patients are not suitable candidates for angioplasty or surgery to restore the vascular flow distal to a stenosis because of age, comorbidities or unfavorable vascular anatomy, and are not adequately treated despite optimal pharmacologic therapy. Therefore, therapeutic angiogenesis could emerge as a stand-alone or also as a concomitant therapy.

A. DEFINITIONS

Therapeutic angiogenesis is a pro-angiogenic therapy that stimulates the growth of micro-vascular structures. Depending on where the process takes place a distinction should be made between angiogenesis and arteriogenesis. Angiogenesis is defined as the expansion of the tissue capillary network from existing vessels. These vessels, with a diameter of 8-12 μm and lacking the tunica media per definition, are responsible for metabolic exchanges and are mostly induced by ischemia. Arteriogenesis refers to the formation of large arterial vessels (20-100 μm), which have a fully developed tunica media. Those larger vessels channel the blood flow around the occlusion site (collateral arteries). It is an enlargement and subsequent maturation of pre-existing small-sized collateral vessels induced by shear stress and inflammatory factors (Fig. 3).

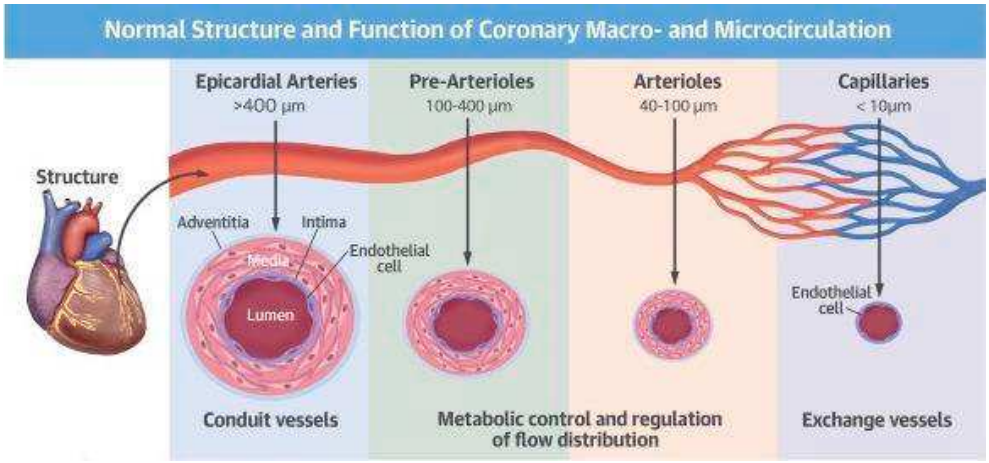

Figure 3. Normal structure and function of the coronary macro- and microcirculation.
From Taqueti VR & Di Carli MF, J Am Coll Cardiol 2018

The two phenomena are interdependent since angiogenesis reduces resistance in downstream capillary beds and induces collateral remodeling, in turn leading to arteriogenesis [9]. As revascularization procedures directly bypass or remove the obstruction in the large conductance arteries, the resulting expansion of the micro-vascular bed is in addition capable of inducing the enlargement of upstream collateral arteries through increased shear stress and gap junction-mediated retrograde signaling along vessel walls, thereby restoring perfusion downstream of the occlusion by way of a biological bypass (Fig. 4) [10, 11].

Several gene and cell therapy approaches showed potential benefit and cardiac function improvement in preclinical studies [12]. However, a suitable adjuvant treatment for chronic cardiac ischemia, capable of providing a long-term and, at the same time, safe and efficacious angiogenic stimulus, still needs to be identified.

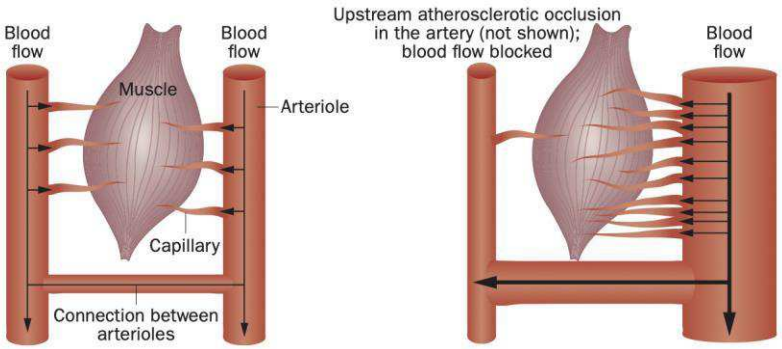

Figure 4. Angiogenesis with arteriogenesis. Left image: two arterioles with capillary beds and a connection from arteriole to arteriole. Right image: an atherosclerotic occlusion in an upstream artery stops blood flow down one of the two arterioles. Subsequent arteriogenesis results in an increase in the size of the connection between the arterioles. Angiogenesis in the muscle bed increases the number and size of the capillaries with enhanced pericyte coverage. Blood flow through these enlarged and additional vessels increases, and flow can also increase all the way back to the site of the occlusion in the artery. This process continues and increases the number of capillaries over time.
From Annex BH, Nat Rev Cardiol 2013

These approaches find application in two related fields within the treatment of cardiac ischemia: (i) direct myocardial revascularization, and (ii) vascularization of engineered cardiac patches. The first approach aims at restoring the blood supply to the chronically ischemic border zone of infarcted tissue, consisting of still viable but dysfunctional (hibernating) myocardium. The second approach aims at improving the function of damaged myocardium by implantation of a contractile cardiac patch: in this setting, rapid vascularization in vivo is crucial to ensure the survival and function of the seeded progenitors inside the thick tissue-engineered construct [13].

B. VEGF

Vascular Endothelial Growth Factor (VEGF) is the master regulator of angiogenesis: this family of factors controls both physiological and pathological growth of blood and lymphatic vessels. The mammalian VEGF family comprises five main ligands (VEGF-A, -B, -C, and -D and placenta-derived growth factor, PlGF) and three receptors (VEGF-R1, -R2, and -R3). While the principal role of VEGF-C and -D is to stimulate lymphatic angiogenesis through VEGF-R3, blood vessel growth is mostly coordinated by the signaling of VEGF-A and -B and PlGF through R1 and R2 (Fig. 5). Despite the multiplicity of players, the molecular target for therapeutic angiogenesis is essentially VEGF-A signaling, as VEGF- B and PlGF play more accessory or tissue-specific roles [14]. Each member of the VEGF ligands is produced in multiple isoforms by either alternative splicing (VEGF-A, -B, and PIGF) or proteolytic processing (VEGF-C and -D) [15]. In all cases, an invariant core cystine-knot domain, which specifically interacts with VEGF-R, is combined with a variable C-terminal domain [16]. VEGF-A display isoforms of 120, 164, and 188 residues in rodents (or 121, 165, and 189 in humans, respectively) due to the presence or absence of heparin-binding domains that interact with the extracellular matrix (ECM) proteoglycans, so that matrix affinity is very low in the shortest isoform and increases with molecular size [17]. Throughout the manuscript VEGF refers to VEGF-A and specifically of its most commonly used isoform, i.e., $VEGF_{164/165}$.

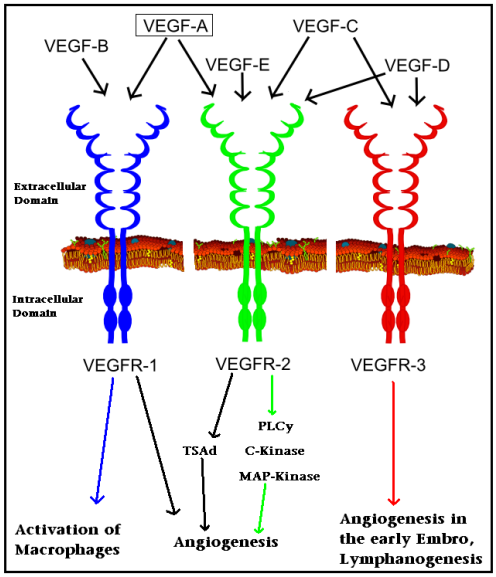

Figure 5. VEGF family and its ligants. *https://proteopedia.org/wiki/images/c/c8/VEGF_receptors.png*

VEGF is the most specific single factor capable of initiating the complex cascade of events leading to angiogenesis. Inactivation of VEGF during development results in embryonic lethality and myocardial defects [18, 19], whereas VEGF delivery has been shown to induce new vascular growth and improved cardiac function in preclinical models of myocardial infarction [20]. Extravasation of plasma occurs immediately after VEGF stimulation, as a consequence of increased vessel permeability by loosening of the endothelial junctions and by detachment from the vascular wall of mural cells, i.e. pericytes and smooth muscle cells. The extravasated plasma provides a provisional matrix that supports endothelial cell migration. VEGF stimulates quiescent endothelial cells to become activated, causing them to migrate and proliferate [21]. The orderly regulation of this morphogenic process is controlled by Notch signaling [22].

Contrary to the widespread effects of VEGF-A, VEGF-B has been shown to induce angiogenesis and arteriogenesis specifically in the myocardium, but not in other tissues [23], together with a function in the maintenance of physiological homeostasis in the heart and an anti-apoptotic effect on cardiomyocytes, leading to restoration of perfusion and functional improvement in large-animal models of myocardial infarction [24]. Furthermore, VEGF-B has been shown to have non-angiogenic functions in the direct regulation of cardiomyocyte metabolism and hypertrophy [25, 26]. These findings suggest a potential to develop heart-specific angiogenic and cardio-protective therapies, which have not yet been explored by the scientific community.

C. THE ANGIOGENIC MICROENVIRONMENT

VEGF binds to the extracellular matrix and forms gradients in the microenvironment around each producing cell [27]. The first cells that are activated by VEGF become specialized tip cells, which do not proliferate and are not involved in the formation of lumen structures, but rather sense the gradient of VEGF in the microenvironment and migrate towards it, thereby initiating the **sprouting** process. In response to VEGF, tip cells upregulate expression of Delta-like-4 (Dll4), which activates Notch-1 signaling on the neighboring endothelial cells and instructs them to acquire a stalk cell phenotype, instead. Contrary to tip cells, stalk cells respond to the total concentration of VEGF by proliferating rather than migrating and form new vessel behind the sprouting tip. Vascular maturation, which involves the return of endothelial cells to quiescence and independence from continued VEGF signaling, requires a complex crosstalk between the endothelium and pericytes (reviewed in [11]), which are recruited by Platelet-Derived Growth Factor-BB (PDGF-BB), produced by activated tip cells [8]. Also playing an active role in vascular maturation are recently identified populations of myeloid cells [12], which are recruited by signaling through the VEGF and Semaphorin receptor Neuropilin-1 and produce a host of pro-maturation paracrine factors, including PDGF-BB, Angiopoietin-1 and Transforming Growth Factor 1 (TGF-1) (Fig. 6) [13].

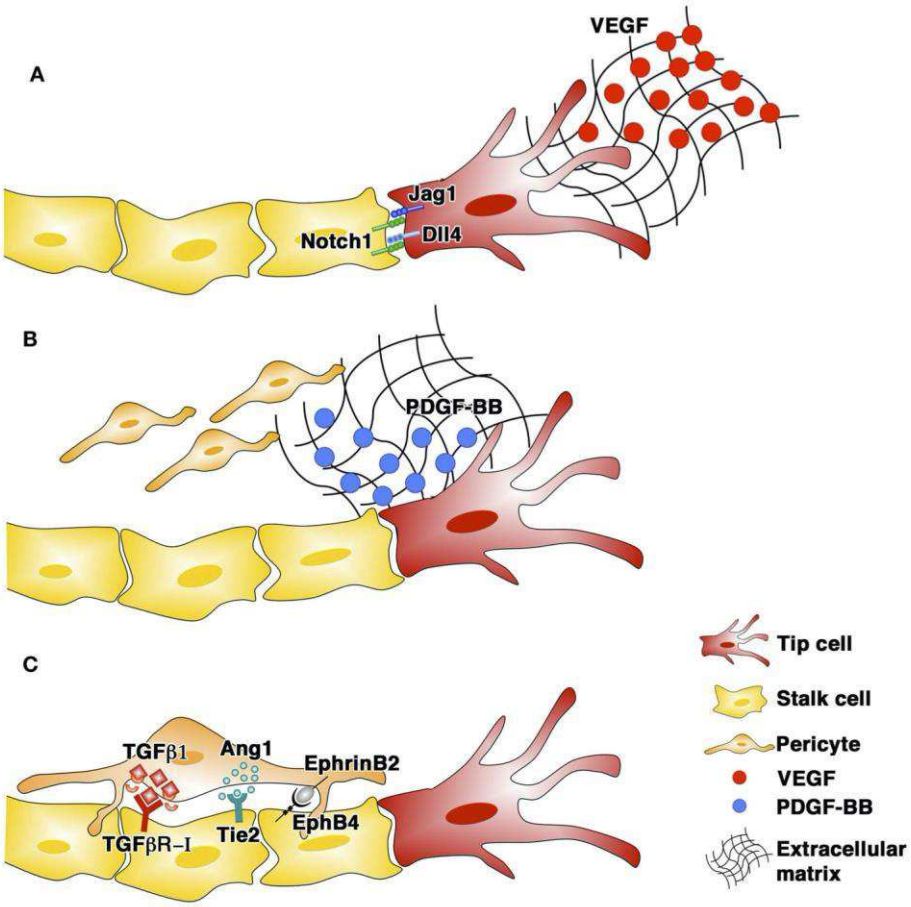

Figure 6. The phases of blood vessel growth and the main signaling pathways involved: (**A**) endothelial morphogenesis, (**B**) pericyte recruitment, and (**C**) stabilization.

From Martino MM et al., Front Bioeng Biotech 2015

An alternative mechanism of vascular network expansion is called **intussusception** (from the Latin meaning "growth within itself") and is referred to as splitting angiogenesis [28]. Initially described as a kind of anatomical curiosity during the development of some organs, such as the lung and the kidney, intussusceptive angiogenesis has been increasingly recognized over the last decade as a common mechanism of vascular growth, with important therapeutic implications [14]. Intussusceptive angiogenesis has been observed also in the heart [29]. Although the recent insights into its functional and molecular regulation have focused on skeletal muscle, several similarities in the structure of vascular networks in skeletal and cardiac muscle suggest a likelihood that similar mechanisms may

apply to myocardial angiogenesis. Intussusception can be initiated very rapidly by increased blood flow and shear stress in the absence of growth factors [30], but it can also follow VEGF upregulation [31]. How VEGF may induce only sprouting or intussusception remains unclear, but its distribution in the matrix matters and the absence of a concentration gradient appears to favor intussusception. On one hand, spontaneous upregulation of VEGF by ischemia leads to sprouting [32], but on the other its over-expression at significantly higher and therapeutic levels, which saturate the little matrix between fibers and abrogate local gradients, causes angiogenesis by intussusception [31]. In the intussusception mechanism [14], endothelial cells respond exclusively by proliferation without migration, without prior activation of tip cells. This leads to circumferential enlargement of the vessel (Fig. 7D-E), which then splits longitudinally into new daughter vessels. Splitting requires the formation of tissue pillars across the vascular lumen, which derive either from a vascular wall invagination that creates a contact between the opposite endothelial cells [33] (Fig. 7F), or by the extension and fusion of intraluminal filopodial-like protrusion from the endothelium [34] (Fig. 7G). Later the endothelial junctions reorganize and myofibroblast invade the core, stabilizing the structures into mature transluminal tissue pillars (Fig. 7H). Finally, they align longitudinally and divide the affected vascular segment (Fig. 7I).

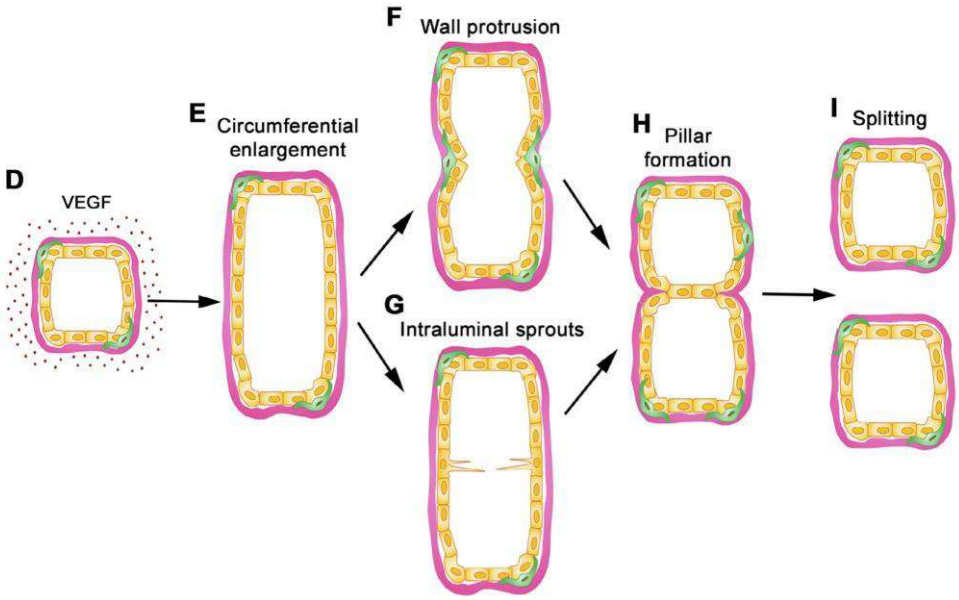

Figure 7. Schematic representation of the processes generating new vascular structures by intussusception (vascular splitting; **D–I**)
From Gianni-Barrera R, Di Maggio N, Melly L et al., Stem Cells Transl Med 2020

Over the last decade, studies with different delivery platforms have identified key requirements to be considered in order to exploit the therapeutic potential of VEGF gene expression, regarding dose, distribution and duration. In fact, uncontrolled over-expression of VEGF has been shown to induce the growth of angioma-like vascular tumors in a variety of tissues, such as skeletal muscle [14,16], subcutaneous fat [15], liver [17] and heart [18,20]. It has been difficult to establish a therapeutic window for VEGF gene delivery, with lower doses of gene therapy vectors being inefficacious and higher doses rapidly causing aberrant vascular growth [20,21], and controlled clinical trials have failed to demonstrate therapeutic efficacy at safe vector doses [22,23].

Taking advantage of a well-characterized cell-based platform for controlled gene delivery, in which clonal populations of transduced myoblasts are used to homogeneously express specific VEGF doses in vivo, Banfi et al. found that the therapeutic window of VEGF does not depend on the total dose administered, but rather on its level of expression in the microenvironment around each producing cell (Fig. 8) [14,24]. In fact, since VEGF remains tightly localized in tissue after being secreted, different growth factor concentrations do not average with each other, even between neighboring muscle fibers, and a few "hotspots" of high expression are sufficient to cause angioma growth even if the total VEGF dose is rather low. However, when a homogeneous distribution of expression levels was achieved by implanting clonal populations in which every cell produced the same amount, it became clear that a wide range of VEGF levels exists that induce only normal, stable and functional capillary networks, and that angiomas are induced only by doses above a discrete threshold level (Fig. 9) [14]. Furthermore, within the safe range there exists a therapeutic window, whereby too low doses efficiently induce normal angiogenesis, but provide no therapeutic benefit, whereas higher ones induce the growth of normal vessels of larger caliber, which are also effective in forming collateral arteries and restoring blood flow in ischemic tissue [24].

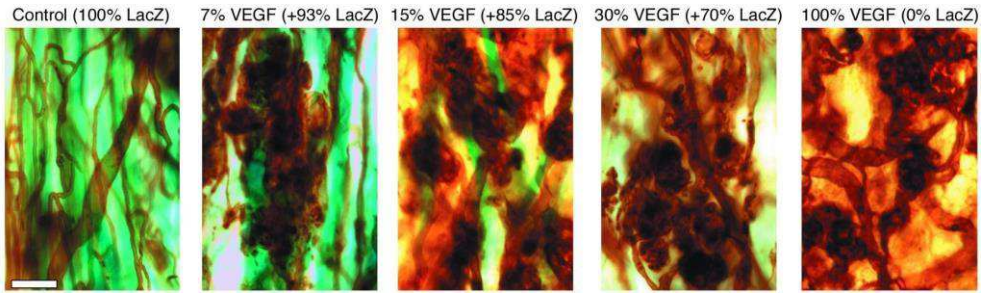

Figure 8. Total VEGF dose. A reduction in the total amount of VEGF does not eliminate abnormal vascular growth. Delivery of a smaller proportion of VEGF myoblasts (less total VEGF) failed to prevent aberrant vascular growth at 28 days.

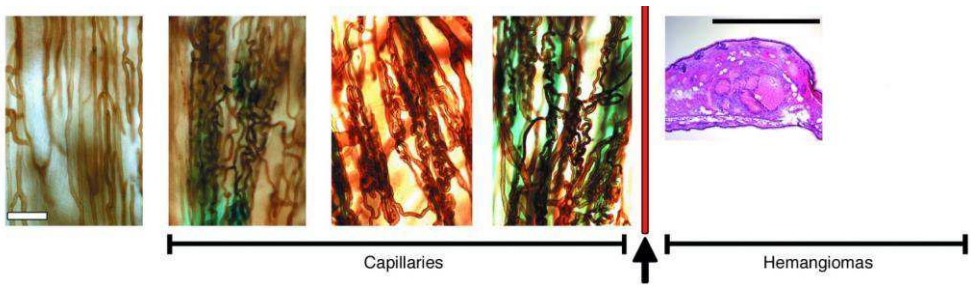

Figure 9. The microenvironmental level of VEGF produced in muscle determines a threshold between the growth of normal capillaries and hemangiomas. Morphologies of vessels at sites implanted with the same clones at 2.5–3.5 months after implantation. The vertical red line and the arrow at the bottom indicate the threshold between the induction of normal capillaries and hemangiomas.

Both figures from Ozawa C, Banfi A et al., J Clin Invest 2004.

A further key parameter to consider in therapeutic VEGF gene delivery is the duration of expression. In fact, although the morphogenic events leading to the formation of new vascular structures are complete within the first 7 days after VEGF gene delivery [25], the newly induced vessels are unstable and depend on continued VEGF stimulation until about 4 weeks and, if expression is lost before this time, they regress and disappear [14,17,26]. Interestingly, the stabilization of VEGF-induced vessels requires more than just pericyte recruitment, since new capillaries are already fully invested by normal pericytes 7 days after induction [25], but remain VEGF-dependent for a longer period of time.

D. PDGF

Platelet-derived growth factor (PDGF) was first isolated from platelet extracts in the early 1970s and classified as a mitogen for fibroblasts and cells of mesenchymal origin. Meanwhile dysfunction of PDGF signaling has been observed in a wide array of pathological conditions, such as cancer, fibrosis, neurological conditions and atherosclerosis [35].

The PDGF family consists of four ligands: A, B, C and D. They function as homodimers with the exception of the heterodimer AB. All PDGF ligands bind two structurally related tyrosine kinase cell surface receptors, α and β, which relay the message internally and initiate signal induction via Ras and phosphatidylinositol-II pathways, which are essential for PDGF-induced cell migration and mitogenesis (Fig. 10). PDGF-AA, AB, -BB and -CC activate the PDGF receptor-α (PDGFR-α) while PDGF-BB and -DD bind to PDGFR-β [35]. Generally PDGF causes neutrophils, macrophages, fibroblasts, and smooth muscle cells to proliferate and migrate into the wound site and it stimulates granulation tissue formation [36]. Specifically in the heart, PGDF stimulates fibroblasts to contract floating collagen matrices and differentiate into myofibroblasts in vitro [37].

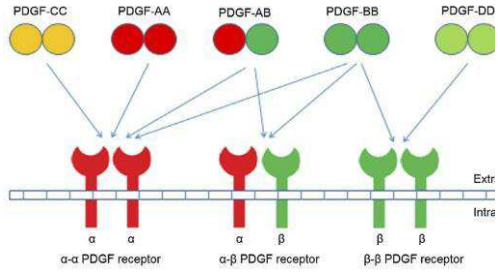

Figure 10. The PDGF family. *From Sadiq MA et al., Saudi J Ophthalmol 2015*

Blood vessel stability depends on the coordinated interaction of multiple signaling pathways in the endothelium and pericytes. As already discussed VEGF promotes endothelial cell growth, while platelet-derived growth factor-BB (PDGF-BB) stabilizes blood vessels by recruiting pericytes [38]. Those pericytes express PDGFR-β, allowing PDGF-BB to play an important role in the maintenance of the vasculature (Fig. 11).

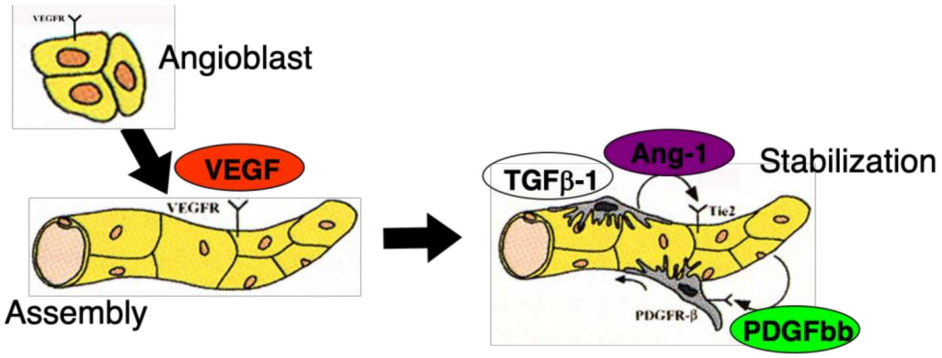

Figure 11. Vessel assembly and stabilization. *With the permission of Banfi A.*

Accordingly, therapeutic strategies that deliver a single angiogenic agent must inevitably depend on the availability of endogenous factors to achieve a balance. Without that balance, the new blood vessels are abnormal, unstable, and inefficient [39, 40].

As elegantly demonstrated by Banfi et al. the co-expression of VEGF and PDGF-BB encoded by separate vectors in different cells or in the same cells only partially corrected aberrant angiogenesis since the endogenous levels of both growth factors play a major role of counterbalancing the effects. Angioma-like structures could be found if VEGF is outweighed PDGF-BB, either by increasing the VEGF dose or by blocking the endogenous PDGF-BB. If PDGF-BB was increased to the same extent as VEGF, normal capillaries were observed. The figure below summarizes their findings (Fig. 12).

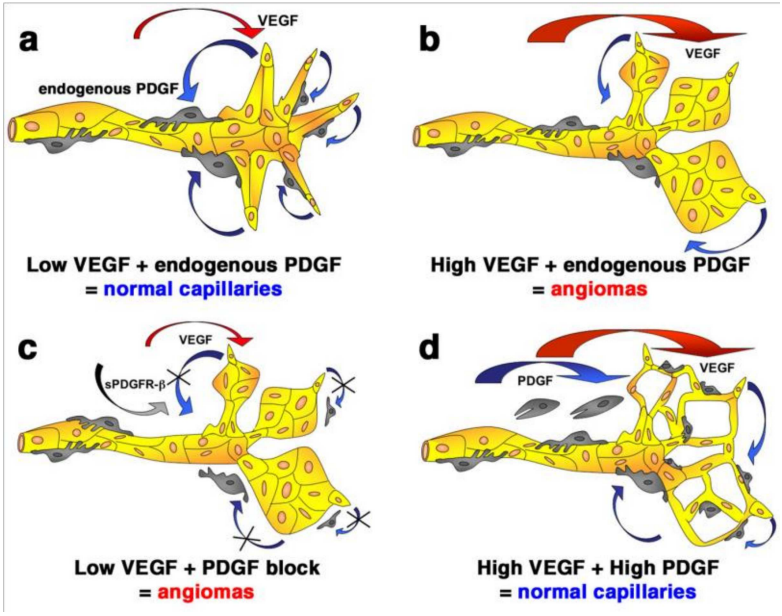

Figure 12. Relative amounts of VEGF and PDGF and their consequences in vivo. *With the permission of Banfi A.*

Taken together these results of complementary gain- and loss-of-function experiments indicate that the threshold between normal and aberrant angiogenesis is not an intrinsic property of VEGF dose alone, but depends on the balance between VEGF and PDGF-BB signaling (Fig. 13).

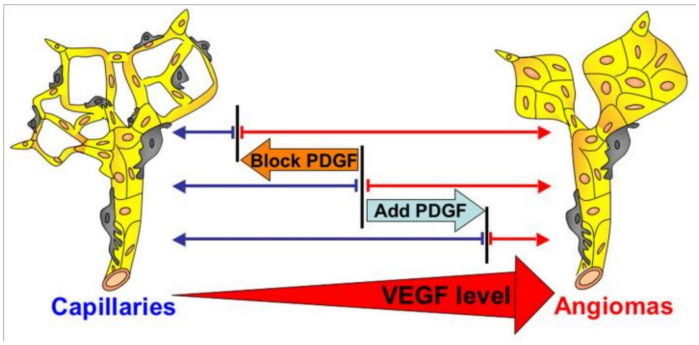

Figure 13. Relative threshold between VEGF and PDGF. *With the permission of Banfi A.*

As a consequence, coordinated co-expression of VEGF and PDGF-BB at fixed relative levels via a single bicistronic vector switched the induction of angioma growth to homogeneous normal capillary networks, despite heterogeneous and high VEGF expression levels [41]. Notably, in an ischemic hindlimb model, single-vector expression led to efficient growth of collateral arteries, revascularization, increased blood flow, and reduced tissue damage. Furthermore, these results were confirmed in a clinically applicable gene therapy approach by adenoviral-mediated delivery of the bicistronic vector [41] .

Furthermore, PDGF-BB co-expression accelerated stabilization of vessels induced by heterogeneous VEGF levels, so that 50% of new vessels were VEGF-independent already after 2 weeks, whereas none were stable when VEGF was expressed alone (Reginato and Banfi, unpublished data).

E. CARDIAC FIBROSIS

Within the injury site the necrosis of cardiomyocytes, induced by oxygen depletion during a myocardial infarction, implies a sequence of events that aims at preventing further damage and rupture of the ventricular wall by preserving the remaining cells and by replacing the dead cells. The healing process of **replacement** fibrosis can be divided into three partially overlapping phases (Fig. 14): the inflammatory phase, the proliferative phase, and the maturation phase [42].

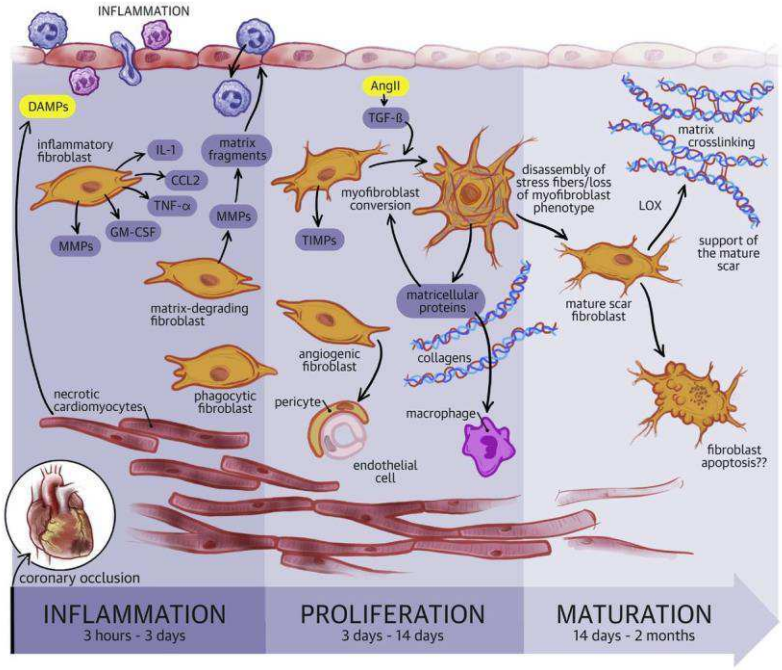

Figure 14. Phases of the replacement of fibrosis and functional diversity of fibroblasts in the infarcted myocardium.
From Humeres C & Fragogiannis G, JACC Basic Transl Sci 2019

The initial inflammatory phase is triggered by massive necrotic cell death in the infarct area [43]. Interstitial fibroblasts, endothelial cells and resident cardiac mast cells seem to be more resistant to ischemic injury than cardiomyocytes; they function as effector cells triggering the post-MI inflammatory reaction [44]. Cardiac fibroblasts produce matrix metalloproteinases (MMP) that degrade the

extracellular matrix (ECM) allowing cell migration into the injured area. The tissue injury activates innate immune signaling, and the secretion of chemokines induces leukocyte (neutrophils and macrophages) infiltration into the injured area [43]. This initial inflammatory phase aims at clearing the dead cells and ECM fragments from the infarcted area in order to allow its repopulation.

At the beginning of the proliferative phase, fibroblasts become the dominant cell type and adopt a proliferative, migratory, and secretory myofibroblast phenotype [44]. The secretion of ECM proteins by those activated myofibroblasts starts from the infarct border zone and progresses toward the core infarct area as the cells migrate along the newly synthesized ECM matrix [45]. Collagen deposition is crucial for increasing tensile strength and preventing ventricular wall rupture. Furthermore, angiogenic signaling stimulates the proliferation and infiltration of endothelial cells and leads to the establishment of a microvascular network to the infarct area [43, 46, 47], which is crucial to provide enough oxygen and nutrients during the repair process.

In the maturation phase, myofibroblasts are removed from the scarred area, possibly through apoptosis because the growth factors and matricellular proteins promoting their survival are depleted [44, 45]. Collagen turnover by the remaining myofibroblasts continues and cross-linking of the fibers leads to increased tensile strength and contraction of the scar, which alters the geometry of the chamber and contributes to remodeling in the remote areas of the ventricular wall [45]. In a normal wound healing response, all myofibroblasts are cleared from the scarred area, but in the heart, they have been found to persist in the infarct scar even decades after the insult [48].

Meanwhile, in the remote myocardium a **reactive** fibrosis takes place, which is called cardiac remodeling. Most often it is not the necrotic cardiomyocyte loss during MI that causes heart failure, but the subsequent remodeling of the non-infarcted left ventricular wall. In this pathological remodeling, the expansion of the ECM is accompanied by the hypertrophic growth of cardiomyocytes as the cells try to compensate for the increased workload by growing in size, in order to increase cardiac function and decrease ventricular wall tension [49]. The increased thickness and stiffness attributable to excessive cross-linked collagen and the tonic contraction of fibrous tissue compromise the diastolic function of the heart [50]. This remodeling process is progressive and eventually leads to the development of heart failure. The exact mechanisms and regulation of reactive fibrosis are unclear. One promoting factor is the increased mechanical stress as well as the activation of latent TGF-β in the non-infarcted ventricular wall. In addition, the persisting activated myofibroblasts in the infarct scar continue to secrete pro-fibrotic factors that might traverse to the remote areas of the

myocardium, inducing activation and proliferation of local fibroblasts and increased collagen deposition in the interstitial compartment (interstitial fibrosis) and in the adventitia of coronary vessels (perivascular fibrosis) [50]. Whereas interstitial fibrosis stiffens the myocardium and thereby leads to diastolic and systolic dysfunction, reactive fibrosis in the adventitia of the coronary arteries and arterioles (perivascular fibrosis) can cause narrowing of the vessel lumen and has been associated with impaired coronary blood flow [51]. This might decrease the oxygen supply to the myocardium, thereby further compromising the survival of cardiomyocytes and predisposing them to ischemic cell death.

PDGF is also involved in cardiac fibrosis. Together with other factors like Transforming Growth Factor β (TGF-β), Angiotensin II (Ang II), endothelin-1 (ET-1) and connective tissue growth factors (CTGF), they result in activation of myofibroblasts (Fig. 15) [52].

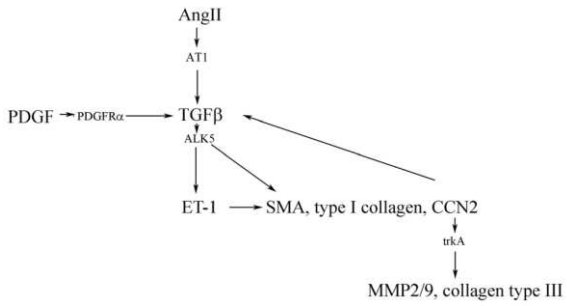

Figure 15. Signaling molecules driving cardiac fibrosis.
From Leask A, Circ Res 2015

Ang II is an oligopeptide that causes vasoconstriction and increased blood pressure. It upregulates TGF-β expression through the angiotensin receptor type 1 (AT-1) in cardiac myocytes and fibroblasts [53]. Ang II and TGF-β appear to act in an autocrine loop (Fig. 15), which ultimately promotes ECM increase by stimulating deposition of collagen type 1 and simultaneously suppressing its resorption through MMP repression [52]. Blockade of the whole cascade through a neutralizing anti-TGF-β antibody, administrated at the time of ligation of the LAD in a mouse model, led to increased mortality and worsened ventricular remodeling, in correlation with a decrease in collagen production and increased MMP [54]. On the other hand, drugs that inhibit the angiotensin pathway either

by inhibiting the angiotensin converting enzyme (ACEI) or as a direct inhibitors of AT-1, such as losartan, are widely used to treat hypertension and various cardiomyopathies and reduce cardiac fibrosis in a variety of animal models and in humans [55, 56]. Aldosterone is part of the renin-angiotensin-aldosterone system and therefore causes fibrogenesis [57]. Aldosterone itself is also capable of inducing fibrotic changes in the myocardium [58], as suggested by experimental animal studies and by the development of reactive myocardial fibrosis in patients with adrenal adenomas [59]. Spironolactone, a specific pharmacologic antagonist of aldosterone, attenuated the myocardial remodeling in Chagas cardiomyopathy, reduced mortality during the chronic phase and reduced inflammatory infiltration in a rodent model [60].

Accordingly, the guidelines of the European Society of Cardiology give a class I A recommendation to use mineralocorticoid antagonist (MRA) for patients with heart failure with reduced ejection fraction, who remain symptomatic despite treatment with (ACEI) and a beta-blocker, to reduce the risk of HF hospitalization and death [61].

III. CELL-BASED GENE THERAPY

Cardiac therapeutic angiogenesis strategies aim at restoring effective perfusion of ischemic myocardium in order to improve regional contractility and global cardiac function. There are three broad categories of pro-angiogenic strategies for myocardial ischemia: (i) cell therapy, (ii) gene therapy, and (iii) cell-based gene therapy. Several identified populations of cardiac progenitor cells hold promise to regenerate lost cardiomyocytes [62]. However, other classes of progenitors, which do not have significant potential for cardiac differentiation, such as endothelial progenitor cells and adult mesenchymal stem cells, have been found to effectively improve the function of infarcted myocardium mainly through pro-angiogenic and anti-apoptotic paracrine effects [63, 64]. My research focuses on cell therapy approaches for cardiac revascularization rather than regeneration. Gene therapy approaches consist instead in the direct delivery of therapeutic genes using viral or DNA-based vector, while cell-based gene therapy is a combination of these two approaches based on the delivery of progenitors previously transduced in vitro to express the therapeutic gene of interest.

A. CELL THERAPY

For cardiac revascularization, endothelial progenitor cells (EPC) derived from either peripheral or umbilical cord blood or from bone marrow have been often used in clinical trials. In particular, $CD34^+$ [65, 66] or $CD133^+$ [64, 67, 68] purified cells have been shown to improve angiogenesis and cardiac function both in animal models and in clinical trials [69]. However, the mechanism or mechanisms by which functional improvement is achieved are controversial. In fact, most evidence points out that so-called EPC are actually not incorporated into new vessels as either endothelial or mural cells, but rather may provide paracrine stimulation of both angiogenesis and tissue protection through the production of as yet not clearly defined combinations of factors [70]. Mesenchymal stem cells (MSC) of different origin, such as from the bone marrow or adipose tissue, have been investigated in several clinical trials as a treatment for the sequelae of myocardial infarction [20] . MSC can release a broad range of factors with pro-angiogenic, anti-apoptotic, anti-inflammatory, immunomodulatory and anti-scarring functions [71]. Through their paracrine effects, MSC have been demonstrated to increase blood vessel growth in numerous in vivo models [72, 73]. A specific advantage of lipoaspirate-derived expanded MSC and the native stromal vascular fraction cells of adipose tissue is their availability, as they can be easily procured in large quantities with very limited donor site morbidity. Cell therapy offers a very attractive approach for the treatment of cardiac ischemia from a safety and regulatory point of view, thanks to the use of autologous cells and the absence of genetic modification. However, a difficulty in using cell-based therapies lies in the identification and characterization of the specific sub-populations responsible for the therapeutic effect. Furthermore, employed cells produce a variety of growth factors, which are also likely to act synergistically, complicating the identification of the specific mechanisms that could be targeted in order to increase therapeutic efficacy. Lastly, a major unsolved issue in this approach is the poor cell retention and survival upon direct intra-myocardial delivery [62, 63, 74].

B. GENE THERAPY

Plasmid DNA, adenovirus (AV) or adeno-associated virus (AAV) are the most commonly used vectors for therapeutic angiogenesis. Plasmid DNA is very easy to produce. However, the gene transfer efficiency in vivo is very low and, as the plasmid DNA is gradually destroyed after uptake, leading to transient expression, lasting up to a couple of weeks. For these reasons, despite their good safety profile, the clinical relevance of plasmid vectors remain unclear [75]. Furthermore, plasmid DNA does not intrinsically allow targeted delivery to the tissue of interest, although methods to overcome this limitation by ultrasound-mediated delivery with microbubbles have been investigated [76].

The efficiency of gene transfer improves with viral vectors. Adenoviruses are easily produced at high titers, can accommodate large expression cassettes and can transduce multiple cell types, both proliferating and quiescent. Therefore, AV have been widely used in gene therapy applications (Fig. 16). On the other hand, AV produce a very high initial level of gene expression, with a peak few days post-injection, but expression drops rapidly, lasting only 10 to 14 days because of a strong vector-directed immune response, which also precludes repeated administration of AV of the same serotype [75].

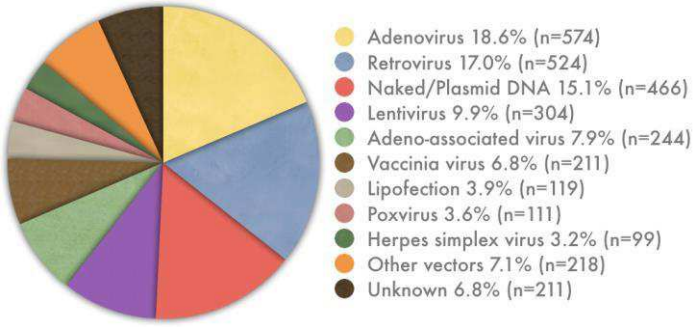

Figure 16. Vectors used in clinical trials for gene therapy.

From http://www.abedia.com/wiley/vectors.php

AAV are small vectors with a limited transgene capacity but possess many advantageous features. AAV exist in different serotypes with different tropisms for target tissues. In particular serotypes 1, 6, 8 and 9 are very effective in transducing adult skeletal muscle and myocardium [77]. Contrary to AV, AAV are

very poorly immunogenic, and are therefore suitable for long-term gene expression up to several months. Importantly, the kinetics of gene expression is very different from AV, i.e., a lower maximal expression level that is achieved gradually with a delayed onset over a couple of weeks after injection, due to the need to convert the single-stranded DNA viral genome to a double-stranded form before transcription can begin [78]. An issue that can diminish efficacy of AAV-based gene therapy is the presence of pre-existing neutralizing antibodies to the capsid proteins [78]. This may be tackled by selecting serotypes for which natural immunity in humans is absent or minimal.

Although several preclinical studies showed positive results, a suitable gene therapy approach providing a long-term, safe and efficacious angiogenic stimulus is still lacking [12]. Some of the key factors that determine the effectiveness of gene therapy for therapeutic angiogenesis have been identified as: (i) the efficacy of gene transfer and effective dose achieved in vivo, (ii) the duration of the angiogenic stimulus, and (iii) the biological potency of the delivered molecule [79]. The specific requirements regarding the dose and duration of VEGF expression as a single factor, which are challenging to satisfy with direct gene therapy approaches, have been analyzed above. In this respect, co-delivery of maturation factors, such as PDGF-BB, which controls pericyte recruitment, or Angiopoietin-1, or factors that are both angiogenic and maturative, like fibroblast growth factor 2, may help to overcome these limitations [79]. In particular, Korpisalo et al. showed that the co-injection into rabbit skeletal muscle of two different adenoviruses carrying VEGF-A and PDGF-BB resulted in a prolonged angiogenic response, despite short-term gene expression. However, this effect was mostly mediated via paracrine effect from recruited mononuclear cells rather than increased pericyte coverage [80].

C. CELL-BASED GENE THERAPY

The use of cells as factor delivery system has the potential to overcome some of the issues that limit the usefulness of VEGF gene therapy. This approach combines the sustained release of the therapeutic factors, characteristic of gene therapy, with the possibility to exploit the production of synergistic paracrine factors by the delivered progenitors, characteristic of cell therapy. Furthermore, it allows a unique opportunity to control the distribution of microenvironmental expression levels in vivo.

For this purpose, the Banfi group has developed a high-throughput, Fluorescence Activated Cell Sorting (FACS)-based technology to identify and rapidly purify cells expressing a specific desired VEGF level from a heterogeneous population of transduced progenitors. This was achieved by linking VEGF expression to that of a FACS-quantifiable syngenic cell surface marker (truncated CD8a), so that the amount of CD8 on the cell surface would reflect the level of secreted VEGF (Fig. 17).

With this technique, populations of VEGF-expressing primary myoblasts purified in this way yielded robust, normal and stable angiogenesis both in normal [81] and chronically ischemic [82] skeletal muscle, while angioma growth was completely avoided.

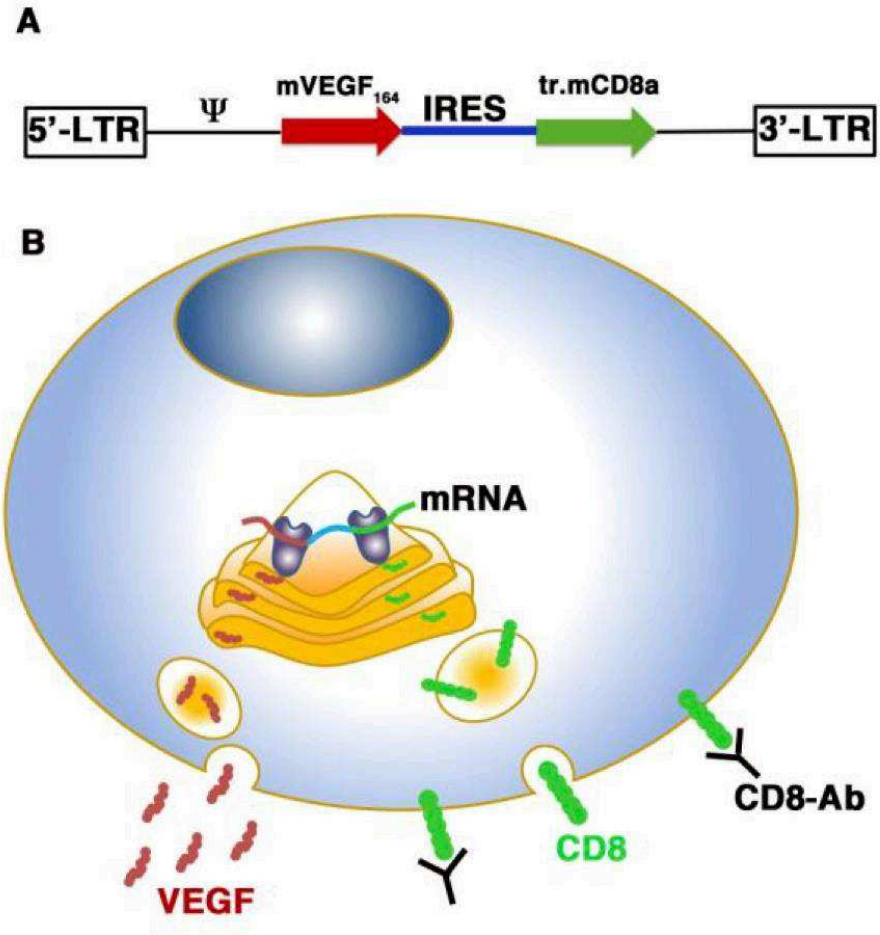

Figure 17. Schematic representation of the FACS-based cell purification technique. (**A**) Structure of the retroviral construct used to co-express VEGF and a truncated version of CD8, linked through an Internal Ribosomal Entry Sequence (IRES). (**B**) In transduced cells, regardless of the amount of expression from each integrated vector copy, the amount of VEGF protein secreted is always proportional to the amount of truncated CD8 on the cell surface, which can be detected by antibody staining (CD8-Ab) and quantified by FACS. *From Melly L et al., Cells 2012*

D. CELL SOURCE

Skeletal myoblasts are not an ideal cell source for cardiac delivery, because they can lead to potentially fatal ventricular arrhythmias. In fact, they have been shown to differentiate into contractile skeletal myofibers that remain electrically uncoupled from the surrounding cardiomyocytes [83].

Taking advantage of the above described FACS-technology, we could also generate purified populations of bone marrow- (BMSC) and adipose tissue-derived mesenchymal progenitors (ASC) expressing specific VEGF levels [84]. Since retroviral vectors efficiently transduce only dividing cells, we determined the earliest time after isolation and plating when ASCs and BMSCs enter the cell cycle and proliferation is at its peak, which was maintained until day 7 (Fig. 18).

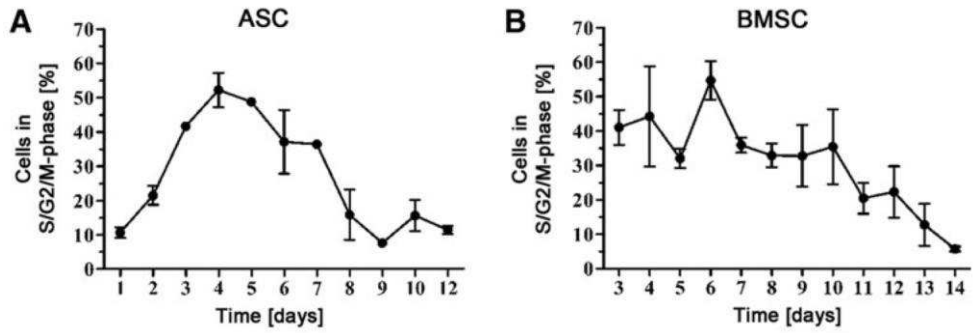

Figure 18. Optimization of MSC retroviral vector trans- duction. The proportion of ASCs (**A**) and BMSCs (**B**) in active proliferation (S/G2/M phases) was assessed by flow cytometry analysis of nuclear DNA content after staining with propidium iodide during the first 12 to 14 days after initial plating (n = 3 each).

From Helmrich U, Marsano A, Melly L et al., Tissue Eng Part C Methods 2012

Transduction and sorting did not affect the intrinsic proliferative potential of MSCs with no major difference between if derived from the bone marrow or the adipose tissue (Fig. 19). Here, we could demonstrate the feasibility of therapeutic approaches based on genetically modified MSCs, by ensuring both high efficiency and minimal in vitro manipulation [84].

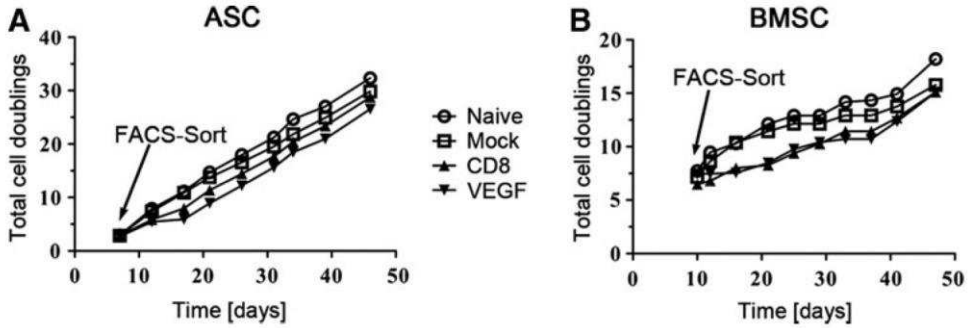

Figure 19. In vitro proliferation of transduced MSCs. The in vitro proliferative potential of CD8- and VEGF-expressing ASCs (**A**) and BMSCs (**B**) was not impaired compared with that of naive and mock- transduced cells over nine passages after FACS sorting.

From Helmrich U, Marsano M, Melly L et al., Tissue Eng Part C Methods 2012

Mesenchymal stem cells are an attractive source for cardiac cell delivery and particularly adipose tissue-derived stem cells (ASC) [69]. Indeed, ASC can be easily procured in large quantities from liposuction material [85], may have had the potential to differentiate into cardiomyocytes [86, 87], and have been reported not to increase the risk of arrhythmias [88].

E. PROOF OF PRINCIPLE IN THE HEART

Adipose-derived stem cells producing a specific and therapeutic level of VEGF (within a narrow therapeutic range) can induce angiogenesis and overall prevent the growth of aberrant angioma-like vascular structures caused by uncontrolled expression [89].

Control cells (CTR), which were transduced with the control virus expressing CD8 alone, were FACS purified to eliminate the few non-transduced cells and yield a purely CD8-positive population. Then, VEGF-expressing ASC were used to generate two distinct populations. Part of the cells were FACS purified through a specific narrow gate, to produce a homogeneous cell population expressing a specific moderate VEGF level (SPEC). The rest of the cells were sorted to purify all CD8-positive cells, in order to generate a population expressing all the heterogeneous VEGF levels present in the primary transduced population (ALL) (Fig. 20).

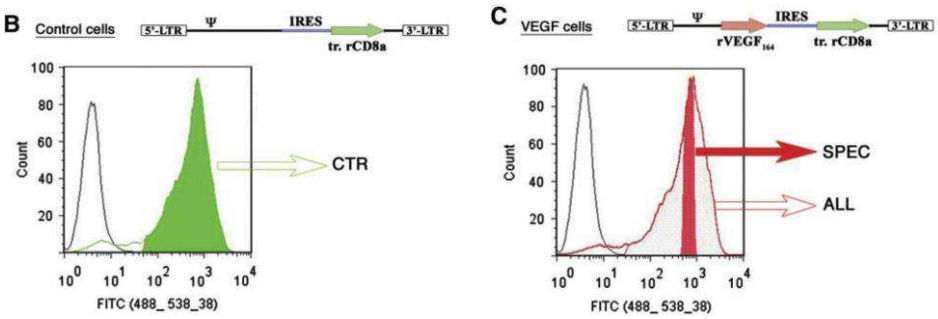

Figure 20. FACS purification of control ASC (**B**), expressing only the cell surface marker CD8 (CTR), or VEGF-expressing ASC (**C**) as populations producing either a specific homogenous level (SPEC) or all heterogeneous levels (ALL).
From Melly L et al., Hum Gene Ther Methods 2012

Both VEGF-expressing populations (SPEC and ALL) produced a similar amount of rat VEGF (about 130ng/10^6 cells/d), which was not detectable in the supernatants of control cells (Fig. 21B). Since ASC were of human origin, expression of endogenous human VEGF was similar, corresponding to only about 10% of the retrovirus-derived rat VEGF, showing that exogenous VEGF overexpression did not influence the basal levels of expression of the endogenous factor (Fig. 21C).

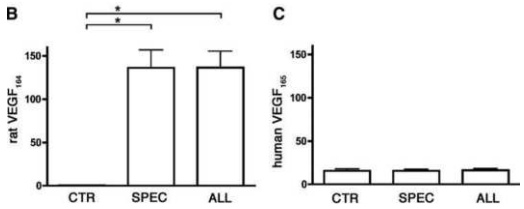

Figure 21. Enzyme-linked immunosor- bent assay (ELISA) quantifi- cation of rat (**B**) and human (**C**) VEGF in the culture su- pernatants of transduced cells (expressed in ng/10^6 cells/d); *p<0.01. *From Melly L et al., Hum Gene Ther Methods 2012*

No significant differences were found in the composition of the three populations in regards to mesenchymal markers (CD73, CD90, or CD105). Less than 4% of the cells were positive for CD31, which is expressed by endothelial as well as some hemopoietic cells. However, the other endothelial markers CD34 and VEGF-Receptor 2 (VEGFR2) were expressed by <1% of cells in all three groups, suggesting that the frequency of endothelial cells in the injected populations was negligible and not affected by VEGF overexpression (Fig. 22).

TABLE 1. PHENOTYPE OF TRANSDUCED ADIPOSE-TISSUE STEM CELL POPULATIONS

	CTR	SPEC	ALL
Mesenchymal			
CD 73	74.2±0.1%	79.9±1.1%	75.8±0.4%
CD 90	69.7±4.4%	78.7±3.0%	70.9±2.3%
CD 105	69.5±10.1%	77.5±6.5%	74.9±0.2%
Endothelial			
CD 31	3.6±4.3%	3.8±2.2%	2.8±0.2%
CD 34	0.7±0.7%	0.6±0.2%	0.9±0.2%
VEGFR2	0.2±0.2%	0.5±0.1%	0.1±0.1%
Cardiac			
Trop I	0.0±0.0%	0.4±0.6%	0.1±0.1%

Figure 22. Expression of the indicated mesenchymal, endothelial, and cardiac makers by the different populations of transduced and purified ASC at the time of in vivo injection, measured by flow cytometry. Data represent the percentage of cells positive for the indicated marker in each population and are expressed as the mean – standard deviation (n=2 independent donors); p was not significant for each marker expression between all groups. *From Melly L et al., Hum Gene Ther Methods 2012*

Both VEGF-expressing populations induced robust angiogenesis when injected in the myocardium compared to control cells (Fig. 23A). Vessel density was quantified by measuring the area fraction occupied by CD31+ endothelial cells, which is not affected by the size of lumens, and the results showed a significant two- to three- fold increase by both VEGF-expressing populations compared to controls (Fig. 23B). Since the vessels induced by the ALL population displayed an irregular morphology, with heterogeneous sizes, vascular growth was independently quantified by measuring vessel length density (VLD), which indicates the total length of vessels in a given tissue area, irrespective of their diameter or endothelial cell content. Both VEGF-expressing populations caused a net increase in VLD by about 60%. However, vessels induced by controlled VEGF expression (SPEC) displayed the morphology of normal and stable capillaries, were homogeneous in diameter, and associated with the slender processes of typical pericytes positive for the chondroitin sulfate proteoglycan NG2, similar in quality to vessels visible in the control group, while occasional regular-shaped arterioles were the only smooth muscle-covered vessels present (arrows in Fig. 23A). By contrast, heterogeneous VEGF expression by ALL cells caused the widespread growth of enlarged aberrant vessels (arrowheads in Fig. 23A), characterized by heterogeneous sizes, the presence of multiple lumens, and a lack of normal pericytes, substituted by a thick coat of smooth muscle cells, positive for both NG2 and smooth muscle actin (SMA; Fig. 23D), similar to the progressively growing angioma-like vascular structures.

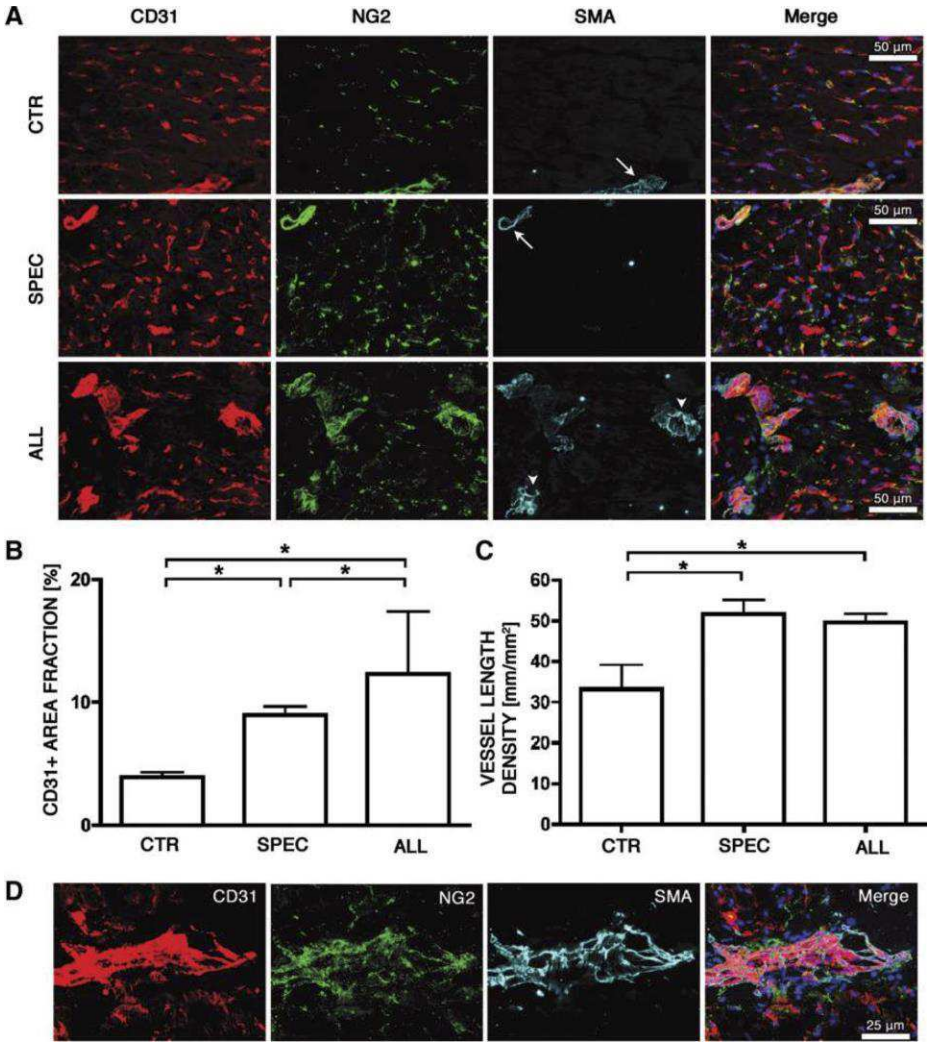

Figure 23. Myocardial angiogenesis. (**A**) Immunofluorescent staining for endothelium (CD31, in red), pericytes (NG2, in green), smooth muscle cells (SMA, in cyan), and nuclei (DAPI, in blue) in sections of myocardium injected with control cells (CTR) or ASC expressing a specific homogeneous VEGF level (SPEC) or uncontrolled heterogeneous levels (ALL). White arrows and arrowheads indicate normal, regular-shaped arterioles and aberrant angioma-like structures, respectively. Angiogenesis was quantified either as the area fraction occupied by CD31-positive pixels (**B**) or as vessel length density (**C**). Results are expressed as the mean–SEM; *p<0.01. (**D**) Immunofluorescent staining showing in greater detail an aberrant vascular structure in the ALL group, displaying irregular, multiple lumens and a thick smooth muscle coat.
From Melly L et al., Hum Gene Ther Methods 2012

In agreement with previous reports [90], we observed very limited human ASC engraftment 4 weeks after intramyocardial injection by two independent methods (Fig. 24). Results in other tissues have shown that approximately 4 weeks of sustained VEGF expression are required before new vessels become independent [38, 91]. Interestingly, newly induced vessels persisted in the injection areas despite the disappearance of most implanted cells, suggesting either of two possible explanations: (1) tissue- specific differences allow vessels in the myocardium to stabilize after VEGF expression shorter than 4 weeks, or (2) the production of other paracrine factors by ASC may accelerate the stabilization of VEGF-induced vessels. Conditional switching of VEGF overexpression specifically in the heart of transgenic mice showed that normal induced vessels were stable after 4 weeks, but not after 2 weeks, whereas aberrant vascular structures always depended on continued VEGF production for their survival [38]. On the other hand, among the many paracrine factors produced by ASC there are some involved in vascular stabilization, such as transforming growth factor ß and basic fibroblast growth factor [92].

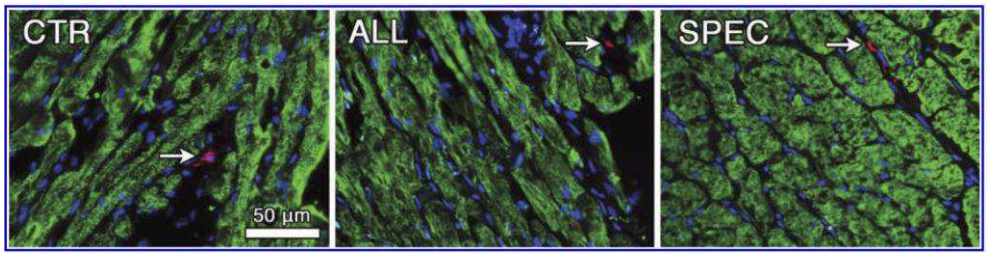

Figure 24. Cell engraftment. Survival of human ASC was assessed by immunostaining for HLA-Class I (red), while cardio- myocytes were detected by troponin I expression (green) and nuclei by DAPI staining (blue) 4 weeks after injection of control cells (CTR) or the two VEGF-expressing populations (ALL and SPEC). White arrows indicate single engrafted human cells. *From Melly L et al., Hum Gene Ther Methods 2012*

In summary we found that transduced and FACS-purified mesenchymal progenitors, homogeneously expressing a specific VEGF level, were effective in inducing robust normal angiogenesis in the myocardium, while preventing the growth of aberrant angioma-like vascular structures caused by uncontrolled expression [89].

IV. HYDROGEL-BASED THERAPY

For therapeutic efficacy and safety, it is desirable to independently control the dose and duration of angiogenic factor delivery in tissues. As we extensively discussed above this is technically challenging with gene transfer, while protein delivery has a short half-life in vivo. However, recently it has been possible to create modified versions of growth factors by protein engineering, so that they can be used to decorate natural matrices while being protected from rapid degradation [93].

A hydrogel is per definition a gel, in which the liquid component is water or hydrophilic. Several fundamental attempts of epicardial applications have aimed at treating hearts with solid hydrogels [94] or even as a spray (Fig. 25) [95] but have failed to be investigated further in clinical trials up to now.

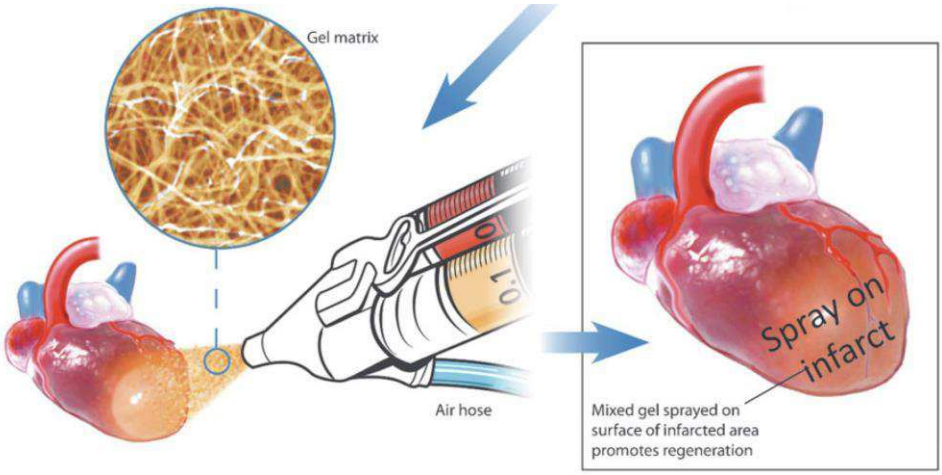

Figure 25. Schematic showing the spray painting of biomaterials on the heart after myocardial infarction. *From Tang J et al., 2017 Tissue Eng Part C Methods*

Here, the main idea resides in the fact that the gel can easily be injected within the target tissue, namely the myocardium. Indeed, the extracellular matrix is a three-dimensional network that provides structural and biochemical support to the surrounding cells. It is mainly composed of macromolecules such as enzymes, glycoprotein and very importantly collagen.

Therefore, most of the hydrogel-based therapies have a collagen core, like the Ultrafoam™ (BD Bard), which is a 3D type I collagen sponge. Compared to other scaffold compositions, collagen is characterized by a poor ability to retain VEGF in the extracellular matrix [96]. Previously, we found that those collagen sponges prevent the formation of localized hot spots of excessive concentration, thereby avoiding the development of aberrant angiogenesis despite uncontrolled expression by a genetically engineered population of ASC, which means that it is possible to induce therapeutic angiogenesis also by modulating the scaffold affinity for the protein [97].

Next to collagen matrices other numerous naturally derived biomaterials including alginate [98], collagen, chitosan, decellularized tissues, fibrin [99], hyaluronic acid (HA), keratin, and Matrigel, along with several synthetic biomaterials composed of polyethylene glycol (PEG) or poly*N*-isopropylacrylamide have been tested [100].

A. FIBRIN AS A DELIVERY SYSTEM

Fibrin is a natural product of blood coagulation and provides unique features, since it is :

(i) injectable as a liquid and solidifies in situ without cytotoxicity
(ii) remodeled by cell-associated enzymes (metalloproteinases, plasmin)
(iii) a natural cell-infiltration matrix [101].

Tissue regeneration after damage starts in all cases with the deposition of a fibrin-based matrix rich in growth factors [102]. So, one way of bringing growth factors is to incorporate them into a fibrin matrix exploiting the coagulation process (Fig. 26A). Over two decades ago, Zisch et al. fused murine $VEGF_{164}$ to an octapeptide, which is the substrate of the transglutaminase coagulation factor XIIIa, allowing its covalent cross-linking into fibrin hydrogels and release only by enzymatic cleavage [103]. However, the brief persistence of fibrin hydrogels in vivo [104] is insufficient to ensure stabilization of newly induced vessels and is a major obstacle to its exploitation for therapeutic angiogenesis [105]. To gain control over fibrin-remodeling rates and significantly prolong gel persistence in vivo, the group of Hubbell engineered an α_2-PI_{1-8}–fused variant of the fibrinolysis inhibitor aprotinin [106]. Finally, a collaboration between the Banfi and Hubbell groups could develop an optimized fibrin platform to ensure both controlled and sustained delivery of α_2-PI_{1-8}-VEGF-A_{164}.

In other words, the parameters controlling angiogenesis in a fibrin-bound delivery system depend on the degradation rate of the matrix in different ways:

- **Dose** = Factor concentration X degradation rate of the matrix
- **Duration of release** = Matrix volume / degradation rate of the matrix

This means that by controlling the degradation rate, it is possible to modulate both the dose and the duration of a growth factor in a tissue. This was achieved by incorporating and fine tuning the aprotinin concentration in the matrix [107].

On the other hand, engineering of any growth factor with a peptide endowing super-affinity for ECM enables in situ decoration of endogenous matrix with exogenously provided therapeutic proteins [108] (Fig. 26B). The increased efficacy of the modified factors avoided the need to deliver supra-physiological doses of VEGF, thereby increasing safety.

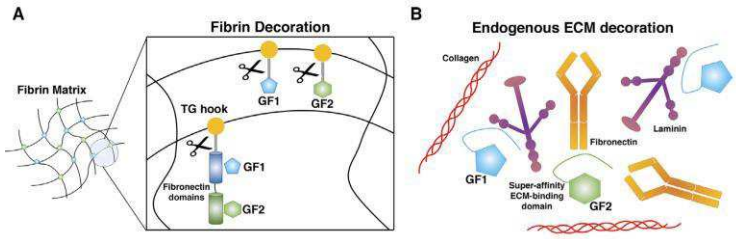

Figure 26. Strategies for matrix decoration with engineered recombinant factors. (A) Fibrin matrices can be decorated with engineered growth factors to mimic ECM functions. Taking advantage of the coagulation cascade, an octapeptide substrate of the transglutaminase Factor XIII (TG hook) can be fused to growth factors (GF), enabling their covalent cross-linking to fibrin. Specific domains of ECM proteins can also be incorporated through a TG hook to exploit their natural affinity for different GFs. (B) Endogenous ECM can be decorated with therapeutic GFs engineered to exhibit super-affinity to a broad range of ECM components.
From Gianni-Barrera R, Di Maggio N, Melly L et al., Stem Cells Transl Med 2020

B. PROOF OF PRINCIPLE IN SKELETAL MUSCLE

The **fibrinogen** content proportionally determines the maximum amount of VEGF that can be incorporated into the gel. In order to be able to inject the gel in vivo in still a liquid form, the gel must have a polymerization time longer than at least 10 seconds. Previous work in the Banfi lab determined the highest usable concentration of fibrinogen to be 25 mg/mL. At the same time the composition with the lowest stiffness (2.9 kPa: fibrinogen 25 mg/mL, FXIII 2 U/mL, thrombin 2 U/mL) was selected to investigate growth-factor delivery in vivo, to maximize compliance and minimize tissue invasiveness (Fig. 27) [107].

Aprotinin inhibits fibrin degradation by proteases, to prolong in vivo persistence of the gel and the duration of VEGF release, required for vascular stabilization. Since gel degradation rate affects both key parameters (rate and duration of the release) controlling angiogenesis in opposite directions, a reduction in degradation rate increases the duration of VEGF release but also reduce its effective delivered dose. The optimal aprotinin concentration was found to be of 56 μg/mL, which allowed a VEGF dose-dependent transition between normal and aberrant angiogenesis (Fig. 27) [107].

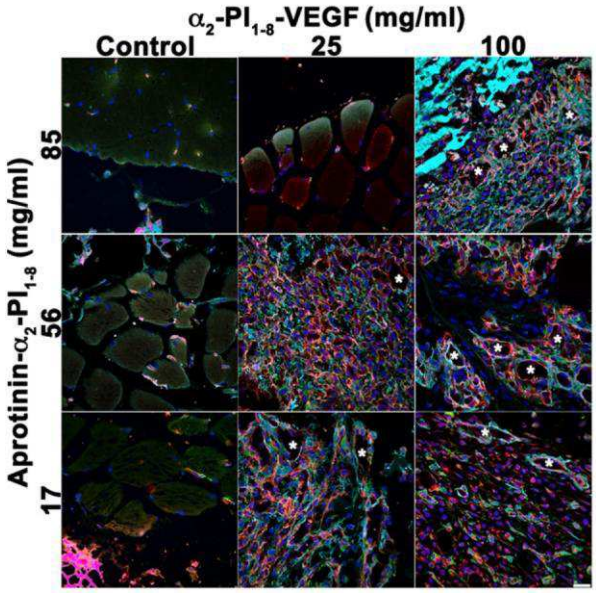

Figure 27. Aprotinin-α2-PI1–8 concentration determines the effective released dose of α2-PI1–8-VEGF164 and the angiogenic outcome. Fibrin gels were injected into the gastrocnemius muscles of SCID mice, and tissues were an- alyzed 9 d later. Two different α2-PI1–8-VEGF164 concentrations (25 μg/mL and 100 μg/mL) were tested in combination with three aprotinin-α2-PI1–8 concentrations (17 μg/mL, 56 μg/mL, and 81 μg/mL). Negative control conditions contained only aprotinin-α2-PI1–8. Frozen sections were immunostained for endothelial cells (CD31, in red), pericytes (NG2, in green), smooth-muscle cells (α-SMA, in cyan) and nuclei (DAPI, in blue). Asterisks, enlarged aberrant vascular structures. n = 3. (Scale bar: 20 μm).
From Sacchi V et al., Proc Natl Acad Sci 2014

In regard to the amount of VEGF delivered to skeletal muscle, it was demonstrated that the concentration of VEGF did not affect the amount of induced vasculature because the maximum had already been achieved with the lowest dose (0.1 mg/mL) and maintained over a 500-fold range (5 mg/mL) (Fig. 28A). But the size of the induced vessels was significantly increased up to the highest dose (5 mg/mL) (Fig. 28B). This is important, because previous studies showed that vascular size affects therapeutic efficacy significantly, as a similar increase in vessel density without increase in size provided no functional benefit [109].

Remarkably, those newly induced vessels did not regress for at least 3 months, whereas the implanted gels were almost completely consumed by 4 weeks, demonstrating that they achieved independence from exogenous VEGF signaling for their survival and suggesting that they could persist indefinitely (Fig. 28C). This finding was particularly relevant for the therapeutic potential of this approach because one of the main limitations of recombinant protein delivery for therapeutic angiogenesis has been the insufficient duration of factor release to achieve persistent effects [105].

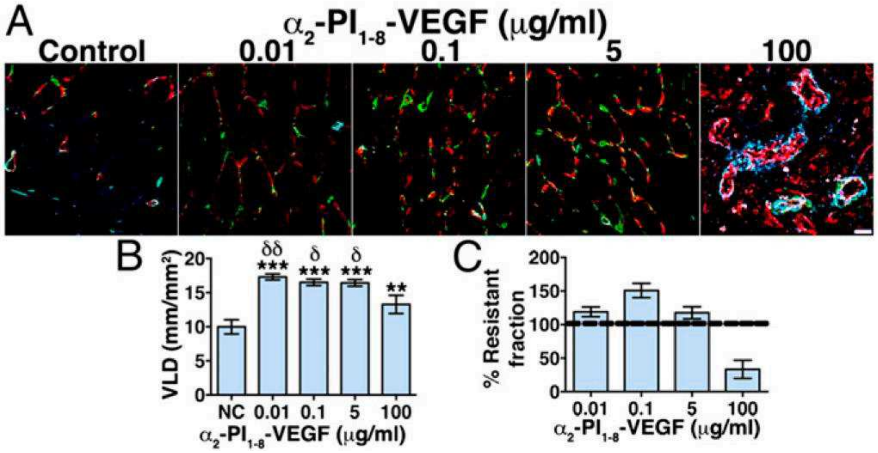

Figure 28. Long-term stability of induced normal, but not aberrant, angiogenesis by optimized delivery of fibrin-bound α2-PI1–8-VEGF164. Fibrin gels containing 56 μg/mL aprotinin-α2-PI1–8 and 0 μg/mL (negative control), 0.01 μg/mL, 0.1 μg/mL, 5 μg/mL, and 100 μg/mL α2-PI1–8-VEGF164 were injected into gastrocnemius muscles of SCID mice. Tissues were analyzed 3 mo later. (A) Frozen sections were immunostained to detect endothelial cells (CD31, in red), pericytes (NG2, in green), and smooth-muscle cells (α-SMA, in cyan). n = 3. (Scale bar: 20 μm.) (B) The amount of angiogenesis was quantified as vessel length density (mean VLD ± SEM; n = 5–10 fields per group); δδ δ ***P < 0.001 or **P < 0.01 vs. negative control, P < 0.01, P < 0.05 vs. the 100 μg/mL condition. (C) The stabilization rate of vessels induced in each condition was calculated as the percentage ratio between VLD 3 mo and 4 wk after gel injection (% Resistant fraction), with a value of 100% or higher indicating complete stabilization and a value lower than 100% indicating vascular regression between the two time points.
From Sacchi V et al., Proc Natl Acad Sci 2014

Results in skeletal muscle showed that 0.5 μg/mL was effective to induce functional improvement as it caused a two-fold increase in the amount of normal capillaries and significantly increased blood flow in ischemic tissue compared with controls (Fig. 29A) [107].

However, 5 μg/mL α_2-PI_{1-8}- $VEGF_{164}$, which induced only normal and stable angiogenesis in nonischemic muscle, actually stimulated the growth of aberrant vascular structures that failed to improve blood flow and collateral arteriogenesis in ischemic tissue (Fig. 29B) [107]. This was due to the accelerated degradation of the fibrin matrix in the highly inflammatory environment of ischemic muscle, causing a greater release of embedded VEGF per unit of time, i.e. a higher effective dose. This observation further validates the concept that the effective dose depends on the factor concentration x the matrix degradation rate, and not simply on the factor concentration. Therefore, the therapeutic concentration may vary depending on the specific application and the target tissue.

On the other hand, aberrant angiogenesis induced by 100 μg/mL VEGF failed to recruit physiological pericyte coverage by 4 weeks, when gel-bound factor was still present, consistently with the described function of VEGF as a negative regulator of pericyte function through formation of nonfunctional VEGFR-2/PDGFR-β complexes and consequent inhibition of PDGFR-β phosphorylation [110].

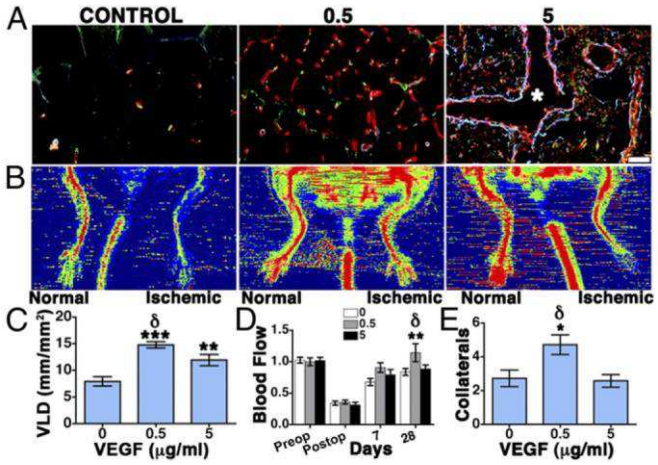

Figure 29. Functional improvement of hind-limb ischemia by α2-PI1–8-VEGF164. Fibrin gels containing 56 μg/mL aprotinin-α2-PI1–8 and 0 μg/mL (negative control), 0.5 μg/mL, and 5 μg/mL α2-PI1–8-VEGF164 were injected into the lower thigh muscles. Tissues were analyzed 4 wk later. (A) Frozen sections were immunostained to detect endothelial cells (CD31, in red), pericytes (NG2, in green), and smooth-muscle cells (α-SMA, in cyan). n = 3. (Scale bar: 20 μm.) (B) Representative laser Doppler images of nonischemic and ischemic limbs (left and right side of each image, respectively) 28 d after treatment with control gels (control) or 0.5 μg/mL and 5 μg/mL α2-PI1–8-VEGF164. (C) The amount of angiogenesis was quantified as vessel length density (mean VLD ± SEM; n = 5–10 fields per group); ***P < 0.001 and **P < 0.01 vs. negative control, P < 0.05 vs. the 0.5 μg/mL condition. (D) Blood flow was mea- sured by laser Doppler imaging before surgery (preop) to set the base- line, immediately after (postop) and 7 and 28 d later. Results were expressed as the ratio between measured flow in the ischemic and the contralateral nonoperated hind limb. (E) The number of collateral arteries was determined histologically in the adductor muscles after 4 wk (mean ± SEM per field; n = 5–10 fields per group); * P< 0.05 vs negative control, P < 0.05 vs. the 0.5 μg/mL condition.
From Sacchi V et al., Proc Natl Acad Sci 2014

AIMS OF THE THESIS

In conditions of inadequate balance between myocardial oxygen supply and demand, such as in angina or after myocardial infarction, revascularization strategies aim at restoring blood flow in the ischemic region. State-of-the-art procedures include percutaneous coronary intervention and coronary artery bypass grafting. Those patients as well as others who are not amenable to interventional procedures could benefit from additional therapeutic angiogenic strategies [111]. Therapeutic angiogenesis aims at promoting the expansion of microvascular networks, which are capable of recruiting increased flow also in upstream collateral arteries through retrograde signals [11], thereby providing effective bypass of the obstructed feeding vessels.

Vascular Endothelial Growth Factor (VEGF) is the master regulator of angiogenesis [112], but it also can induce aberrant and dysfunctional vascular growth if its expression is not tightly controlled [14]. A large body of investigations has identified specific features of VEGF biology that need to be considered to exploit its therapeutic potential while ensuring safety: these principally relate to dosing and duration of delivery. Results in the heart and other tissues have shown that approximately 4 weeks of sustained VEGF expression are required before new vessels become independent from the exogenous VEGF trigger, so that transient delivery is ineffective, although desirable for safety reasons [91]. On the other hand, since VEGF binds tightly to the extracellular matrix, the induction of normal or aberrant angiogenesis depends strictly on its amount localized in the microenvironment [91] and not on the total dose. This finding helps to explain the apparently narrow therapeutic window for VEGF gene delivery and its lack of efficacy at safe doses in clinical trials of therapeutic angiogenesis [113], in which only the total dose of vector could be controlled, but not its expression in individual cells, leading to a heterogeneous distribution of microenvironmental levels within the tissue [114]. A high throughput Fluorescence Activated Cell Sorting (FACS)-based technology was developed by linking VEGF expression to that of a FACS-quantifiable syngenic cell surface marker (truncated CD8a), so that the amount of CD8 on the cell surface would reflect the level of secreted VEGF, thereby enabling rapid purification of cells expressing a specific desired VEGF level from a heterogeneous population of transduced progenitors [81]. Populations of VEGF-expressing primary myoblasts purified in this way yielded robust, normal and stable angiogenesis both in normal [81] and chronically ischemic [82] skeletal muscle, while angioma growth was completely avoided. Since skeletal myoblasts are not a suitable candidate for cardiac cell delivery [115], adipose-derived stem cells (ASC) have attracted considerable attention. Indeed, beside the yield of large quantities of ASC from liposuction material [116] and their potential to differentiate into cardiomyocytes [117], they have a demonstrated ability to reduce the infarct area [118], to significantly improve the

left ventricular ejection fraction [119], and the cardiac mechanical and electrophysiological functions post-myocardial infarction [120]. Previously, we could demonstrate in a rodent model that, upon injection of genetically engineered and FACS-purified ASC, only cells homogeneously expressing a specific desired level of VEGF could induce normal and stable angiogenesis compared to control cells, despite very sparse cell engraftment in the normal myocardium [89].

In the first aim of this thesis we investigated the potential of a human ASC-based platform for controlled VEGF expression to induce safe angiogenesis and to improve cardiac function in a rat model of myocardial infarction.

Recombinant VEGF protein delivery has several desirable features for a clinical application: 1) it could avoid safety concerns associated with the genetic modification of progenitors, and 2) it could also ensure a homogeneous in vivo distribution of the delivered dose. However, sustained duration of protein delivery is necessary to ensure the stabilization and the persistence of induced angiogenesis [121], but it is challenging to obtain, due to the rapid degradation of VEGF protein in vivo. An optimized platform for the controlled delivery of recombinant VEGF after cross-linking into a fibrin hydrogel allows its release by cell-demanded enzymatic cleavage like metalloproteinases and plasmin, while protecting the factor from degradation until the time of release. Fibrin, a natural product of blood coagulation, provides unique features for physiological presentation of angiogenic signals: 1) it is injectable as a liquid and solidifies in situ without cytotoxicity, and 2) it is at the same time a natural cell-infiltration matrix [107]. After optimization of this fibrin-based delivery method, induction of normal, stable, and functional angiogenesis was demonstrated in rodent models of hind-limb ischemia and wound healing [107]. Further, it has also been shown that if the pericyte-recruiting factor Platelet-Derived Growth Factor-BB (PDGF) is co-expressed with VEGF in every cell at a fixed relative level via a single bicistronic vector, aberrant vascular structures are prevented and a greater arteriogenic effect is induced with higher VEGF doses [41]. Therefore, the combination of VEGF and PDGF proteins in the optimized fibrin-based delivery platform, which provides a convenient, clinically approved and off-the-shelf product, appears to be a very promising strategy to increase both safety and efficacy of VEGF delivery for a rapid clinical translation. In the second aim of this thesis we tested the feasibility and the potential of VEGF- and PDGF-BB-decorated fibrin matrices to induce therapeutic angiogenesis, as well as the possible untoward effects on safety in the myocardium.

Taken together, both aims evaluate therapeutic angiogenesis in the heart by the controlled delivery of growth factors within the myocardium to stimulate the micro-vascularization.

EXPERIMENTAL RESULTS

J. Cell. Mol. Med. Vol 22, No 5, 2018 pp. 2580-2591

Myocardial infarction stabilization by cell-based expression of controlled Vascular Endothelial Growth Factor levels

Ludovic Melly [a, b, c, *, #], Giulia Cerino [b, #], Aurélien Frobert [d], Stéphane Cook [d], Marie-Noëlle Giraud [d], Thierry Carrel [e], Hendrik T. Tevaearai Stahel [e], Friedrich Eckstein [b], Benoît Rondelet [c], Anna Marsano [b, #], Andrea Banfi [a, *, #]

[a] *Cell and Gene Therapy, Departments of Biomedicine and Surgery, University and University Hospital Basel, Basel, Switzerland*
[b] *Cardiac Surgery and Engineering, Departments of Biomedicine and Surgery, University and University Hospital Basel, Basel, Switzerland*
[c] *Department of Cardiac Vascular and Thoracic Surgery, CHU UCL Namur, Yvoir, Belgium*
[d] *Department of Cardiology, University of Fribourg, Fribourg, Switzerland*
[e] *Department of Cardiovascular Surgery, Inselspital, Bern University Hospital and University of Bern, Bern, Switzerland*

Received: August 23, 2017; Accepted: November 23, 2017

ABSTRACT

VEGF can induce normal or aberrant angiogenesis depending on the amount secreted in the microenvironment around each cell. Towards a possible clinical translation, we developed a FACS-based technique to rapidly purify transduced progenitors that homogeneously express a desired specific VEGF level from heterogeneous primary populations. Here we sought to induce safe and functional angiogenesis in ischemic myocardium by cell-based expression of controlled VEGF levels. Human adipose stromal cells (ASC) were transduced with retroviral vectors and FACS-purified to generate two populations producing similar total VEGF doses, but with different distributions: one with cells homogeneously producing a specific VEGF level (SPEC), and one with cells heterogeneously producing widespread VEGF levels (ALL), but with an average similar to that of the SPEC population. 70 nude rats underwent myocardial infarction by coronary artery ligation and 2 weeks later VEGF-expressing or control cells, or saline were injected at the infarction border. Four weeks later, ventricular ejection fraction was significantly worsened with all treatments except for SPEC-cells. Further, only SPEC-cells significantly increased the density of homogeneously normal and mature microvascular networks. This was accompanied by a positive remodeling effect, with significantly reduced fibrosis in the infarcted area. We conclude that controlled homogeneous VEGF delivery by FACS-purified transduced ASC is a promising strategy to achieve safe and functional angiogenesis in myocardial ischemia.

KEYWORDS

Myocardial infarction, adipose stem cells, VEGF, angiogenesis, cell therapy

INTRODUCTION

Ischemic heart pathologies are caused by inadequate balance between myocardial oxygen supply and demand such as in angina or after myocardial infarction. Percutaneous coronary intervention (PCI) and coronary artery bypass grafting (CABG) typically restore the macrovascularization in the ischemic area of the either acutely or chronically affected myocardium. But many patients could also benefit from additional therapeutic angiogenic strategies that would improve the microvascularization [111].

Vascular Endothelial Growth Factor (VEGF) is the master regulator of angiogenesis [122], but it can also induce aberrant and dysfunctional vascular growth if its expression is not tightly controlled [39, 123]. We previously found that, since VEGF binds tightly to extracellular matrix, the induction of normal or aberrant angiogenesis depends strictly on its amount localized in the microenvironment around each producing cell and not simply on the total dose delivered [91, 109]. This finding helps explaining the apparently narrow therapeutic window for VEGF gene therapy and its lack of efficacy at safe vector doses in first-generation clinical trials for therapeutic angiogenesis [113]. In these trials, only the total dose of vector could be controlled, but not the level of expression achieved in individual cells, leading to a heterogeneous and unpredictable distribution of VEGF within the tissue [114].

In order to overcome this limitation and the ensuing loss of therapeutic potential, we previously developed a high-throughput, Fluorescence Activated Cell Sorting (FACS)-based technology to identify and rapidly purify cells expressing a specific desired VEGF level from a heterogeneous population of transduced progenitors. This was achieved by using a retroviral construct expressing the VEGF sequence quantitatively linked through an internal ribosome entry site (IRES) to a FACS-quantifiable syngenic cell surface marker (truncated CD8a), so that the amount of CD8 on the cell surface would reflect the level of secreted VEGF [81]. Populations of so-purified VEGF-expressing primary myoblasts could ensure robust, normal and stable angiogenesis both in normal [81] and chronically ischemic [82] skeletal muscle, while angioma growth was completely avoided. However, skeletal myoblasts are not suitable for cardiac cell therapy, due to their inability to electrically couple and integrate with the surrounding cardiomyocytes, leading to fatal arrhythmias [115]. On the other hand, adipose tissue-derived stromal cells (ASC) possess several desirable features for cell therapy approaches to cardiac repair [120]. In fact, ASC 1) can be easily obtained in large quantities from autologous liposuction material [116], 2) have differentiation potential into cardiomyocytes [117] and 3) have been reported to reduce the infarct area [118] and to significantly improve the left ventricular ejection fraction [119], as well as

the electrophysiological function after delivery in animal models of myocardial infarction [120]. Recently, we have shown that injection of genetically engineered VEGF-expressing human ASC in normal myocardium, FACS-purified to homogeneously produce a specific controlled and safe level of VEGF, could induce normal and stable angiogenesis while completely preventing aberrant vascular growth [124].

In this study, we tested the hypothesis that delivery of human ASC FACS-purified to express controlled VEGF levels at the infarct border zone could efficiently induce safe angiogenesis and ultimately improve cardiac function in a rat model of myocardial infarction.

METHODS

Cell culture

Human adipose tissue was obtained from three healthy patients undergoing plastic surgery after informed consent and according to a protocol approved by the Ethical Committee of the Basel University Hospital. All investigations conformed to the Declaration of Helsinki. Tissue was minced and digested with 0.15% collagenase (Worthington Biochemical Corporation, Lakewood, NJ) in phosphate-buffered saline (PBS) at 37°C under continuous shaking for 60 min. After centrifugation at 1500 rpm for 10 min, the lipid-rich layer was discarded, and the cellular pellet was washed once with PBS. Released cells were strained through a 100-µm nylon-mesh followed by a 70-µm nylon-mesh in order to remove fibrous debris, plated at a density of 10^5 cells/cm^2, and cultured in high-glucose Dulbecco's modified Eagle's medium with 10% fetal bovine serum, as described [125]. After 4 days, cells were retrovirally transduced twice a day according to a recently optimized high-efficiency protocol [84] for a total of six rounds. The retroviral vectors expressing rat $VEGF_{164}$ and truncated rat CD8a have been previously described [82]. We have previously found that neither the transduction procedure nor VEGF expression affected the surface marker expression profile, proliferative ability, and multi-lineage differentiation potential of the transduced ASC [84]. After 12 days, (approximately 90% confluence), cells were FACS-sorted with a BD Influx Cell Sorter (BD Biosciences, Basel, Switzerland) to generate the three different treatment groups (*CD8, ALL, SPEC*), according to a previously published protocol [81, 124]. Briefly at the first passage, control cells, which were transduced with the control virus expressing CD8 alone, were FACS purified to eliminate the few non-transduced cells and yield a purely CD8-positive population (CD8). Part of the cells transduced with the virus containing VEGF were FACS purified through a specific narrow gate to produce a homogeneous cell population expressing a specific moderate VEGF level (SPEC) and the rest of the cells were sorted to generate a population expressing all the heterogeneous VEGF levels (ALL).

VEGF ELISA measurements

The production of rat $VEGF_{164}$ and human $VEGF_{165}$ was quantified as previously described [124]. Briefly, species-specific Quantikine VEGF ELISA kits (R&D Systems, Abingdon, UK) were used according to manufacturer's protocol. One milliliter of medium was harvested from ASC cultured in a 60-mm dish, following 4 hours of incubation, filtered, and analyzed in duplicate. Results were normalized by the number of cells and time of incubation and expressed as ng of VEGF/10^6 cells/day. Four separate dishes of cells were assayed for each cell type from 3 independent donors.

Animals

All animals were treated in compliance with Swiss Federal guidelines for animal welfare and all procedures were approved by the Veterinary Office of the Canton Bern (Bern, Switzerland) and conform to the Directive 2010/63/EU of the European Parliament. Immunodeficient male nude rats, (Hsd: RH-rnu/rnu, Harlan, Venray, Netherlands) were used to prevent rejection of human ASC.

Myocardial infarction and in vivo cell implantation

Anesthesia was performed with isoflurane (5% of oxygen for induction and 2.5% for maintenance) and additional buprenorphine (10 mg/kg). Animals were placed on a warming pad (37°C) and intubated with a 14G tracheal cannula (Abbocath, Abbott, Sligo, Ireland) and ventilated at 80 cycles/min (Small Animal Ventilator 683, Harvard Apparatus, Inc., Holliston, MA). Hearts were exposed through a left thoracotomy [126]. After opening the pericardium, a myocardial infarction was created by a permanent ligation of the left anterior descending (LAD) coronary artery using a 7/0 polypropylene suture. Distal ligature allowed the induction of an initial small infarct with limited mechanical overload and consequently reduced animal mortality over the study period. Two weeks after coronary ligation, a pre-treatment echocardiography (E1) was performed to exclude animals with an ejection fraction above 60% (i.e. with no significant infarction) or under 45% (i.e. already close to heart failure), before randomization to one of the 4 treatment groups. Animals received five direct intramyocardial injections into the anterior wall around the infarction for a total of 150 μL of either phosphate buffered saline (PBS) alone or containing 10^7 cells for each of the three selected conditions (CD8, ALL, SPEC). Four weeks post-treatment, rats were sacrificed by exsanguination under the same anesthesia conditions as already described, and the hearts were then collected, embedded in optimal cutting temperature (OCT) compound (Sakura Finetek Inc.), and frozen in isopentane cooled in liquid nitrogen.

Functional assessment

Before sacrifice at 28 days animals were anesthetized by mask and placed on the left lateral position. A single examiner evaluated left ventricular function in a blinded manner by transthoracic echocardiography equipped with a 9–11 MHz linear phase array transducer system (AcusonSequoia, Siemens, Inc., Malvern, PA). Echocardiographic assessments were performed on animals under anesthesia induced by 2.5% isoflurane at the beginning of the study in non-infarcted heart (E0), 2 weeks after induction of the myocardial infarction at the time of randomization (E1), and finally 4 weeks after treatment (E2). The fraction shortening (FS) and ejection fraction (EF) were recorded with M-mode and 2D echocardiography. For each data point, 3 different heart cycles were averaged.

Immunofluorescence

Histological analyses were performed on heart 10 µm-thick cryosections. Immunofluorescence was performed using the following primary antibodies and dilutions: mouse-anti-rat CD45 (BD Biosciences Allschwil, Switzerland; 1:200), mouse anti-rat CD31 (Clone TLD-3A12; AbD Serotec, Düsseldorf, Germany; 1:100), rabbit anti-mouse NG2 (Millipore, Zug, Switzerland; 1:200), mouse anti α-smooth muscle actin (Clone 1A4; MPBiomedicals, Basel, Switzerland; 1:400), anti-human leukocyte antigen (HLA) (Biolegend, San Diego, CA; 1:200), mouse anti-Human Nuclei (HuNu) (Millipore, Billerica, MA; 1:100), goat anti-VE-Cadherin (VE-Cad; Santa Cruz, Dallas, TX; 1:100) and goat anti-rat VEGF (R&D Systems, Abingdon, UK; 1:100). Fluorescently labeled Alexa488, Alexa546 or Alexa647 secondary antibodies (Invitrogen, Basel, Switzerland) were used at 1:200.

Fibrosis evaluation

Histological analyses were performed on heart cryosections stained with Masson Trichrome according to standard protocols. Images were acquired using an Olympus BX61 microscope (Olympus, Münster, Germany) and processed using Image J (National Institutes of Health, Bethesda, MD) by color recognition. In all experimental groups, the total amounts of fibrotic tissue (green color) and muscle tissue (red tone) were determined on a standardized set of 10 cross-sections, starting at the level of the papillary muscle and moving towards the apex every 300 µm. The percentage of fibrosis was calculated from the ratio of the green area over the total (red + green) area.

Vessel measurements

The amount of blood vessels was quantified on images taken from CD31-stained sections. Eighteen representative fluorescent images per group (6 images/heart and 3 hearts/group) were acquired with a 20x objective on an Olympus BX61 microscope (Olympus, Münster, Germany) on cross-sections of the anterior wall taken at 300-µm intervals starting from the level of the papillary muscle, in the area where injections were performed. Blind analysis was performed with either Image J software (National Institutes of Health, Bethesda, MD) or AnalySIS D software (Soft Imaging System, Münster, Germany). The area fraction occupied by endothelial cells was calculated by measuring the number of CD31-positive pixels in each image with Image J software and normalizing it to the total area. Alternatively, vessel length density (VLD) was quantified as previously described [127] by tracing the total length of CD31-positive vessels in AnalySIS D software (Soft Imaging System, Münster, Germany) and dividing it by the total area of each field.

Statistics

Data are presented as means ± standard deviation and were analyzed with the statistical software Prism 5.0a (GraphPad, La Jolla, CA). For quantifications of VEGF expression, cardiac fibrosis and vascularization, comparison between groups was performed with the non-parametric Kruskal-Wallis test for multiple comparisons and Dunn's post-hoc test. All quantifications were analyzed using the means of multiple individual measurements in each sample (n = number of independent samples). Echocardiography data, which represent measurements from the same animals before and after treatment, were analyzed by Repeated Measures ANOVA and Bonferroni post-hoc test. The normal distribution of data sets representing differences between pre- and post-treatment (ΔEF and ΔFS) was verified and multiple comparisons were performed with the parametric 1-way analysis of variance (ANOVA) followed by the Bonferroni test. Differences were considered statistically significant when $p<0.05$.

RESULTS

VEGF-producing ASC were generated by transduction with a retrovirus carrying a bicistronic cassette that co-expresses rat $VEGF_{164}$ and a truncated version of rat CD8a as a FACS-quantifiable cell surface marker. The primary transduced cells were used to generate two distinct populations. Part were FACS-purified through a specific narrow gate, designed according to a previously published technique [81], to produce a homogeneous cell population expressing a specific moderate VEGF level (SPEC; Fig. 30a). The rest were sorted to eliminate only non-expressing cells and generate a population heterogeneously expressing all the VEGF levels present after retroviral transduction (ALL; Fig. 30a). The mesenchymal identity of the different ASC populations used here was previously confirmed by their robust expression of classical mesenchymal markers (CD73, CD90, CD105) and essentially absent expression of endothelial (CD31, CD34, VEGFR2) or cardiac (Troponin I) markers [124]. Further, the ASC phenotype was not affected by retroviral transduction, FACS-sorting or VEGF expression [84, 124]. In agreement with this, we have also previously shown that both control CD8 and ALL VEGF-expressing cells maintained their *in vitro* differentiation potential towards the adipogenic or osteogenic lineages compared to the naïve ASC [84]. In vitro VEGF release by cells from the different groups was quantified before in vivo injection. As shown in Fig. 30b, negative control CD8 cells, which were transduced with a retrovirus carrying only the surface marker CD8, but no VEGF gene, produced negligible amounts of rat VEGF (CD8 = 1.0±0.3 ng/10^6 cells/day). On the other hand, both VEGF-expressing populations (SPEC and ALL) produced similar total amounts of rat VEGF (ALL = 109.8±15.8 ng/10^6 cells/day; SPEC = 83.1±21.1 ng/10^6 cells/day) (Fig. 30b), in agreement with the fact that the purified SPEC population represents the middle portion of the levels present in the unpurified ALL population, which further comprises both higher and lower ones, as visible on the FACS distribution of fluorescence intensities (Fig. 30a). On the other hand, since ASC were of human origin, expression of the endogenous human VEGF was also quantified. All three populations secreted very low amounts of human $VEGF_{165}$, without any difference between conditions (CD8 = 13.8 ±5.2; SPEC = 15.6 ±6.0; and ALL = 15.3 ±4.8 ng/10^6 cells/day). Lastly, neither the genetic modification of the cells nor their sorting affected their morphology, which was uniformly fibroblast-like, typical of early-passage ASC (Fig. 31).

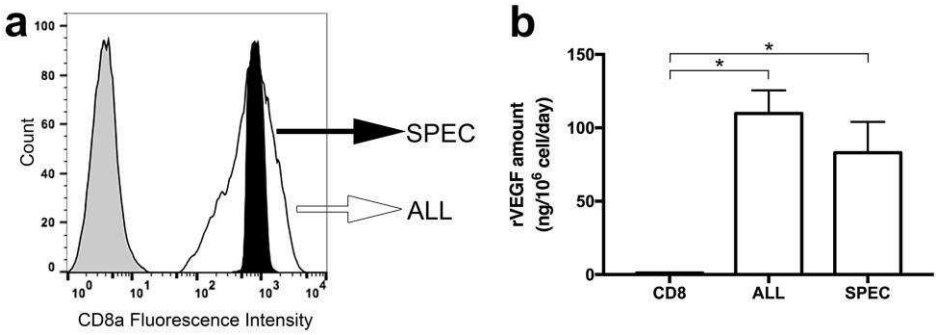

Figure 30. Cell generation and VEGF quantification. **(a)** VEGF-expressing ASC were FACS-sorted to generate two populations producing either a specific homogenous level (SPEC) or all heterogeneous levels (ALL) of VEGF. In the FACS plots: grey tinted curve = negative control; black open curve = purified ALL cells; black tinted curve = purified SPEC cells. **(b)** ELISA quantification of rat VEGF production in the culture supernatants of the different populations, expressed in ng/10^6 cells/day; * $p<0.05$.

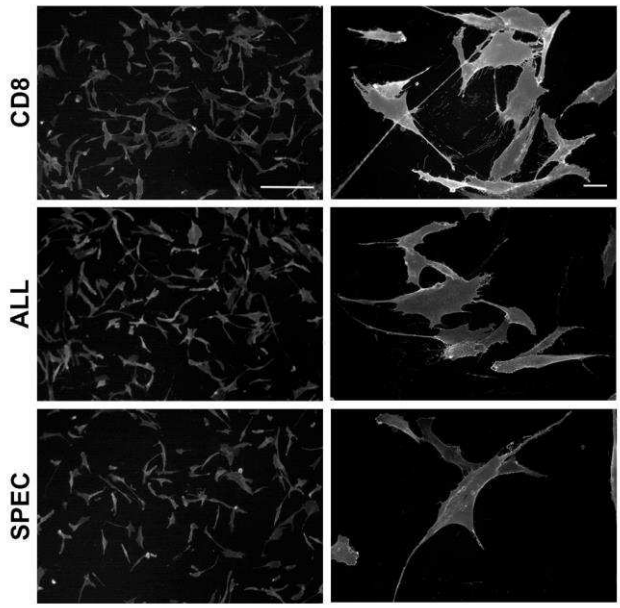

Figure 31. Cell morphology. Before in vivo injection, cell morphology was assessed by fluorescence microscopy after in vitro staining for cell surface CD8a expression for control cells (CD8) or the two VEGF-expressing populations (ALL and SPEC). Size bar: left column = 500µm, right column =50µm.

Surgical induction of myocardial infarction (MI) caused a moderate 24-hour mortality of 15.7% (11/70 rats). In order to ensure a homogeneous functional state before randomization to the different treatment groups, 20 rats (33.8% of the surviving animals) were excluded because the echocardiographic control after 2 weeks indicated either a very mild or no infarction, evidenced by a left ventricular ejection fraction (EF) above 60%, or on the contrary a too severe infarction zone with a corresponding EF under 45%. Therefore, a total of 39 animals weighing 252±16 grams with an EF of 45-60% were randomized into the 4 treatment groups. This very selective randomization of animals with only an ejection fraction within a narrow range was necessary to ensure the standardization of the model and homogeneous functional groups for comparison [126]. Mortality following the second thoracotomy and the intramyocardial injection was 10.3% (4/39). No further mortality was observed until follow-up was completed at 6 weeks. Finally, 35 animals could be analyzed in the 4 treatment groups: PBS n=7, CD8 n=9; ALL n=8; SPEC n=11 (Fig. 32).

		n	%
Number of animals initially included		70	
Mortality post infarction [1]		11	15.7
Drop-out [2]		20	33.8
Mortality post treatment		4	10.2
Completed follow up @ 6 weeks - **Total**		35	50.0
	PBS	7	
	CD8	9	
	ALL	8	
	SPEC	11	

Figure 32. Mortality throughout the study.

[1] during the first 24 hours after coronary ligation.
[2] criteria for a drop-out were a left ventricular ejection fraction (EF) > 60% or < 45%

Controlled VEGF expression prevents cardiac function deterioration after infarction

Cardiac functionality was assessed before infarction (E0), 2 weeks after ligation of the LAD right before treatment (E1) and 4 weeks post-treatment (E2) by echocardiography (Fig. 33a). On day 14, E1 echocardiography analysis showed that at the time of randomization before treatment the ejection fraction was significantly reduced compared to the non-infarcted heart (E0) (53±6% versus 70±3%). After randomization, all groups had a similar EF before treatment with no statistical difference. Four weeks after treatment, EF further decreased in the PBS (-8±7%), the CD8 (-6±7%) and the ALL (-13±10%) groups, but remained stable in the SPEC group (+1±7%), (Fig. 33b-c). Interestingly, EF data suggested a statistically non-significant trend towards an even greater degree of deterioration after injection of cells expressing VEGF at uncontrolled levels (ALL) compared to PBS and control cells (CD8). Analysis of fractional shortening showed similar results (Fig. 33d-e), with a significant decrease between E1 and E2 for the PBS (-4±3%), the CD8 (-4±3%) and the ALL (-7±6%) groups, but a stabilization for the SPEC treatment group (+1±5%).

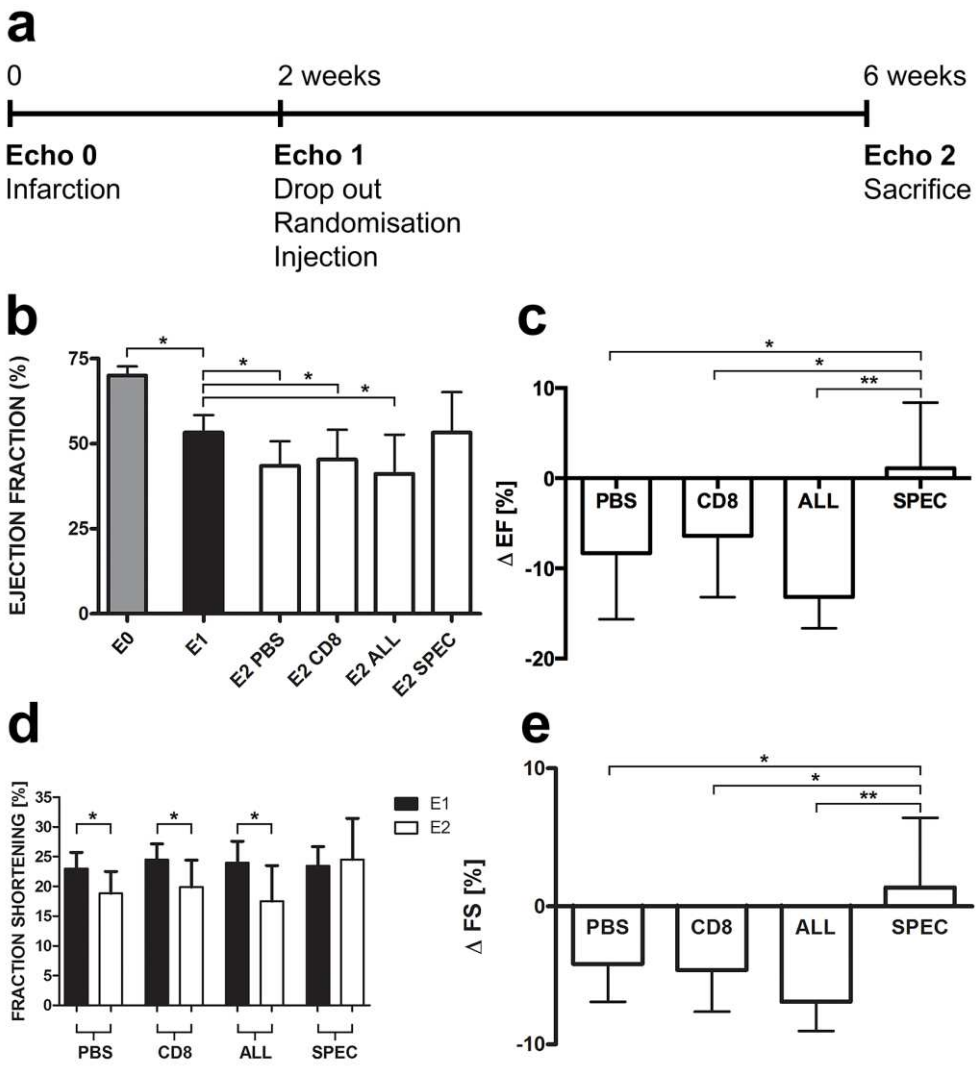

Figure 33. Echocardiographic cardiac functionality. (**a**) Time line of the experiment. Three echocardiography studies were performed: at pre-infarction (E0), 2 weeks after ligation of the LAD but before treatment (E1) and 4 weeks post-treatment (E2). Treatment consists in the injection of PBS, CD8 cells or VEGF-producing cells with controlled levels (SPEC) or heterogenous levels (ALL). Ejection fraction (2D-mode) in non-infarcted hearts and pre-treatment, as well as post-treatment per group (**b**) or expressed as difference between E1 and E2 per animal in the same group (**c**). Fraction shortening (M-mode) per treatment group (**d**), or as a difference between E1 and E2 per animal of the same group (**e**). PBS n=7; CD8 n=9; ALL n=8; SPEC n=11; * $p<0.05$, ** $p<0.01$.

Controlled VEGF expression reduces myocardial fibrosis

To assess the effects of the angiogenic treatment on ventricle remodeling, we evaluated the fraction of the left ventricular myocardium that was substituted by a scar tissue 6 weeks after coronary ligation. Masson's Trichrome staining of heart sections was used to detect the high collagen content typical of fibrotic scarring (Fig. 34a, showing representative images corresponding to the median value of each group). In all the groups, fibrous tissue and a corresponding thinning of the regional wall thickness substituted a significant portion of the left ventricle. This was however greatly reduced only in the SPEC-treated hearts. Quantification of the scar fraction (Fig. 34b) confirmed that only controlled VEGF delivery (SPEC) could significantly reduce fibrosis (11±5%) compared to all other groups (PBS = 27±6%; ALL = 22±3%; CD8 = 21±3%), which were not statistically different from each other.

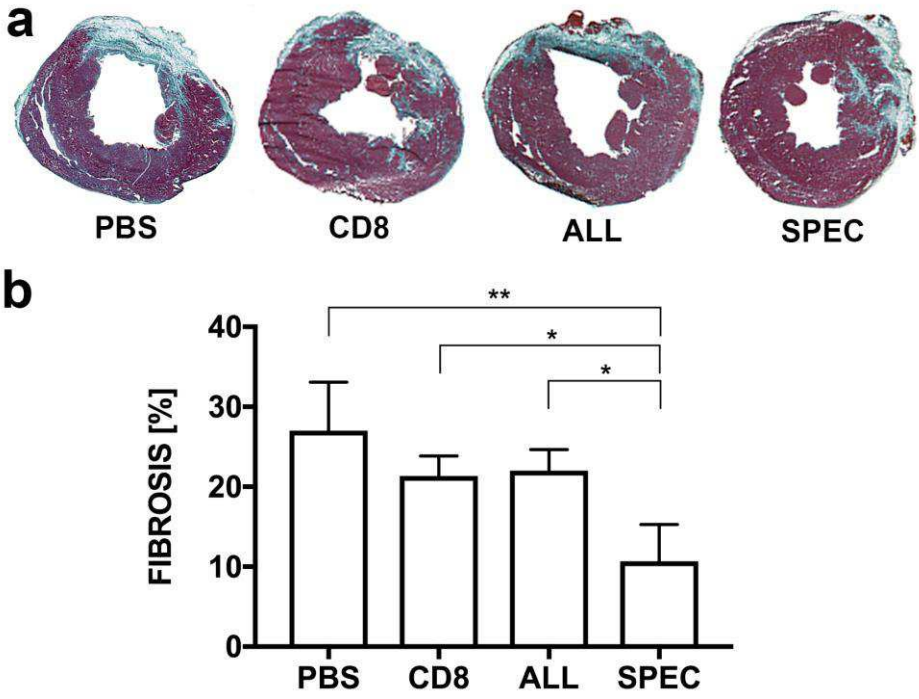

Figure 34. Fibrosis quantification. (**a**) Representative cryosections stained with Masson-Trichrome for the four treatment groups, corresponding to the median value of the quantification. (**b**) Fibrosis quantification measured in the percentage of green pixels over the total colored pixel numbers for all treatment groups (CD8 and PBS n=3; ALL and SPEC n=4); * $p<0.05$, ** $p<0.01$.

Controlled VEGF expression improves normal myocardial angiogenesis

The quality and quantity of vascular growth induced by controlled or heterogeneous VEGF expression were assessed by immunofluorescence staining 4 weeks after treatment. Both VEGF-expressing populations induced robust endothelial expansion compared to PBS or control CD8 cells (Fig. 35a). However, vessels induced by controlled VEGF expression (SPEC) displayed the morphology of normal and mature capillaries, homogeneous in size and associated with typical pericytes positive for the chondroitin sulfate proteoglycan NG2 and negative for smooth muscle actin (SMA) expression. These were similar in quality to the normal pre-existing vasculature visible in the PBS and CD8 groups. A few SMA-positive vessels of regular caliber had the morphology of arterioles feeding into the newly formed microvascular networks. In contrast, heterogeneous VEGF expression by ALL cells caused the growth of enlarged vessels, characterized by heterogeneous diameters, the presence of multiple lumens, and a lack of normal pericytes, substituted by a thick coat of smooth muscle cells expressing both NG2 and SMA, similar to the progressively growing angioma-like vascular structures previously observed in similar conditions [39, 91, 124].

Quantification of the area fraction occupied by CD31-positive endothelial cells (Fig. 35b) showed that both VEGF-expressing populations caused a significant expansion of vascular structures compared to controls (ALL 13±5% and SPEC 9±1% vs PBS 6±1% and CD8 6±1%). Since the vessels induced by the ALL population displayed an irregular morphology and heterogeneous sizes, vascular growth was independently quantified by measuring vessel length density (VLD), which indicates the total length of vessels in a given tissue area, irrespective of their diameter or endothelial cell content [91]. As shown in Fig. 35c, the endothelial expansion induced by uncontrolled VEGF expression did not translate into a corresponding increase in actual vessel length compared to controls (ALL 11±6 mm/mm^2 vs PBS 12±3 mm/mm^2 and CD8 12±4 mm/mm^2), whereas only the homogeneous VEGF-expressing population caused a significant increase in VLD by about 60% (SPEC 17±9 mm/mm^2, $p<0.01$ vs all other groups). Taken together, these data show that, although heterogeneous VEGF expression was efficient in inducing endothelial expansion, this contributed mostly to vascular enlargement rather than the generation of new capillary networks, which were instead efficiently induced by controlled expression of a homogeneous specific VEGF level.

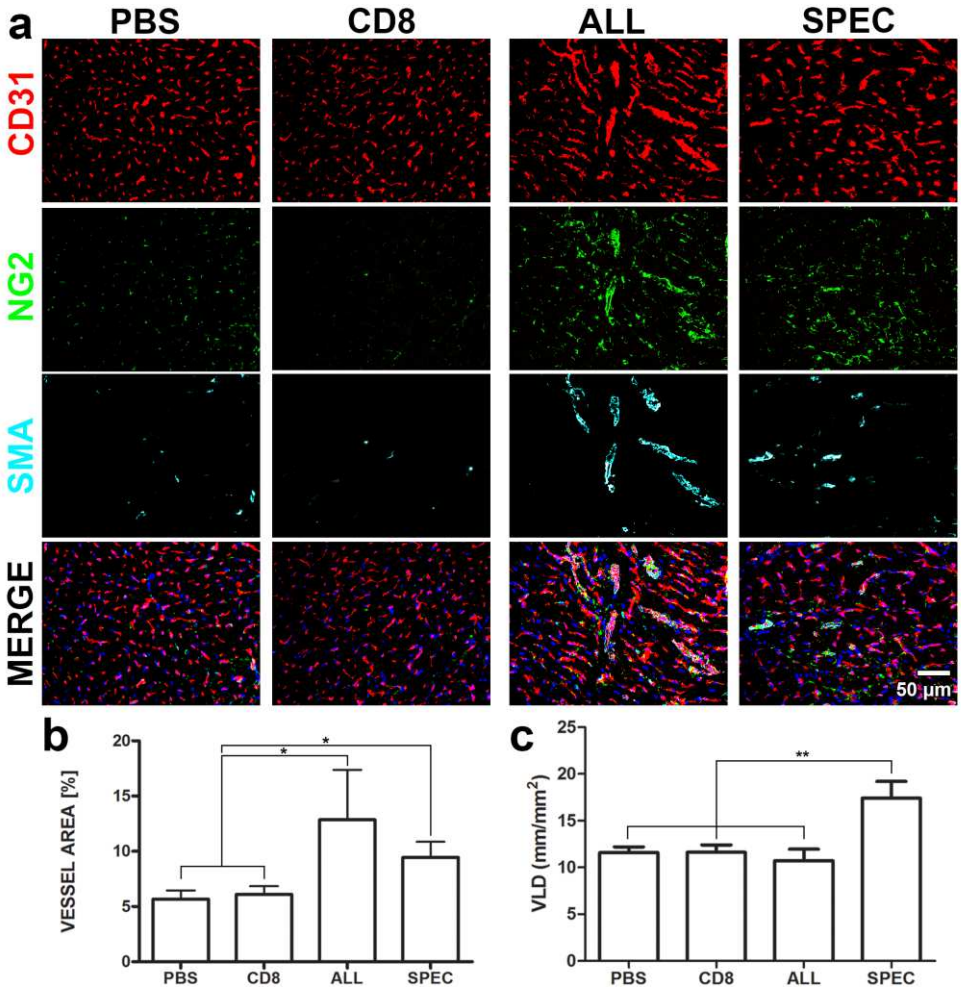

Figure 35. Myocardial angiogenesis**.** (**a**) Immunofluorescence staining for endothelium (CD31, in red), pericytes (NG2, in green), smooth muscle cells (SMA, in cyan), and nuclei (DAPI, in blue) in sections of myocardium injected with PBS, control cells (CD8), or ASC expressing uncontrolled heterogeneous levels (ALL) or a specific homogeneous VEGF level (SPEC). Angiogenesis was quantified either as the area fraction occupied by CD31-positive pixels (**b**) or as vessel length density (**c**); n=3 per group; * $p<0.05$, ** $p<0.01$.

Cell engraftment and fate

In order to determine the degree of stable engraftment of the injected cells, human ASC were tracked in harvested tissue by immunofluorescence staining for human-specific histocompatibility antigens of class I (HLA-class I), which are ubiquitously and specifically expressed on human cells. Four weeks after injection, only rare human ASC were still detectable in the rat myocardium (Fig. 36), which did not appear integrated with the cardiomyocytes, but rather remained as isolated single cells in between CD31-positive vessels. No differences were observed between the three cell-based treatment groups (CD8, ALL, SPEC), suggesting that VEGF expression did not influence the rate of ASC survival in the myocardium. Although unlikely, it remains theoretically possible that some injected cells may have down-regulated HLA-class I expression in vivo. Therefore, ASC engraftment was also analyzed by in situ hybridization to the human-specific Alu-sequence, present in the genomic DNA of all human cells. This unrelated technique confirmed that ASC engraftment 4 weeks after injection was very limited, without noticeable differences between the groups (data not shown).

Lastly, we sought to determine whether engrafted ASC might contribute to vessel growth by acquiring a vascular cell fate. For this purpose, injected ASC were identified by staining with a human nucleus antibody (HuNu), which is specific for human cells, and co-localized with endothelial or pericyte markers (VE-Cadherin and NG2, respectively). Most human nuclei appeared located in between vascular structures and did not co-localize with either endothelial cells or pericytes (arrows in Fig. 37) both for the control group (CD8) and the VEGF-expressing populations (ALL and SPEC). However, the few human cells from both VEGF-expressing populations that were present in the myocardium 4 weeks after injection could be shown to still produce VEGF, whereas control CD8 cells did not, as expected (Fig. 38). Immunofluorescence staining showed that: 1) the most part of rat VEGF protein was visible in association with surviving human cells, suggesting that endogenous VEGF is not significantly expressed in comparison with the exogenous delivered factor; and 2) VEGF protein was tightly associated with the surface of producing cells, with no significant staining visible even a few μm away, providing a visual evidence of the concept of microenvironmental localization. Due to the essentially non-quantitative nature of immunostaining, levels of expression by different cells could not be visualized by this technique.

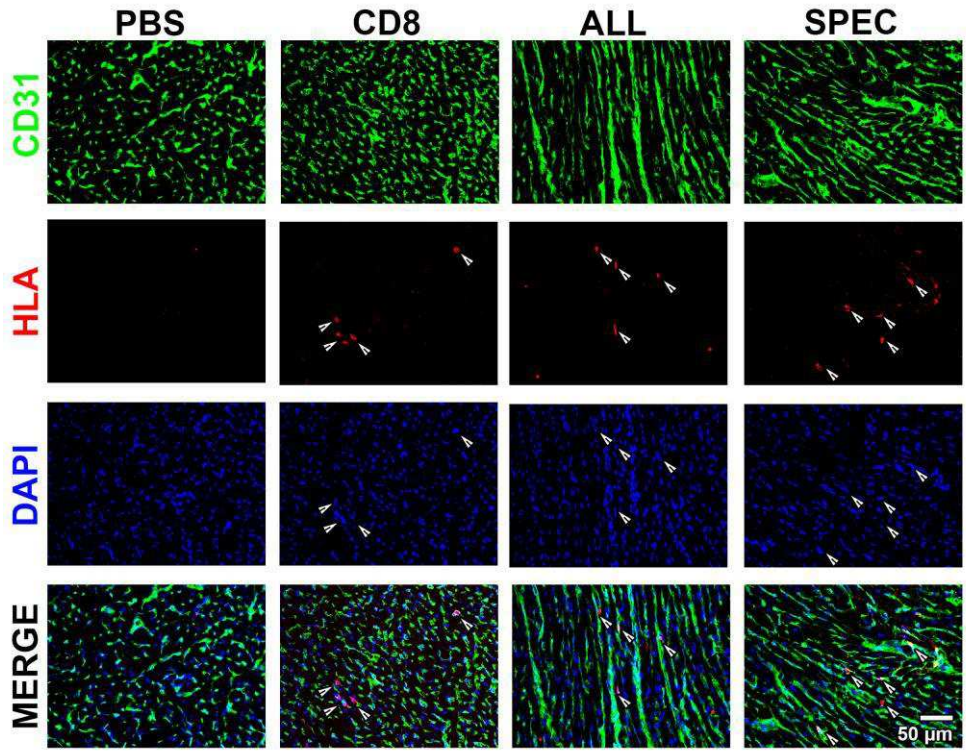

Figure 36. Cell engraftment. Survival of human ASC was assessed by immunostaining for HLA-Class I (red), while endothelium was detected by CD31 expression (green), and nuclei by DAPI staining (blue) 4 weeks after injection of PBS, control cells (CD8) or the two VEGF-expressing populations (ALL and SPEC). White arrows indicate single engrafted human cells.

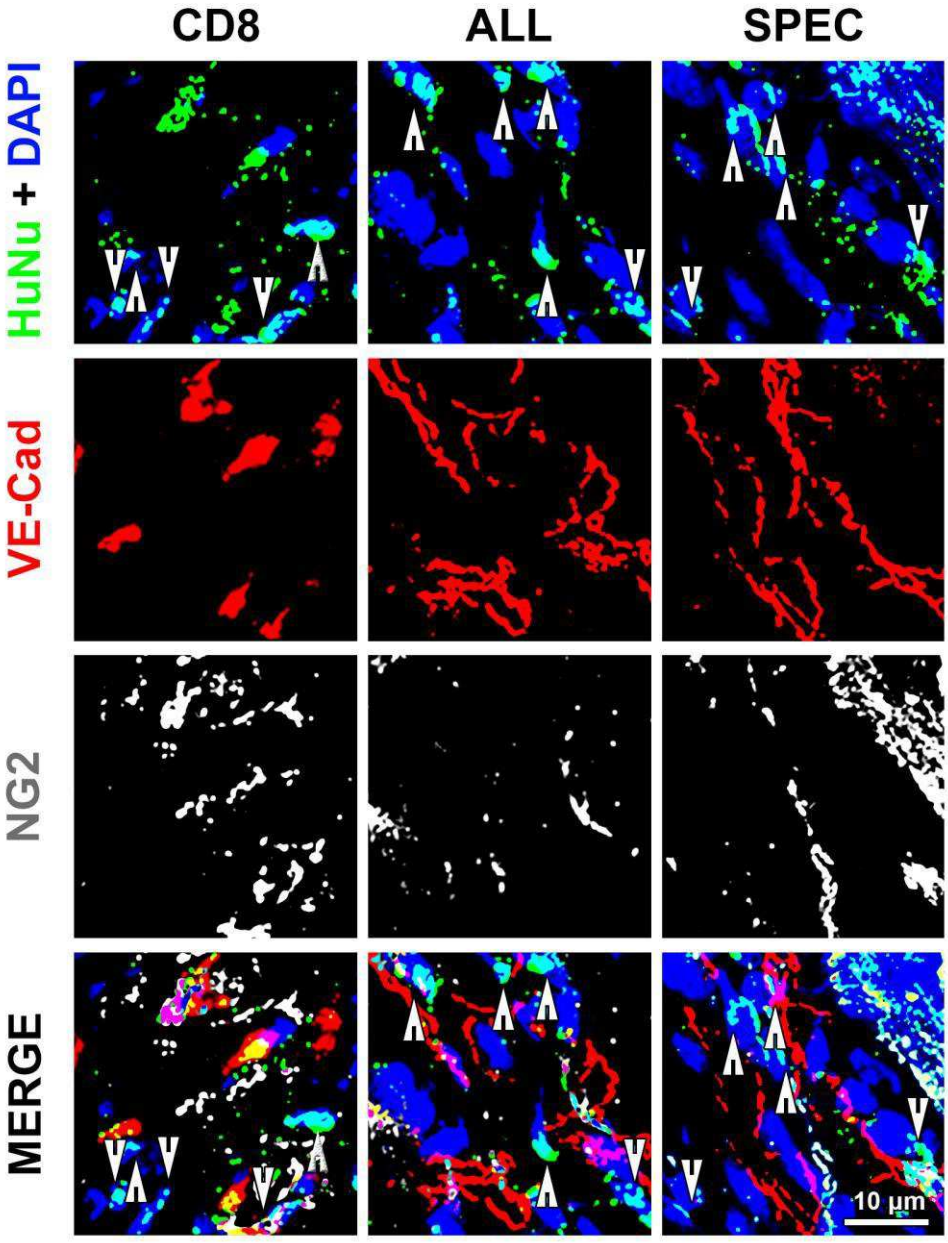

Figure 37. Cell fate. Fate of human ASC was assessed by immunostaining for the endothelial junctional marker VE-Cadherin (VE-Cad, in red), pericytes (NG2, in white), human nuclei (HuNu, in green) and nuclei by DAPI staining (blue) 4 weeks after injection of control cells (CD8) or ASC expressing uncontrolled heterogeneous levels (ALL) or a specific homogeneous VEGF level (SPEC).

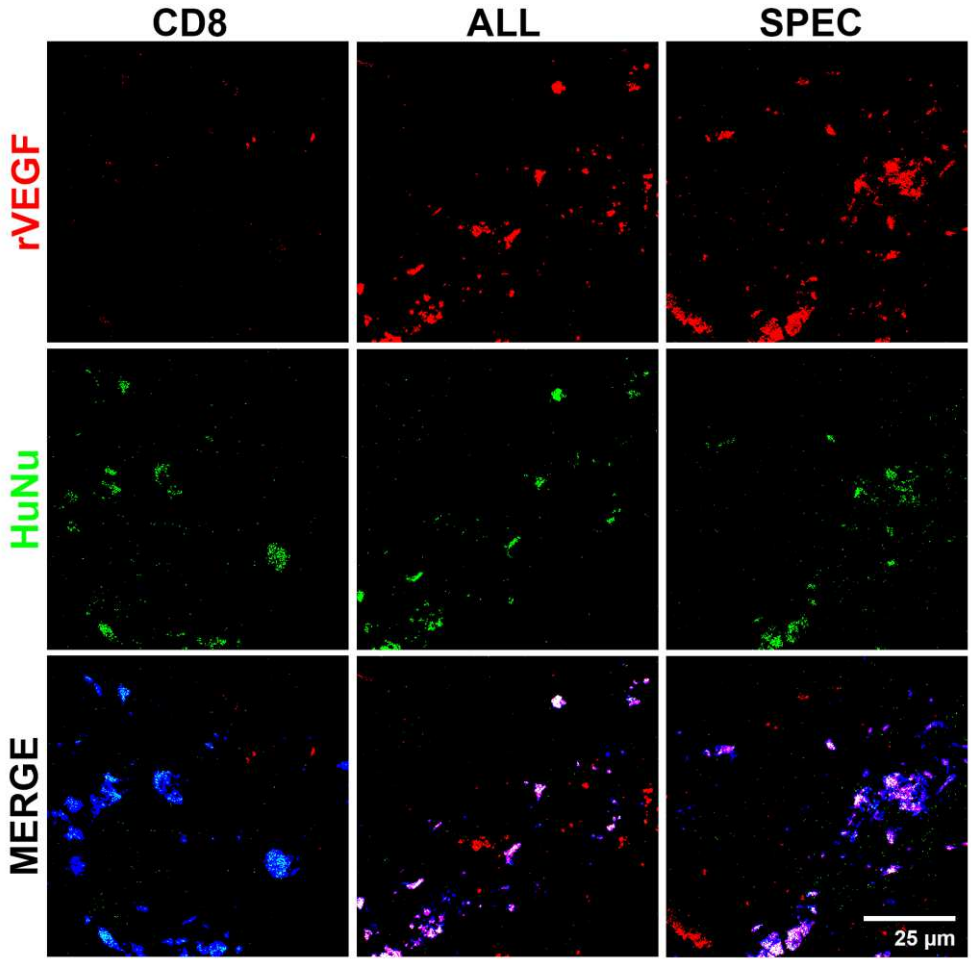

Figure 38. VEGF production. Production of rat VEGF by the injected human cells (control cells CD8; VEGF-producing cells ALL and SPEC) after 4 weeks in vivo assessed by immunostaining for rat VEGF (rVEGF, in red), human nuclei (HuNu, in green) and nuclei by DAPI staining (blue).

DISCUSSION

In the present study, we have provided proof of principle that cell-based homogeneous expression of a specific moderate VEGF level in post-infarction myocardium is effective to: 1) induce robust growth of normal and mature microvascular networks; 2) prevent deterioration of cardiac function; and 3) limit fibrotic scarring.

Myocardial ischemia leads to thinning of the ventricle wall, myocyte slippage, and ventricular dilatation, with progressive deterioration of cardiac function until end-stage heart failure [128]. Therapeutic angiogenesis, aiming at growing new blood vessels from pre-existing vasculature through delivery of exogenous factors, is an attractive strategy to restore blood flow in the ischemic myocardium for many patients that cannot be treated by coronary revascularization, or as an adjunct to surgery [129]. VEGF is the master regulator of both developmental and postnatal angiogenesis [130]. However, despite promising results obtained in various animal models of acute or progressive ischemia, phase I/II clinical studies based on VEGF gene therapy failed to show evidence of benefit and conflicting outcomes were reported for cardiac functionality after myocardial infarction [131]. Retrospective analyses identified several issues underlying these negative results, including the low local transfection efficacy at safe vector doses, resulting in limited amount and duration of protein expression [113, 132]. VEGF gene delivery by different vectors and in a variety of tissues has been shown to produce significant adverse effects, such as vascular hyperpermeability and edema [133], exacerbated scar tissue formation [134], and aberrant endothelial cell proliferation with growth of angioma-like tumors [123, 135]. Growing evidence supports the notion that the difficulty of controlling the VEGF dose distribution in the tissue in vivo underlies the paradox between the crucial biological functions of VEGF and its apparent lack of a therapeutic window [114]. In fact, VEGF binds to the extracellular matrix [136] and remains localized in the immediate microenvironment around each producing cell in vivo [91]. While this property is crucial for the physiological function of VEGF to guide vascular growth through the formation of gradients in the matrix [21], it also prevents heterogeneous levels of expression from diffusing in tissue and averaging with each other [91]. Therefore, the challenge is to avoid that increasing delivered dose and efficacy leads to excessive localized expression and loss of safety.

The use of stably transduced and FACS-purified ASC can overcome this limitation, ensuring that every delivered cell produces the same dose and therefore allowing efficient and sustained VEGF expression without compromising safety. Controlled VEGF expression by the SPEC cells could induce angiogenesis that was both robust, leading to a 60% increase in vessel density, and safe, by completely

preventing the appearance of aberrant vasculature. These results are in agreement with our previous results in healthy heart [124] and notably extend those findings to show that cell-based controlled VEGF expression is safe even in ischemic myocardium, where endogenous factors are upregulated in response to hypoxia and during the ensuing inflammatory reaction.

It is interesting to note that ASC expressing heterogeneous levels of VEGF completely failed to rescue cardiac functionality and, if at all, showed a non-significant trend towards a worse outcome in contractility compared to no treatment. This observation is in agreement with previous findings in skeletal muscle that uncontrolled VEGF expression failed to improve blood perfusion and induce collateral arteriogenesis in hindlimb ischemia [109] and likely reflects the fact that the aberrant vascular structures induced by excessive and uncontrolled VEGF doses behave as functional arterio-venous shunts that paradoxically reduce perfusion of the downstream microcirculation despite the robust angiogenic effect [137].

The better outcomes in terms of vascularization obtained with the SPEC population likely explain the observed reduction in fibrosis and infarction stabilization. In fact, after both clinical and experimental MI, unless reperfusion is performed within six hours, acute and permanent coronary obstruction induces myocardial necrosis in the central infarct zone. This acute phase occurs during the first week and is associated with extensive inflammation and the recruitment of fibroblasts. On the other hand, in the border zone of the infarction cardiomyocytes survive the acute injury, but are still critically under-perfused and will eventually also die during the subsequent sub-acute phase. This takes place up to six weeks after MI, is characterized by the gradual formation of a scar, associated with a further worsening in cardiac function, and can progressively result in heart failure [42, 126]. Clinical and experimental evidences [66, 138] suggest that the rarefaction of cardiac capillaries increases apoptosis of hypertrophied myocytes in the peri-infarct region and promotes tissue hypoxia and its replacement through fibrosis. The fate of the border-zone myocytes plays a key role in determining the sequelae of the acute MI, as their loss will lead to scar enlargement and worsening cardiac function, while their rescue will limit both processes. Therefore, the improved angiogenesis induced by controlled VEGF expression, delivered to the border zone during the early sub-acute phase of MI remodeling (2 weeks after LAD ligation), is expected to be beneficial by preventing cardiomyocyte death, fibrosis expansion and decline in contractility and cardiac function over the subsequent weeks, as shown here. A central role for cardiac angiogenesis is further supported by findings that inhibition of new blood vessel formation accelerates the development of left ventricular (LV) dysfunction [139], whereas stimulation of angiogenesis improves cardiac function and delays

the onset of heart failure [140, 141]. Further, VEGF has been demonstrated to promote several beneficial outcomes in the cardiovascular unit, such as recruitment and activation of cardiac progenitors [142], cardiomyocyte protection from apoptosis [143], and recruitment of bone marrow-derived mononuclear cells, which contribute to the maturation of arterial walls [144].

The observed very limited engraftment of human ASC 4 weeks after intra-myocardial injection is in agreement with previous reports [145] and has been attributed to two distinct events. First, the cell transfer is inefficient because of cell losses due to leakage through trans-epicardial puncture holes, wash-out through the venous system or squeezing of cells by the heartbeats. Second, many of the originally injected cells die because of ischemia of the target areas and apoptosis subsequent to the loss of cell anchorage to matrix [145].

Interestingly, newly induced vessels persisted in the injection areas despite the low engraftment of implanted cells, while results in different tissues have shown that approximately 4 weeks of sustained VEGF expression are required before new vessels stabilize and can persist independently of further stimulation [91, 146]. It is unlikely that this may reflect tissue-specific differences in the stabilization kinetics of myocardial vessels, as experiments with conditional switching of VEGF expression showed that newly induced cardiac microvessels are still unstable after 2 weeks, but persist after 4 weeks [146]. On the other hand, ASC have been described to secrete cytokines involved in vascular stabilization, such as transforming growth factor-β1 (TGF-β1) and basic fibroblast growth factor [92]. Interestingly, we have recently identified a pericyte-independent mechanism for vascular stabilization, whereby a specific subset of circulating monocytes expressing the VEGF co-receptor Neuropilin-1 (NEM) are recruited to sites of VEGF-induced angiogenesis by the axon-guidance factor Semaphorin3A and accelerate stabilization of newly formed vessels by activating endothelial TGF-β1 signaling [147]. Whether ASC may produce Semaphorin 3A and contribute to NEM recruitment remains to be investigated.

ASC can also produce angiogenic and antiapoptotic paracrine factors that contribute to cardioprotection [148]. However, the findings reported here show that only VEGF over-expression at controlled levels by the SPEC population induced efficient and normal angiogenesis with functional benefit on cardiac function, whereas ASC alone did not cause any improvement compared to PBS injection, nor did any ASC population directly take part in new vessel formation as endothelial or mural cells. These controls support the conclusion that the observed functional improvements could be ascribed prevalently to the direct angiogenic effects of VEGF delivery.

The findings reported here provide proof of principle for the therapeutic potential of controlling the distribution of VEGF expression levels in the myocardium. The outcome of preventing further decline in cardiac functionality and therefore avoiding progression towards heart failure is consistent with the histological correlate of limiting the extension of fibrotic scar and is in agreement with other pre-clinical results obtained in the same small rodent model of acute infarction, recently reviewed in a meta-analysis by Kanelidis et al. [149].

In view of a potential clinical translation, the use of retroviral vectors raises some safety concerns due to the possible neoplastic transformation of transduced stem cells by insertional mutagenesis [150]. However, the same approach is readily applicable to progenitors transduced with clinically compliant new-generation vectors, such as self-inactivating lentiviruses with chromatin insulator elements that ensure stable and sustained transgene expression in the absence of oncogenic potential [151].

In conclusion, we obtained functional evidence that controlled VEGF expression by transduced and FACS-purified ASC is safe and effective in inducing robust growth of uniformly normal blood vessels in ischemic myocardium, preventing the loss of cardiac functionality and reducing heart fibrosis after myocardial infarction. These results suggest that this cell-based gene delivery approach, by affording precise control over the distribution of expression levels *in vivo*, could help overcome a significant obstacle towards safe and effective therapeutic angiogenesis in the heart.

ACKNOWLEDGMENTS

We gratefully acknowledge Ms Brigitta Gahl (Inselspital, Berne) for help with the statistical analysis. This work was supported in part by an intramural grant of the Department of Surgery (Basel University Hospital), a Swiss National Science Foundation grant [127426], a U.S. National Institutes of Health R21 grant [HL089913-02], and European Union FP7 grants MAGISTER [CP-IP 214685] and ANGIOSCAFF [CP-IP 214402] to A.B.

AUTHOR DISCLOSURE STATEMENT

No competing financial interests exist.

FIBRIN HYDROGELS PROMOTE SCAR FORMATION AND PREVENT THERAPEUTIC ANGIOGENESIS IN THE HEART

L. Melly[1,2], A. Grosso[2], C. Stanciu Pop[3], C. Yu-Hsuan[4], MC. Nollevaux[3], C. Schachtrup[4], A. Marsano[5], N. Di Maggio[2], B. Rondelet[1*], A. Banfi[2*]

1 *Cardiac, Vascular and Thoracic Surgery Department, CHU UCL Namur, Yvoir, Belgium.*
2 *Cell and Gene Therapy, Department of Biomedicine, Basel University Hospital and University of Basel, Basel, Switzerland.*
3 *Pathology Department, CHU UCL Namur, Yvoir, Belgium.*
4 *Institute of Anatomy and Cell Biology, Department of Molecular Embryology, University of Freiburg, Germany.*
5 *Cardiac Tissue Engineering, Department of Biomedicine, Basel University Hospital and University of Basel, Basel, Switzerland.*

** Equally contributing authors*

Correspondence

Dr. Ludovic MELLY (e-mail: ludovic.melly@uclouvain.be)

or Dr. Andrea BANFI (e-mail: andrea.banfi@usb.ch)

ABSTRACT

Therapeutic angiogenesis is the delivery of factors to promote vascular growth and holds promise for the treatment of ischemic heart conditions. Recombinant protein delivery to the myocardium by factor-decorated fibrin matrices is an attractive approach, thanks to the ability to precisely control both dose and duration of the treatment, the use of a clinically approved material like fibrin and the avoidance of genetic modification. Here we investigated the feasibility of inducing therapeutic angiogenesis in the rat myocardium by a state-of-the-art fibrin-based delivery platform that we previously optimized. Engineered versions of $hVEGF_{165}$ and hPDGF-BB were fused with an octapeptide substrate of the transglutaminase coagulation factor fXIIIa (TG) to allow their covalent cross-linking into fibrin hydrogels and release by enzymatic cleavage. Hydrogels containing either 100 μg/ml TG-VEGF alone or in combination with 10 μg/ml TG-PDGF-BB or no factor were injected into rat myocardium. Surprisingly, vascular density was severely reduced in all conditions, both in and around the injection site, where large fibrotic scars were formed. Scar formation was not due to the presence of growth factors, adaptive immunity to human proteins, damage from injection, nor to mechanical trauma from the hydrogel stiffness or volume. Rather scar was induced directly by fibrin and persisted despite hydrogel degradation within 1 week. These results caution against the suitability of fibrin-based platforms for myocardial growth factor delivery, despite their efficacy in other tissues, like skeletal muscle. The underlying molecular mechanisms must be further investigated in order to identify rational targets to prevent this serious side-effect.

KEYWORDS

Fibrin; Hydrogel; VEGF; PDGF; Intramyocardial injection; Rat.

INTRODUCTION

Ischemic heart disease still remains one of most frequent causes of death worldwide. Therapeutic angiogenesis promotes expansion of microvascular networks, which can lead to increased flow also in upstream collateral arteries (arteriogenesis) through retrograde signals [9], thereby providing effective bypass of the obstructed feeding vessels. Thus, stimulation of microvascular growth has the potential to treat several ischemic conditions, either alone or in combination with revascularization strategies, such as percutaneous angioplasty or coronary artery bypass grafting.

Vascular Endothelial Growth Factor-A (VEGF) is the master regulator of angiogenesis [112] and its combination with Platelet-Derived Growth Factor-BB (PDGF-BB) has been shown to provide optimal stimulation of both angiogenesis and arteriogenesis [152]. However, VEGF can also induce aberrant and dysfunctional vascular growth if its distribution and duration of expression are not carefully controlled in vivo [14]. In fact, since VEGF binds tightly to the extracellular matrix, different levels of expression do not average in tissue, but rather remain localized in the microenvironment around each producing cell [91]. Cell-based gene therapy approaches, whereby progenitor populations are genetically engineered and FACS-purified to homogenously produce desired levels of the genes of interest [81], have been show to enable precise control of VEGF dose distribution in vivo and ensure only physiological and functional angiogenesis in the myocardium [89, 153]. However, the clinical application of such approaches is challenging due to both the difficulty to achieve sufficient expansion of the transduced populations and the safety issues concerning stable genetic transduction of progenitors [150]. On the other hand, gene therapy vectors (e.g. adenoviruses) have been the most investigated tool for clinical trials of therapeutic angiogenesis because they afford two very desirable features: a) efficient gene transfer with robust expression, and b) transient duration that is limited by the immune response. However, these same features compromise safety (by uncontrolled distribution of high levels) and efficacy (by regression of unstable vessels).

Controlled delivery of recombinant protein factors from bio-compatible matrices has recently emerged as a clinically attractive approach to control both the dose and duration of treatment, while ensuring a homogeneous distribution in vivo, therefore improving both safety and efficacy [93]. We previously optimized a fibrin-based platform for the controlled delivery of recombinant VEGF, engineered to contain an octapeptide sequence that is a substrate for the transglutaminase factor XIIIa [107]. This modification allows its cross-linking into a fibrin hydrogel during fibrinogen coagulation and ensures its controlled release only by cell-

demanded enzymatic cleavage. Fibrin is a natural product of blood coagulation and provides unique features for physiological presentation of angiogenic signals. Fibrin is also injectable as a liquid, becomes a hydrogel in situ without cytotoxicity, and last also provides the universal matrix for tissue regeneration after damage. We previously sowed that controlled VEGF delivery by this optimized factor-decorated fibrin matrix was therapeutically effective in rodent models of hind limb ischemia and wound healing [107].

Fibrin-based delivery of therapeutic factors to the heart has not been attempted. Therefore, here we investigated the feasibility and safety of factor-decorated fibrin matrices to deliver an optimal combination of the angiogenic and arteriogenic factors VEGF and PDGF-BB to the myocardium of immune-competent normal rats.

METHODS

Gel preparation

Fibrin matrices were prepared by mixing human fibrinogen in different concentrations (2.5 to 25 mg/mL; Enzymes Research Laboratories), factor XIIIa (2 U/mL; CSL Behring), thrombin (2 U/mL; Sigma-Aldrich), if needed aprotinin (51 µg/mL), combined with VEGF alone (100 µg/mL) or together with PDGF (10 µg/mL) and 2.5nM Ca^{+2}in 4-(2-hydromethyl)-1-piperazineethanesulfonic acid (Hepes). Fibrin gels were created with the highest feasible dose of transglutaminase-VEGF to ensure maximum arteriogenic potential, in a ratio of 10:1 with transglutaminase-PDGF-BB (V: 100 µg/mL and P: 10 µg/mL) based on previous results. Matrices containing aprotinin-α_2-$PI_{1–8}$ and α_2-$PI_{1–8}$-$VEGF_{164}$ were obtained by adding the engineered proteins to the cross-linking enzymes solution before mixing with fibrinogen. Before injection the two components were mixed to allow in situ polymerization. For the degradation trial the unlabeled fibrinogen (25mg/mL) was mixed with a 647-flurochrome marked fibrinogen (0.5 mg/mL; Invitrogen).

In vivo gel injection

Animals were treated in compliance with Swiss Federal guidelines for animal welfare and all procedures were approved by the Veterinary Office of the Canton Basel (Basel, Switzerland) and conform to the Directive 2010/63/EU of the European Parliament. Sprague-Dawley (RjHan:SD) or nude (Crl: NIH-*Foxn1*^{rnu}, Charles River) rats were anesthetized with 2.5% isoflurane and 10 mg/kg buprenorphine with tracheal ventilation at 80 cycles/min (Small Animal Ventilator 683, Harvard Apparatus). The heart was exposed through a left thoracotomy. The gel was injected into four sites of the anterior wall for a total volume of 100 µL. At sacrifice, rats were anesthetized under the same anesthesia conditions as already described. Hearts were perfused in a retrograde manner through the descending aorta with paraformaldehyde 0.5% for three minutes. Hearts were then collected, embedded in OCT compound (Sakura Finetek), and frozen in isopentane cooled in liquid nitrogen.

Tissue staining

Histological analyses were performed on heart cryosections. Masson Trichrome staining was performed according to standard protocols. Immunofluorescence was performed using the following primary antibodies and dilutions: mouse anti-rat CD31 (Clone TLD-3A12; AbD Serotec; 1:100), mouse anti-α-smooth muscle actin (Clone 1A4; MPBiomedicals; 1:400), rabbit anti-PDGF Receptor α (Clone D1E1E; Cell Signaling; 1:500), goat anti-ionized calcium-binding adapter molecule 1 (Abcam; 1:500). Fluorescently labeled secondary antibodies (Invitrogen) were used at 1:200. Immunohistochemistry was performed using the rabbit-anti-rat CD31 (Clone EPR17259; Abcam; 1:1000).

Vessel and scar measurements

The amount of blood vessels was quantified on images taken from CD31-stained sections. Representative images on immunohistochemistry staining were acquired with a 20x objective on a Leica DM 2002 LED microscope on cross-sections of the anterior wall, as well as the border zone and the contralateral myocardium. Six different injection sites per group (with each one averaged two quantifications per injection) were quantified by using the absolute number of CD31-positive structures on a given circular area of 100µm in diameter and then normalized per mm^2. Measures were made within the injection site, on the border zone and in the remote contralateral myocardium of the same section. For the maximal scar area, six representative images with per injection per group, acquired with a 2.5x objective, were chosen among 8 sections per animal taken at 300-µm intervals. Blind analysis of the maximal scar area was calculated using the Fiji software (BSD license).

Statistics

Data are presented as mean ± standard deviation and were analyzed with the statistical software Prism 8 (GraphPad) for significance of differences. The normal distribution of all data sets was tested and, depending on the results, multiple comparisons were performed with the parametric one-way analysis of variance (ANOVA) followed by the Tukey test, or with the nonparametric unpaired t test. $p < 0.05$ was considered statistically significant.

RESULTS

Intramyocardial injection of fibrin hydrogels is feasible

The liquid fibrinogen mixtures completely polymerized within 60 to 90 seconds after mixing with cross-linking enzymes. This time allowed successful injection into the front wall of the left ventricle in all 50 animals, which had an average weight of 349±128 g. No neurological deficits were observed, indicating the absence of intra-ventricular injections and potential embolization to the brain. Peri-procedural mortality remained null and all animals could complete their planned time-point without side-effects.

Fibrin hydrogels severely reduce vascular density regardless of angiogenic factor decoration

In order to assess the angiogenic potential of factor-decorated fibrin matrices, hydrogels were decorated either with 100 µg/ml of TG-VEGF alone (V) or in combination with 10 µg/ml of TG-PDGF-BB (VP) and injected in the left ventricle myocardium as 4 individual volumes of 25 µL each. Empty fibrin hydrogels without any growth factor served as negative control (Ctr). These doses of the VP combination were previously determined to provide the maximum angiogenic and arteriogenic effect in skeletal muscle (Sacchi et al. unpublished results). Surprisingly, only sparse vascular structures were found within the injection sites in all groups, regardless of angiogenic factor presence (Ctr = 772±130, V = 746±316, VP = 830 ±259 CD31+ structures/mm^2, p=n.s.). Not only no angiogenic effect was observed in the factor-decorated hydrogels compared to fibrin alone, but the vascular density in all injection sites was severely reduced compared to the immediately adjacent border zones (Ctr = 2515±371, V = 2410±359, VP = 2897±342 CD31+ structures/mm^2, $p<0.0001$ vs the respective injection sites) and even more compared to normal myocardium in the remote posterior wall of the ventricle (Ctr = 3677±510, V = 3714±287, VP = 4074±128 CD31+ structures/mm^2, $p<0.0001$ vs both the respective injection sites and border zones) (Fig. 39). On the other hand, the reduction of vascular density in the injection sites was accompanied by the infiltration of an amorphous cellularized tissue with abundant extracellular matrix in place of the normal cardiomyocyte fibers (Fig. 39A).

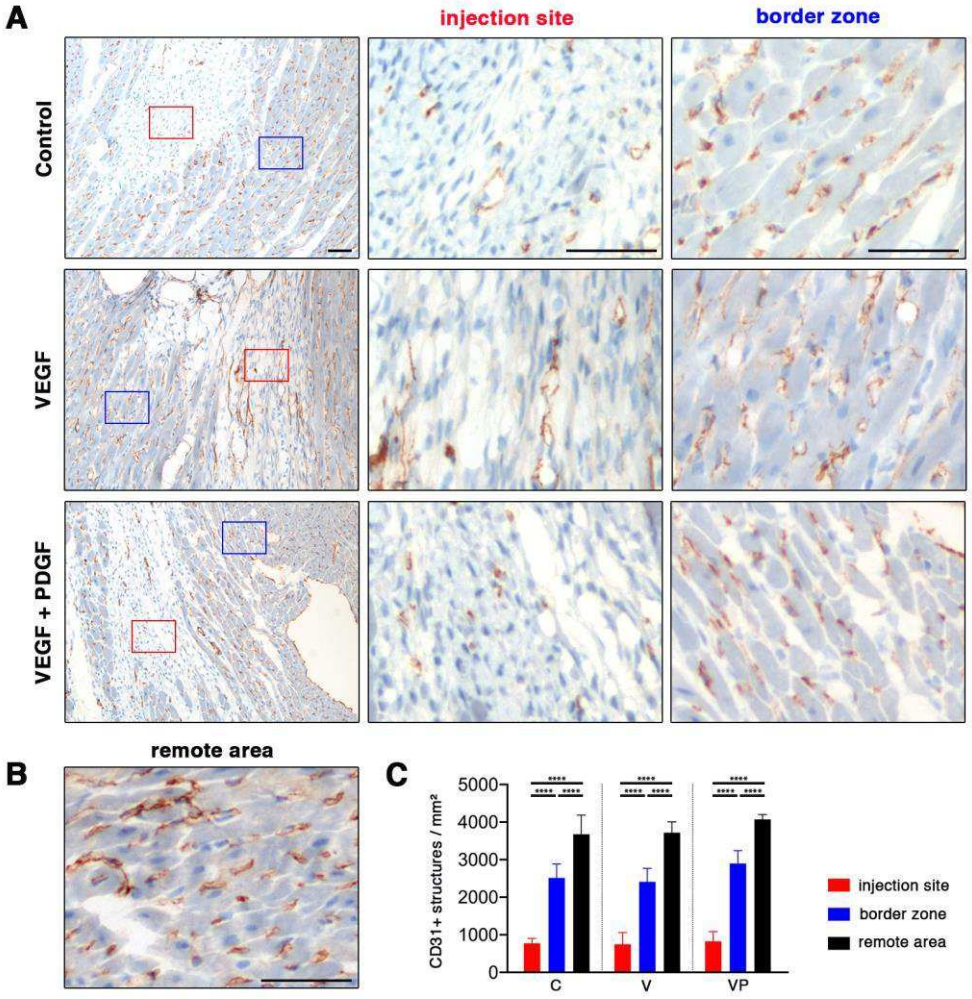

Figure 39. (A) Angiogenesis analysis in immunohistochemistry (CD31, in brown) at one week after intramyocardial delivery of the hydrogel for all three treatment groups: empty gel, loaded with VEGF only and in combination with PDGF. **(B)** As negative controls, the remote areas in the posterior wall of the myocardium were used. Size bar = 50µm. **(C)** Quantifications were made for all treatment groups (n=6 for each group) within the injection site (red squares in A), at the border zone (blue squares in A) and in a remote area (black). **** $P < 0.0001$.

Fibrin hydrogels induce a fibrotic scar similar to myocardial infarction

Masson Trichrome staining revealed that the newly formed tissue within the injection sites displayed the typical features of a fibrotic scar and was similarly composed of abundant collagen fibers in all three groups (Fig. 40A). To determine whether the scar could be due to tissue damage induced by the injection, a similar volume of phosphate-buffered saline (PBS) was injected using the same 30 Gauge syringe (Fig. 40B). Quantification of the collagen area after Masson Trichrome staining revealed that all three fibrin-containing treatments induced a significantly larger scar than PBS after 1 week (Fig. 40C, Ctr = 1.31±0.36; V = 1.16±0.20; VP = 0.76±0.24 mm^2 vs PBS = 0.17±0.10 mm^2) after 1 week. Interestingly, fibrin matrices decorated with both TG-VEGF and TG-PDGF-BB induced smaller scars than fibrin alone or with TG-VEGF alone. Quantification after 4 weeks confirmed similar results (Fig. 40D, Ctr = 0.97±0.33, V = 1.08±0.25, VP = 0.55±0.13 vs PBS = 0.19±0.14 mm^2). These results suggest that scar formation is not determined by injection trauma, but rather by the presence of fibrin itself.

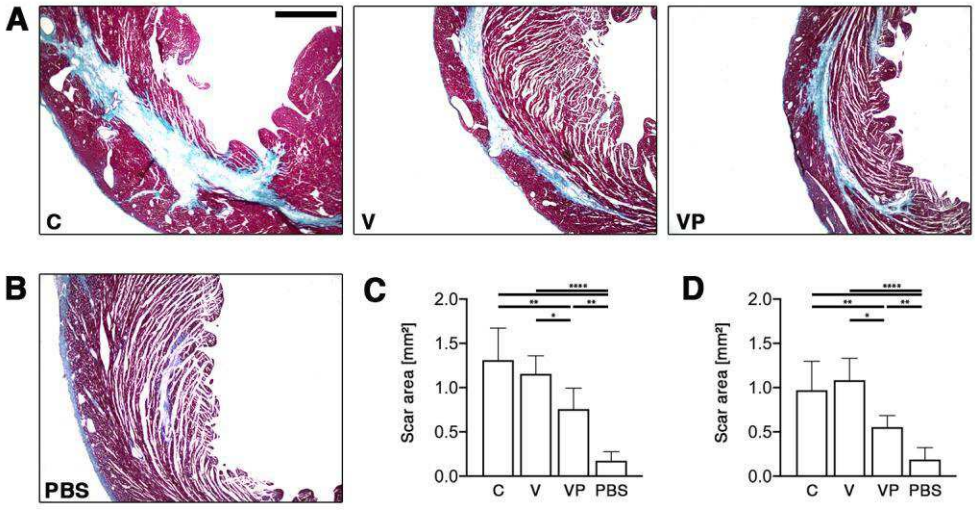

Figure 40. Presence of a fibrotic scar. **(A)** Fibrosis analysis on Masson Trichrome sections for all three treatment groups. **(B)** A negative control with phosphate-buffered saline (PBS) injection was added.). Size bar = 1 mm. Scar area was quantified at one **(C)** and four **(D)** weeks (n=6). * $P < 0.05$, ** $P < 0.01$, **** $P < 0.0001$.

The most prevalent cause of cardiac scarring is the sequelae of myocardial infarction. The early stages of scar formation after infarction comprise an inflammatory phase (up to 3 days), characterized by invasion of the damaged area by PDGF-Rα+ inflammatory fibroblasts, and a proliferative phase (until 7-14 days), during which activated fibroblasts up-regulate α-SMA expression, convert to myofibroblasts and start collagen deposition [154]. As shown in Fig. 41, a few hours after fibrin injection the hydrogel is essentially acellular and only rare macrophages can be seen to be the first cells infiltrating the hydrogels (Fig. 41A). Consistently with the evolution of post-infarction scar formation, fibrin hydrogels were progressively invaded by PDGF-Rα+ cardiac fibroblasts [155] over the first 5 days, which subsequently converted to α-SMA+ myofibroblasts [156] with a maximum frequency by 7 days after injection (Fig. 41B).

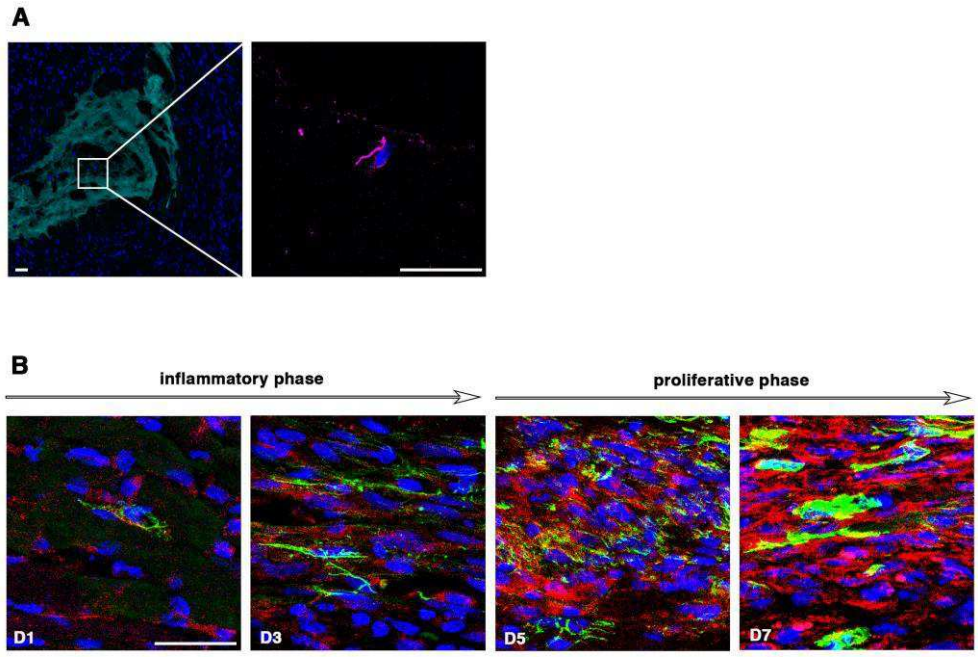

Figure 41. Cell population in the gel and in the injection site. (**A**) Immunofluorescence 3 hours after injection with 647-labeled fibrinogen (in cyan) and nuclei (DAPI, in blue) and at higher magnification for the specific ionized binding adaptor molecule IBA1 (in magenta). (**B**) Immunofluorescence for activated (αSMA in green) cardiac fibroblasts (PDGFRα in red), and during the first week at days 1,3,5,7 (D1, D3, D5, D7). Size bar = 30μm.

Scar formation is independent of adaptive immune response

Next, we sought to determine whether scar formation might be promoted by an immune response against the hydrogel components of human origin, i.e. fibrinogen and the cross-linking enzymes. Therefore, both empty and VEGF-decorated fibrin hydrogels were injected in the left ventricle myocardium of nu/nu nude rats, which lack T-lymphocytes and cannot mount an adaptive immune response, providing a tolerogenic environment to xenogenic cells and proteins. As a further control, hearts were implanted also with human adipose-derived mesenchymal cells (ASC) alone or over-expressing VEGF after genetic modification with a retroviral vector [89]. Quantification of sections stained with Masson Trichrome confirmed that both fibrin groups induced significantly larger scars than the cell groups, regardless of VEGF presence (Fig. 42A-B; Ctr gel = 1.85±0.50 and V gel = 1.61±0.40 mm^2 vs Ctr cells = 0.74±0.25 and V cells = 1.08±0.31 mm^2). Interestingly, immunofluorescence staining for endothelium (CD31) and smooth muscle cells (α-SMA) showed that cell-based VEGF expression could induce effective angiogenesis at the border of the injection area, as previously reported [89], in contrast with the VEGF-decorated fibrin hydrogels (Fig. 42C). These results show that fibrin-associated scar formation is independent of adaptive immune response and that it prevents VEGF-induced myocardial angiogenesis.

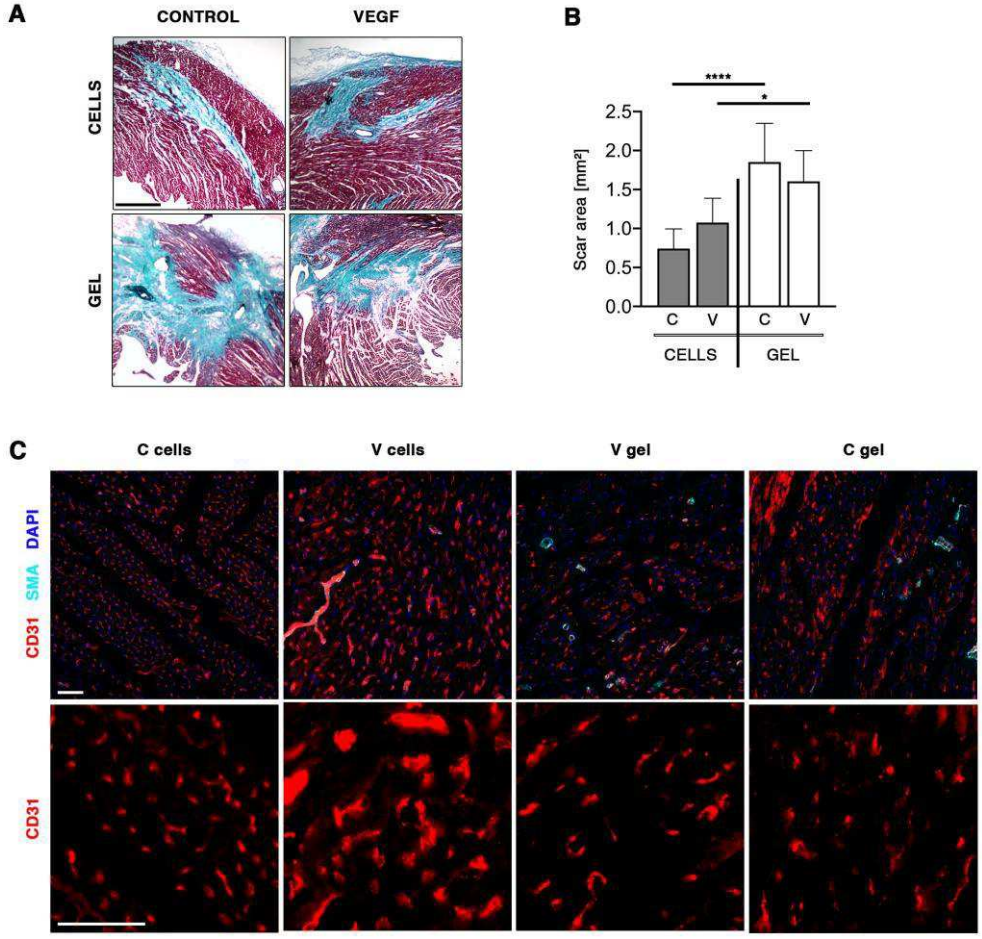

Figure 42. Effect of the gel on T-cell deficient animals with cell-based versus hydrogel-based delivery at four weeks. Adipose-derived mesenchymal stem cells alone (control cells) or transduced to express VEGF (VEGF cells), empty gel and/or loaded with VEGF. (**A**) Morphology of the scar in Masson Trichrome. (**B**) Scar area quantification at four weeks (n=6). Size bar = 1 mm. * $P < 0.05$, **** $P < 0.0001$. (**C**) Morphology of the angiogenesis in immunofluorescence staining for endothelium (CD 31, in red), for smooth muscle cells (SMA, in cyan) and nuclei (DAPI, in blue) and at higher magnification for CD31 only. Size bar = 50µm.

Scar formation is independent of hydrogel volume or mechanical stiffness

Lastly, we investigated whether scar formation may correlate with mechanical trauma to the tissue due to the presence of the solid hydrogel in the actively contracting myocardium. Therefore we evaluated the effects on scar formation of reducing mechanical disturbance to the tissue by changing the size or the stiffness (fibrinogen concentration) of the hydrogels: a) a 2.5-fold smaller volume (10 µl) without changing hydrogel composition (Vol); or b) a 10-fold lower concentration of fibrinogen (2.5 mg/ml) without changing injection volume (Fib). Quantification of tissue sections after 4 weeks showed that neither smaller nor softer hydrogels reduced the scar size compared to the control injections of 25 µl with a fibrinogen concentration of 25 mg/ml (Ctr = 0.79±0.28, Vol = 0.91±0.19, Fib = 0.93±0.23 mm^2, p=n.s.) (Fig. 43).

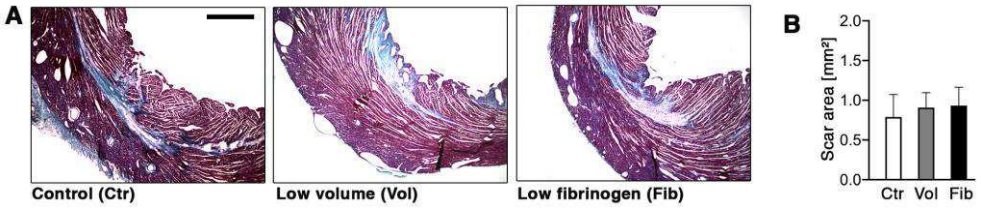

Figure 43. (**A**) Masson Trichrome after the injection of a reduced volume (Vol) of 10 µL and of a 10-fold reduced fibrinogen concentration of 2.5 mg/mL (Fib) compared to the control, (Ctr, injection of 25uL [Fibirnogen] of 25 mg/mL). Size bar = 1 mm. (**B**) Quantification of the scar area at 1 week (n=6).

Fibrin hydrogel persistence increases scar formation

Taken together, these data indicate that scar formation is induced exclusively by the presence of fibrin itself. Therefore, we sought to confirm this finding by the opposite approach and investigated whether prolonging fibrin persistence in the myocardium could increase scar size. First, we labelled the injected hydrogels with fluorescent fibrinogen in order to track its degradation kinetics in the myocardium. As shown in Fig. 44A, fibrin is clearly visible and it is rapidly degraded during the first few days after injection, until traces can still be found at day 5 and it is completely absent by day 7. Hydrogel duration was increased by incorporating 51 μg/ml of the fibrinolysis inhibitor aprotinin, which has been shown to slow fibrin degradation and prolong hydrogel persistence up to 4 weeks in skeletal muscle [107]. As shown in Fig. 44B-C, after three weeks aprotinin-containing hydrogels caused significantly larger scars than the fast-degrading controls (Ctr = 0.81±0.34 vs Apro = 1.81±0.56 mm^2, $p<0.01$).

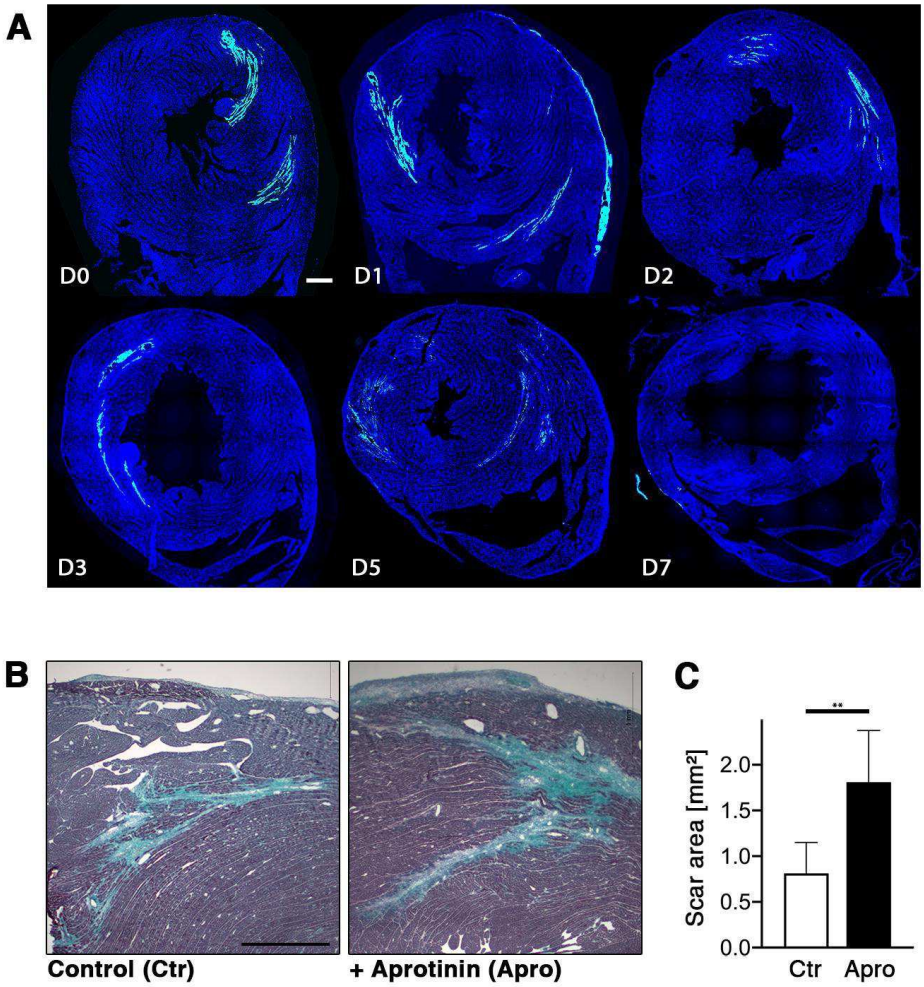

Figure 44. (**A**) Gel degradation for the first week in immunofluorescence with 647-labeld fibrinogen (in cyan) and nuclei (DAPI, in blue). Size bar = 1 mm. (**B**) Aprotinin (51 µg/mL) was added to the hydrogel and the maximal scar area (**C**) was assessed at 3 weeks (n=6). ** $P < 0.01$.

DISCUSSION

Fibrin is widely used in clinical surgery and provides an attractive platform for the controlled delivery of therapeutic factors, thanks to the development of protein engineering strategies that enable their crosslinking to fibrinogen by coagulation factor XIII and therefore the decoration of the resulting matrix with desired doses and combinations of factors [93]. Here we identified a serious side-effect of fibrin-based factor delivery to the myocardium, on one hand causing the formation of large fibrous scars similar to the sequelae of myocardial infarction, and on the other jeopardizing the therapeutic effect of delivered factors. Scar formation was not due to tissue damage associated with injection of the hydrogel, its mechanical stiffness or volume, nor to an immune reaction against the human components. Rather, the presence of fibrin *per se* was sufficient to kick-off the myocardial scarring response. Interestingly, the process appeared to be irreversible, since fibrin was degraded within 5 days in the myocardium, but the resulting scars persisted at least 4 weeks without showing signs of resolution.

The observed scar formation is not a universal property of fibrin, but rather a tissue-specific effect. In fact, the same fibrin-based platform was previously investigated to deliver controlled doses of TG-VEGF in both normal and ischemic skeletal muscle or to ischemic skin wounds in mice, and in both tissues it induced robust and functional angiogenesis without any sign of scar or fibrosis, restored blood flow and promoted healing [107]. Fibrin has been also extensively investigated as a delivery system for growth factors in wound healing, both exploiting its natural binding for a variety of therapeutic factors [99] and with different modifications to tailor factor release [157] and no skin fibrosis has been observed. Bladder smooth muscle has also been targeted with a bioactive fibrin-based bulking material to treat urinary incontinence, without any report of ensuing fibrosis [158].

Upon ischemia or other kinds of injury, cardiomyocyte death rapidly activates innate immune pathways that trigger cytokine, chemokine and adhesion molecule expression, initiating the inflammatory phase that subsequently evolves into fibrosis [159]. Taken together our results show that fibrin per se is capable of starting this inflammatory process. In fact, fibrous scars were induced also when fibrinogen concentration was reduced by 10-fold, which is in the range of a physiological blood clot [160]. The addition of VEGF alone did not reduce the scar. However, when PDGF-BB was added to VEGF, a positive trend toward a smaller scar was observed. This finding is compatible with the activation of the PGDF-Receptor β (PDGF-Rβ) signaling pathway in the perivascular and mononuclear cells that takes place after myocardial infarction [161]. Whereas PDGF-Rα signaling does not regulate vascular maturation, it promotes collagen deposition

[161]. On the contrary, the activation of PDGF-Rβ plays a crucial role in vascular maturation by regulating the recruitment of mural cells to growing microvessels, and its inhibition by a neutralizing antibody critically impaired vascular maturation in healing infarcts [162]. The role of PDGF-Rβ signaling in healing infarcts likely involves a paracrine interaction between endothelial cells that secrete PDGF-BB and mural cells like pericytes and smooth muscle cells that express the receptor [163].

Fibrous tissue accumulation relies on the balance between collagen synthesis and degradation. Collagen synthesis is primarily stimulated by Transforming Growth Factor-β (TGF-β), whereas matrix metallo-proteases are central to collagen degradation [154]. Myofibroblasts play a key role in fibrous tissue formation in the infarcted myocardium as they are not present in the normal and non-infarcted myocardium, but accumulate in the infarcted myocardium [156]. During cardiac remodeling, fibroblasts differentiate into myofibroblasts, which are fast-proliferating, α-smooth muscle cell actin (α-SMA)-positive cells with pronounced contractile and secretory properties [164]. After depositing collagen in the normal repair process myofibroblasts undergo apoptosis, but if this does not occur then their persistent activity causes excessive matrix accumulation and detrimental fibrosis [165]. Myofibroblasts can also be induced by TGF-β itself and lead to excessive matrix accumulation [45]. TGF-β plays therefore an important role in modulating fibroblast phenotype towards fibrosis gene expression, and in promoting extracellular matrix deposition in the infarct region [166].

Interestingly, fibrinogen has been recently found to trigger astrocyte scar formation in the central nervous system through TGF-β signaling [167]. Fibrinogen is one of the first blood proteins that leaks out of broken vessels immediately after injury and it acts as a multi-faceted signaling molecule by interacting with integrins and non-integrin receptors, as well as by functioning as a carrier of growth factors and regulator of their bioavailability [168]. In a murine model of traumatic injury to the brain cortex, genetic or pharmacologic depletion of fibrinogen prevented astrocytic scar formation, whereas the simple injection of fibrinogen into the cortex induced scarring even in the absence of trauma [167]. Mechanistically, fibrinogen-bound latent TGF-β was found to interact with local perivascular astrocytes, leading to active TGF-β formation, which induces reactive astrocytosis by regulating the TGF-β/Smad signaling pathway, resulting in scar formation[167]. Local provisional fibrin matrix thus functions as a primary astrocyte activation signal initiating scar formation in the CNS by regulating the bioavailability of active TGF-β at sites of vascular damage. Based on the function of fibrinogen to activate TGF-β signaling and to promote astrocytic gliosis in the central nervous system, it is tempting to speculate that a similar mechanism

might underlie the ability of fibrinogen to induce fibrotic scarring in the myocardium that we identified here.

Several lines of evidence suggest that a complex interaction involving TGF-β, Endothelin-1 (ET-1) and the renin-angiotensin-aldosterone system cause fibrogenesis [57]. Angiotensin-II (Ang-II) causes vasoconstriction and its circulating concentration is elevated in patients with fibrotic hearts [169]. In rats with myocardial fibrosis, Ang-II is both expressed and activated by macrophages and myofibroblasts [170]. In cardiac fibroblasts, Ang-II induces expression of collagen through TGF-β/Smad3 and extracellular signal–regulated kinase by an interleukin 6 (IL-6)–dependent mechanism. Angiotensin receptor inhibitors, such as losartan, are effective in reducing cardiac fibrosis in both animals and humans [57]. Losartan is believed to reduce cardiac fibrosis through the inhibition of the endothelial to mesenchymal transition, as was demonstrated in mitral valve endothelial cells, by acting to block the AngII-elicited, TGF-β–induced phosphorylation of ERK1/2 [171]. Losartan also reduces collagen I synthesis and fibroblast activation in response to stimulation by AngII [172]. Several other pathways are playing a role in activating TGF-β and are currently under investigation in clinical trials. As aldosterone promotes myocardial fibrosis [173], Spironolactone, a specific pharmacologic antagonist of aldosterone, seems to have an influence on serum markers of collagen metabolism and on other cardiovascular structures [174]. Pirfenidone, a broad anti-inflammatory drug, has an effect of blocking TGF-β and Ang-II–induced fibrosis by controlling the feedback loop between the Ang-II type 1 receptor, the phsoph-p38 mitogen-activated protein kinase pathway and the renin-angiotensin system, which provides its cardio-protective effect [175]. TGF-β and hypoxia are important stimuli for the expression of the collagen cross-linking enzyme lysil oxidase (LOX) in a number of cells and tissues, and its inhibition with beta-amino-propionitrile (BAPN) resulted in a significant reduction in both collagen cross-linking and content [176].

Future studies should investigate the loss of function of the TGF-β pathway to possibly overcome the scaring process and then eventually test the potential of both growth factors in ischemic conditions.

In conclusion intramyocardial delivery of growth factors by fibrin-based matrices poses significant risks of unwanted fibrosis. In order to overcome this issue, it will be important to identify the underlying molecular mechanism, especially investigating the role of TGF-β signaling.

ACKNOWLEDGMENTS

We gratefully acknowledge Ms. M. Ast-Dumbach and Mr. P. Thurion for their expertise in histology and their technical assistance with tissue staining. This work was supported in part by an intramural grant of the CHU UCL Namur (Mont Godinne Foundation) to L.M., as well as grants by the Swiss National Science Foundation (163202) and the European Union FP7 (ANGIOSCAFF, CP-IP 214402) to A.B.

CONFLICT OF INTEREST

None to declare.

DISCUSSION

I. LIMITATIONS

All the animals used in the above described studies were healthy at the time of entering experiments and therefore do not reflect other pathological factors and comorbidities that are commonly found in human patients.

Focus has been given to the effects on the heart. Other sub-phenomena could have occurred in other tissues by a possible systemic action of our different treatments with growth factors. Macroscopically the animals behave as always but no other tissue has been investigated in detail.

In ischemic tissue, maximum blood supply is limited by the degree of arterial obstruction, and the opening of collateral arteries (arteriogenesis) is required to restore physiological flow levels to meet the metabolic demands of regenerating tissue. The model of myocardial infarction that was used here sought to reproduce as much as possible the clinical situation of a chronic sequela of myocardial infarction by including 2-week latency period between the ligation of the coronary artery and the treatment (cell injection). Despite this, the model still might not reflect the exact pathophysiological changes that would develop in a slowly developing condition in humans, particularly in regard to the potential of arteriogenesis in ischemic tissues with already diseased arteries.

The models in the cardiac and skeletal muscle presented above are state-of-the-art in the field and both these limitations reflect common issues concerning animal models of disease or therapeutic intervention in general. Therefore, it is important to limit the conclusions of such pre-clinical work to the proof of principle on the investigated strategies, whereas therapeutic efficacy and safety need to be investigated in clinical studies, for which these results provide supportive evidence.

In both studies we deliberately chose to deliver syngenic rodent factors instead of the clinically used human homolog because the experiments were performed in a rat model. In fact, the Banfi group found previously that the dose-dependent effects of VEGF are species-specific, and this may specifically mask the toxic effects of high doses of the human factor. In fact, previous experiments showed that human $VEGF_{165}$ was significantly more effective in activating VEGF receptor signaling in human endothelial cells than rodent $VEGF_{164}$, while the opposite was true in rodent endothelial cells [177].

Specifically, for the fibrin gel experiments, some disparate effects were observed for similar concentration within the groups. It may be attributable to the elevated levels of inflammatory cells and proteases [107] caused for instance by the size of the triggered intra-myocardial infarction, which could in some animals accelerate gel degradation and thus the effective rate of growth factor release. This highlights the need to determine the therapeutic window of fibrin-bound growth factor delivery specifically for each envisioned clinical application.

II. GENERAL CONCLUSIONS

There is a significant need for therapeutic angiogenesis in the treatment of ischemic cardiac condition. Indeed, restoring the blood flow by coronary interventions is not suitable for all patients and certainly not sufficient as a definitive solution. In my eyes, therapeutic angiogenesis could become part of the arsenal of the modern cardiac surgeon and/or surgical cardiologist in the near future.

Cell-based therapies were identified as an elegant method to control the dose and distribution of the therapeutic gene while at the same time ensuring a sufficiently prolonged duration of expression. First, we set the basis and the proof of principle for ASC [84] in the normal myocardium [84, 89] in investigations preceding the work for this thesis.

In the first part of the thesis we aimed at testing the cell-based gene therapy strategy that we had previously developed in ischemic conditions after ligation of the LAD in a rodent model. We obtained functional evidence that controlled VEGF expression by transduced and FACS-purified ASC is safe and effective in inducing robust growth of uniformly normal blood vessels in the ischemic myocardium, preventing the loss of cardiac functionality and reducing heart fibrosis after myocardial infarction. Our findings demonstrate the therapeutic potential of controlling the distribution of VEGF expression levels in the ischemic myocardium. The outcome of preventing further decline in cardiac functionality and therefore avoiding progression towards heart failure was consistent with the histological correlate of limiting the extension of fibrotic scarring.

A serious limitation of this approach in view of a potential clinical translation is the use of retroviral vectors, which raise safety concerns due to the possible neoplastic transformation of transduced progenitors by insertional mutagenesis [150]. Such issue could be overcome by the use of clinically compliant new-generation integrating vectors, such as self-inactivating lentiviruses with chromatin insulator elements that ensure stable and sustained transgene expression in the absence of oncogenic potential [151]. Nevertheless, the degree of an in vitro progenitor expansion required to obtain clinically relevant numbers of transduced and purified cells in a practical challenge for the treatment of human subject, is shared by all cell-based gene therapy approaches for different pathologies.

In parallel, significant advances in the field of protein engineering, spearheaded among others by our long-standing collaborator, Professor Hubbell (University of Chicago), have revolutionized the possibilities offered by recombinant protein

delivery. His findings made it possible to crosslink therapeutic protein to fibrinogen by coagulation factor XIII and therefore the decoration of the resulting matrix with desired doses and combinations of factors, while protecting them from degradation [93].

In the second part of the thesis, we investigated the feasibility and potential of fibrin-based factor delivery for cardiac pro-angiogenic treatments. In fact, fibrin is already widely used in clinical surgery and provides an attractive platform for the controlled delivery of therapeutic factors. Further, the same approach yielded promising results for therapeutic angiogenesis in skeletal muscle. However, we unexpectedly have identified a serious side-effect of fibrin-based factor delivery to the myocardium, on one hand causing the formation of large fibrous scars similar to the sequelae of myocardial infarction, and on the other jeopardizing the therapeutic effect of the delivered factors. Scar formation was not due to tissue damage associated with injection of the hydrogel, its mechanical stiffness or volume, nor to an immune reaction against the human components, and we showed that the presence of fibrin per se was sufficient to kick-off a scarring response, resulting in harmful fibrosis.

It is important to underline that this study was conducted in the normal and healthy myocardium. The results show the importance of rigorous testing in normal tissue as a first step, before moving to pathological models, such as the rodent myocardial infarction model that had already been established in the first part of the thesis. In fact, the experiments in the normal myocardium allowed us to clearly identify this deleterious reaction to fibrin delivery in the absence of relevant confounding factors such as the inflammation and fibrosis that are caused by myocardial infarction.

Based on these results, the next efforts should be directed towards identifying the underlying mechanism of cardiac-specific fibrotic scarring by fibrin, e.g. involving the TGF-β signaling pathway in order to overcome this serious side-effect.

III. PERSPECTIVES

A. ALTERNATIVE DELIVERY METHODS

The clear promotion of fibrotic scarring by intramyocardial delivery of fibrin poses significant concerns for a clinical application. Nevertheless, fibrin matrices have a very desirable features for the safe and effective delivery of angiogenic factors, namely: a) the use of recombinant proteins rather than genetic vectors, avoiding the possibility of excessively prolonged expression; and b) the ability to precisely and homogenously control the delivered dose, preventing the formation of toxic hotspots of factor.

Many authors have claimed increased effect through different delivery pathways such as intracoronary injection/perfusion in an anterograde or retrograde manner, as well as through an endomyocardial approach. Although the route of delivery admittedly seems to play a role in modulating at least the mesenchymal cardiac cell therapy [149], no method is without pitfalls and has emerged as the one and only solution. Meta-analysis in Phase I/II clinical trials suggest that patients with recent AMI enrolled in cell therapy trials and receiving cell treatment by **intracoronary** delivery seem to profit most. But it seems that **intramyocardial** delivery of cell, either by surgical or percutaneous intervention, seems to be the preferred route of delivery for chronic heart failure (CHF). [178]. Therefore, future work should also investigate alternative strategies to avoid or prevent the fibrotic scarring associated with intramyocardial injection.

One such approach is to avoid injection altogether and apply the therapeutic factor-decorated fibrin matrix on the epicardium, for instance combined with a scaffold. In previous works [96, 97], we showed that the composition of a scaffold applied on the epicardium can impact the functional effect of the incorporated growth factors. We demonstrated how an egg white-derived material could lead to VEGF hotspots that favor the formation of angioma-like structures because of its significant biochemical affinity to VEGF.

Epicardial delivery might be a valid alternative since the epicardium is always easily accessible during cardiac surgery, for instance. Therefore, we have started to investigate the potential of epicardial delivery of growth factor-decorated fibrin matrices. In this approach fibrin is not allowed to gelify in suit as a 2-component liquid, but rather it is pre-formed as a gel of 100 µL in an 8-mm mold (Fig. 45). Various techniques to glue the gel to the epicardial surface have been tested, since the brittle consistency of the material does not allow its suturing. The best

approach has been found to fix the gel in place by overlaying it with a larger patch of Tachosil™ (Baxter Inc.), which is composed of human fibrinogen [5,5 mg /cm^2] and human thrombin [2,0 UI], thereby ensuring a similar composition to the factor-decorated hydrogel.

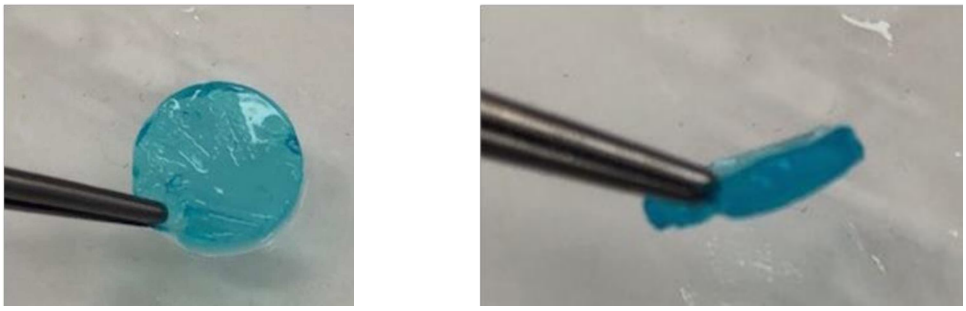

Figure 45. Preformed gel of 8 mm in diameter.

In order to analyze the effects on vascular growth, at the time of sacrifice animals were perfused through the descending aorta in a retrograde manner with μAngiofil™ (Funmedica Inc.) to fill the coronary circulation. This polymer solidifies inside the perfused vessels and allows imaging of the vessels down to 10 μm in diameter by a micro-Computed Tomography (μCT). Collaborative work has previously demonstrated an excellent correlation of the obtained μCT 3D reconstruction with standard histology observed under light microscopy [179].

Preliminary results obtained after 1 week show that fibrin matrices containing both growth factors (VEGF+PDGF-BB) induced more angiogenesis starting from the epicardium compared with the controls composed of empty fibrin or the Tachosil™ only (Fig. 46).

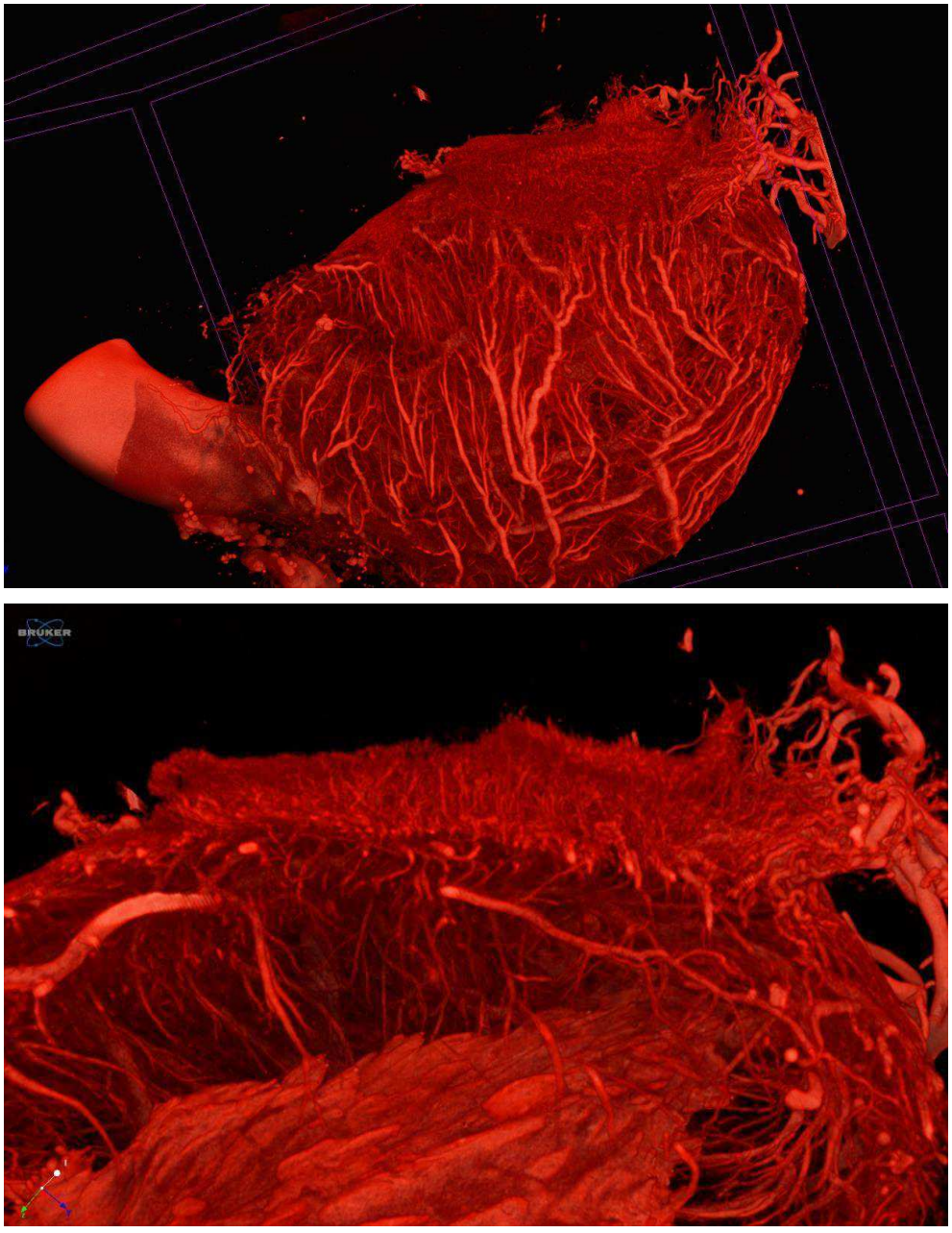

Figure 46. MicroCT analysis of an epicardial scaffold decorated with VEGF and PDGF after μAngiofil perfusion at 1 week.

B. NEW TARGETS TO CORRECT VEGF ISSUES

Moving away from protein delivery by fibrin matrices, adenoviral vectors also have desirable features for clinical delivery, including robust expression (efficacy) and transient duration (safety). However, these same features pose challenges for VEGF-based therapy, because: a) expression shorter than about 4 weeks is insufficient to stabilize normal newly induced vessels, leading to their regression after stimulus cessation, and thus jeopardizing efficacy and b) heterogeneous expression leads to hotspots of excessive dose and can cause angioma growth. Approaches to accelerate vascular stabilization and prevent aberrant angiogenesis associated with VEGF-expressing adenoviral vectors would be key to improve their safety and efficacy and exploit their attractive clinical features.

Recent work in the Banfi group aimed at elucidating novel molecular targets to overcome these issues in VEGF biology. Specifically, they found that: a) endothelial Semaphorin3A (Sema3A) is required for stabilization of VEGF-induced angiogenesis by recruiting a specific class of Neuropilin-1-expressing monocytes (NEM) and treatment with the recombinant protein Semaphorin3A (Sema3A-Fc) can ensure persistence of newly induced vessels despite transient adenoviral delivery of VEGF (Fig. 47) [180] and b) EphB4 signaling modulates the rate of endothelial proliferation rate by specific VEGF doses, independently of pericyte recruitment, and EphB4 stimulation by treatment with a recombinant EphrinB2-Fc protein prevents aberrant angiogenesis by uncontrolled and excessive VEGF doses, switching it to robust normal vascular growth (Fig. 48) [181].

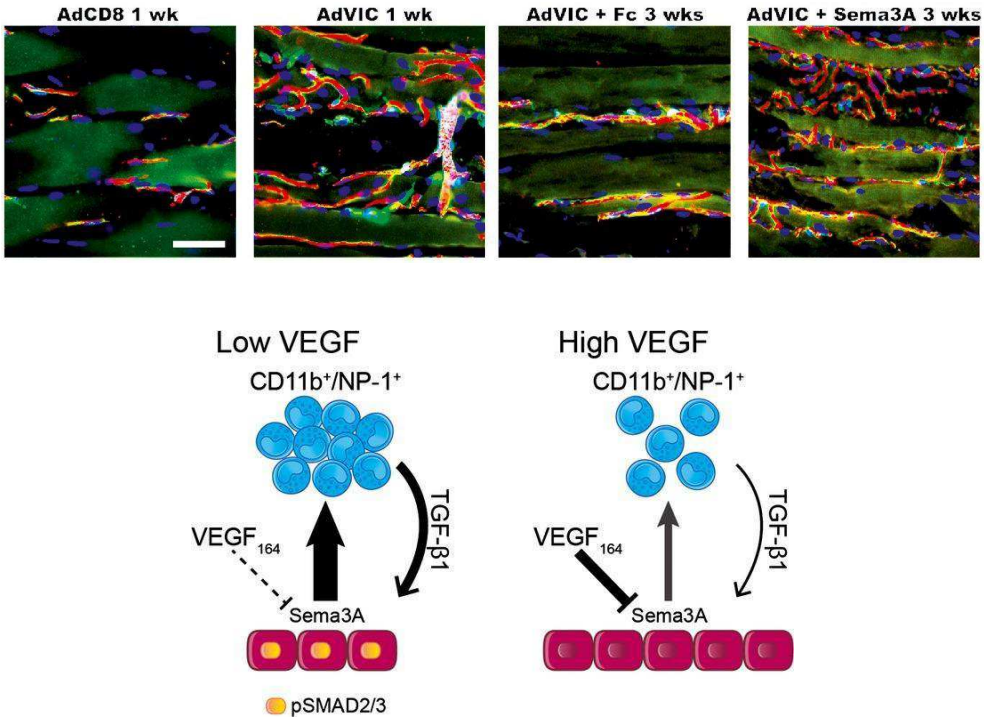

Figure 47. Above: Treatment with recombinant Sema3A rescues vascular stabilization impaired by high VEGF doses and prevents regression of newly induced angiogenesis after transient VEGF delivery by adenoviral vectors. Below: Working model for the VEGF-dose dependent regulation of vascular stabilization with Semaphorin3A (Sema3A), Neuropilin1-expressing monocytes (NEM) and TGF-β1 pathway.

From Groppa E et al., EMBO Mol Med 2015

In summary, investigations of the mechanisms underlying for the vascular stabilization showed that:

1. Sema3A is required for recruitment of NEM, which promote survival of endothelial cells independently of VEGFand the persistence of newly formed vessels by secreting TGF-β1 and activating endothelial SMAD2/3 signaling.
2. The stabilizing signals are amplified and maintained by a novel positive feedback loop, whereby TGF-β1, produced by Sema3A-recruited NEM, stimulates further Sema3A secretion by the endothelium.
3. Sema3A production in vivo requires TGF-β1, whereas VEGF directly and dose-dependently inhibits Sema3A expression by activated endothelium.

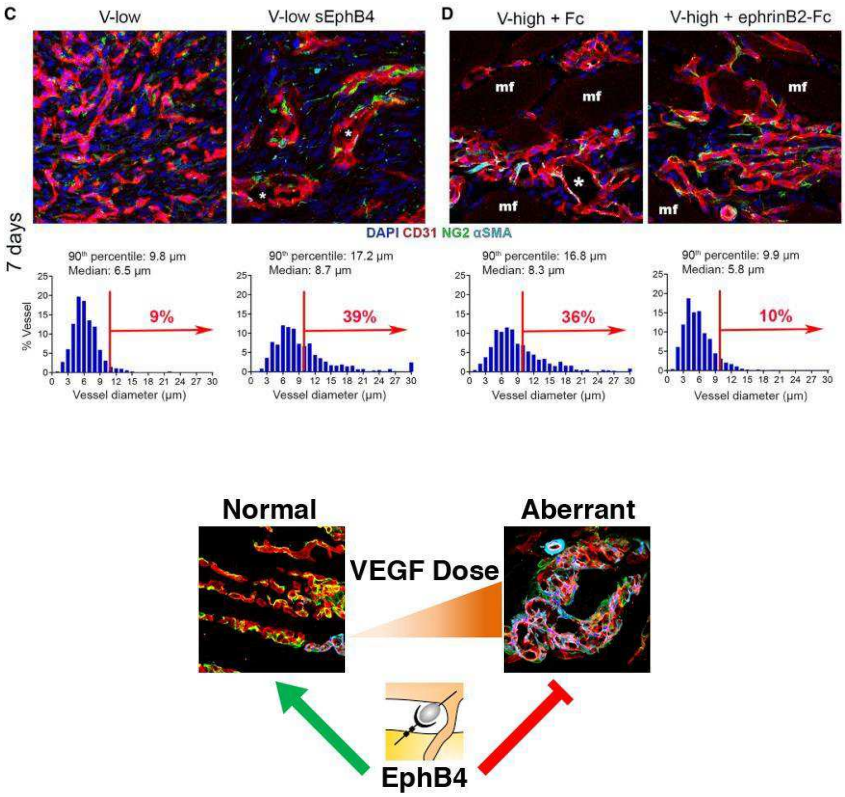

Figure 48. EphrinB2/EphB4 signalling between pericytes and endothelium regulates the switch from normal to aberrant angiogenesis caused by increasing VEGF doses. Above: By 7 days, after completion of the remodeling EphB4 inhibition normal angiogenesis by V-low to aberrant (C) and its stimulation converted aberrant structures form V-high to normal capillary networs (D). Red arrows and numbers indicate the fraction of vessel diameters < 10 um . * lumen f aberrant structures; mf, muscle fibers; scale bar, 25 um. Below: Schematic representation of the switch. *From Groppa E et al., EMBO Reports 2018*

In summary, investigations of the mechanisms underlying the switch between physiological and aberrant vascular growth showed that:

1. The endothelial tyrosine kinase receptor EphB4 finely tunes the degree of endothelial proliferation by specific VEGF doses in vivo.
2. EphB4 does not affect VEGF-R2 activation or internalization, but regulates its downstream signaling through p-ERK1/2.
3. EphB4 stimulation limits the size of circumferential vessel enlargement induced by VEGF, thereby enabling splitting into normal capillaries and preventing aberrant growth into angiomas.

Based on these findings, it can be envisioned to exploit treatments with recombinant Sema3A-Fc for a rapid stabilization of the newly formed vessel and with recombinant EphrinB2-Fc to ensure physiological angiogenesis regardless of VEGF dose control. This could be an elegant strategy to solve both the dose and duration issues of VEGF delivery. Practically, we could aim at translating these two biological concepts as pro-angiogenic strategies for the myocardium. First, the VEGF gene will be delivered by adenoviral vectors to normal hearts of immune-competent rats, while systemic Sema3A treatment will be evaluated to ensure long-term persistence of newly induced vascular networks despite rapid vector clearance by the immune system and transient VEGF expression. Secondly, systemic treatment with EphrinB2-Fc protein will be assessed to induce normalization of aberrant structures, thereby ensuring effective generation of normal microvascular networks despite uncontrolled levels of VEGF expression by adenoviral delivery. The final goal is to apply novel biological mechanisms to overcome existing issues of VEGF gene therapy and enabling its clinical application to myocardial ischemia.

IV. ACKNOWLEDGMENTS

A thesis is about science and fundamental research. But not only ... This journey allowed me to get to know wonderful people from many different horizons, to interact with them regularly over the years, to exchange ideas and knowledge in a privileged and stimulating environment. At the same time this experience taught me not to take anything for granted, but to go deeper and understand the motivation, the sense or the essence of each thought.

First of all, I would like to thank Pr Rondelet for having given me the opportunity to structure my research into a PhD thesis as I moved to Belgium. His support and his trust in my time management between quite a few travels back and forth was important to me. My colleagues from the hospital played an important role on a daily basis by agreeing to move some of the on-call shifts when needed for organizational purposes: Thank you Grégory, Philippe, Asmae and Aurélie, as well as our secretaries Dorothée and Viviane.

Research is teamwork, and this ambitious project would have never taken place without the active contribution of all my research colleagues in Basel. Andrea and Nunzia deserve a special thanks as they were always available for me while in Basel and over skype otherwise. Roberto, Andrea, Adelin cheered me up when needed and gave precious advice. Last, but not the least, Andrea, the guide, and friend over the last decade. He supported my ideas, my tight schedules, he encouraged me when failure was looking around. Without his expertise, his long and precise explanations, the work could not have been wrapped together as it is today. Thank you Andrea.

My first steps in basic research in 2010 were possible thanks to my first clinical and research mentors, Pr Eckstein and Pr Heberer, who believed in me and gave me the first opportunities to ally daily clinical work and protected time in the lab.

Various and numerous experiments were performed to come up with this thesis. Many collaborators were involved in this over-a-decade work. Each one of them deserves a personal acknowledgment. Anna, Laia, Giulia, Diana, Ema, Stefano and Gregory in Basel; Stéphane, Marie-Noëlle and Aurélien in Fribourg (CH); Ruslan and David as well as Brigitta and Pr Carrel in Berne; Hendrik in Zürich; Christian, Chu and Meinke in Freiburg (D); Claudia and Pascal in Godinne (B).

A special thanks goes to Jean-Luc, who offered me an opportunity to move to Belgium and travel around the world, connect with other peers interested in using and developing new technologies such as a robotic program in cardiac surgery.

Of course, sponsoring is mandatory in research. I would like to thank the “Fondation Mont-Godinne” for its financial support over the last years. I would also like to thank my accompanying committee and PhD Jury, Pr Poncelet, Pr Michaux, Pr Nollveaux, Pr Gourdin, Pr Gianello and particularly Pr Korpisalo and Pr Bonaros, the 2 external members, who virtually traveled across Europe in order to refine the last ideas of this project.

A very special thanks goes to all my friends who supported me and cheered me up over the years. As the journey took quite some time, they are too many for an exhaustive and accurate list. Each one of them, though, deserves my gratitude.

Last, the people who took care of me over the last 4 decades, I thank my whole family, especially my parents, who have given me the open-mindedness to grab every opportunity in life; my brother Nicolas, who means so much to me and our long business discussions, which gave my mind some scientific pauses for a while; and here, in my country of adoption, my reasons to be in Belgium, Delphine and Chloé, who were sharing my day-to-day evolution and particularly for their support and smiles during the redaction of the manuscript in a closed hearing during the confinement.

REFERENCES

1. Benjamin, E.J., et al., *Heart Disease and Stroke Statistics-2019 Update: A Report From the American Heart Association.* Circulation, 2019. **139**(10): p. e56-e528.

2. Taqueti, V.R. and M.F. Di Carli, *Coronary Microvascular Disease Pathogenic Mechanisms and Therapeutic Options: JACC State-of-the-Art Review.* J Am Coll Cardiol, 2018. **72**(21): p. 2625-2641.

3. Weiss, A.J. and A. Elixhauser, *Trends in Operating Room Procedures in U.S. Hospitals, 2001-2011: Statistical Brief #171*, in *Healthcare Cost and Utilization Project (HCUP) Statistical Briefs*. 2006: Rockville (MD).

4. Head, S.J., et al., *Current Practice of State-of-the-Art Surgical Coronary Revascularization.* Circulation, 2017. **136**(14): p. 1331-1345.

5. Melly, L., et al., *Fifty years of coronary artery bypass grafting.* J Thorac Dis, 2018. **10**(3): p. 1960-1967.

6. Gruntzig, A., *Transluminal dilatation of coronary-artery stenosis.* Lancet, 1978. **1**(8058): p. 263.

7. Sigwart, U., et al., *Intravascular stents to prevent occlusion and restenosis after transluminal angioplasty.* N Engl J Med, 1987. **316**(12): p. 701-6.

8. Simard, T., et al., *The evolution of coronary stents: a brief review.* Can J Cardiol, 2014. **30**(1): p. 35-45.

9. Annex, B.H., *Therapeutic angiogenesis for critical limb ischaemia.* Nat Rev Cardiol, 2013. **10**(7): p. 387-96.

10. Pries, A.R., et al., *The shunt problem: control of functional shunting in normal and tumour vasculature.* Nat Rev Cancer, 2010. **10**(8): p. 587-93.

11. Rissanen, T.T., et al., *Blood flow remodels growing vasculature during vascular endothelial growth factor gene therapy and determines between capillary arterialization and sprouting angiogenesis.* Circulation, 2005. **112**(25): p. 3937-46.

12. Giacca, M. and S. Zacchigna, *VEGF gene therapy: therapeutic angiogenesis in the clinic and beyond.* Gene Ther, 2012. **19**(6): p. 622-9.

13. Melly, L., et al., *Cell and gene therapy approaches for cardiac vascularization.* Cells, 2012. **1**(4): p. 961-75.

14. Gianni-Barrera, R., et al., *Therapeutic vascularization in regenerative medicine: Concise Review.* Stem Cells Transl Med, 2020.

15. Holmes, D.I. and I. Zachary, *The vascular endothelial growth factor (VEGF) family: angiogenic factors in health and disease.* Genome Biol, 2005. **6**(2): p. 209.

16. Parker, M.W., et al., *Structural basis for VEGF-C binding to neuropilin-2 and sequestration by a soluble splice form.* Structure, 2015. **23**(4): p. 677-87.

17. Ferrara, N., *Binding to the extracellular matrix and proteolytic processing: two key mechanisms regulating vascular endothelial growth factor action.* Mol Biol Cell, 2010. **21**(5): p. 687-90.

18. Ferrara, N., et al., *Heterozygous embryonic lethality induced by targeted inactivation of the VEGF gene.* Nature, 1996. **380**(6573): p. 439-42.

19. Haigh, J.J., et al., *Conditional inactivation of VEGF-A in areas of collagen2a1 expression results in embryonic lethality in the heterozygous state.* Development, 2000. **127**(7): p. 1445-53.

20. Mitsos, S., et al., *Therapeutic angiogenesis for myocardial ischemia revisited: basic biological concepts and focus on latest clinical trials.* Angiogenesis, 2012. **15**(1): p. 1-22.

21. Gerhardt, H., et al., *VEGF guides angiogenic sprouting utilizing endothelial tip cell filopodia.* The Journal of cell biology, 2003. **161**(6): p. 1163-77.

22. Hellstrom, M., et al., *Dll4 signalling through Notch1 regulates formation of tip cells during angiogenesis.* Nature, 2007. **445**(7129): p. 776-80.

23. Li, X., et al., *Reevaluation of the role of VEGF-B suggests a restricted role in the revascularization of the ischemic myocardium.* Arterioscler Thromb Vasc Biol, 2008. **28**(9): p. 1614-20.

24. Lahteenvuo, J.E., et al., *Vascular endothelial growth factor-B induces myocardium-specific angiogenesis and arteriogenesis via vascular endothelial growth factor receptor-1- and neuropilin receptor-1-dependent mechanisms.* Circulation, 2009. **119**(6): p. 845-56.

25. Karpanen, T., et al., *Overexpression of vascular endothelial growth factor-B in mouse heart alters cardiac lipid metabolism and induces myocardial hypertrophy.* Circ Res, 2008. **103**(9): p. 1018-26.

26. Zentilin, L., et al., *Cardiomyocyte VEGFR-1 activation by VEGF-B induces compensatory hypertrophy and preserves cardiac function after myocardial infarction.* FASEB J, 2010. **24**(5): p. 1467-78.

27. Park, J.E., G.A. Keller, and N. Ferrara, *The vascular endothelial growth factor (VEGF) isoforms: differential deposition into the subepithelial extracellular matrix and bioactivity of extracellular matrix-bound VEGF.* Mol Biol Cell, 1993. **4**(12): p. 1317-26.

28. Gianni-Barrera, R., et al., *Split for the cure: VEGF, PDGF-BB and intussusception in therapeutic angiogenesis.* Biochem Soc Trans, 2014. **42**(6): p. 1637-42.

29. Patan, S., *TIE1 and TIE2 receptor tyrosine kinases inversely regulate embryonic angiogenesis by the mechanism of intussusceptive microvascular growth.* Microvasc Res, 1998. **56**(1): p. 1-21.

30. Egginton, S., et al., *Unorthodox angiogenesis in skeletal muscle.* Cardiovasc Res, 2001. **49**(3): p. 634-46.

31. Gianni-Barrera, R., et al., *VEGF over-expression in skeletal muscle induces angiogenesis by intussusception rather than sprouting.* Angiogenesis, 2013. **16**(1): p. 123-36.

32. Al Haj Zen, A., et al., *Inhibition of delta-like-4-mediated signaling impairs reparative angiogenesis after ischemia.* Circ Res, 2010. **107**(2): p. 283-93.

33. Makanya, A.N., R. Hlushchuk, and V.G. Djonov, *Intussusceptive angiogenesis and its role in vascular morphogenesis, patterning, and remodeling.* Angiogenesis, 2009. **12**(2): p. 113-23.

34. Egginton, S., *Invited review: activity-induced angiogenesis.* Pflugers Arch, 2009. **457**(5): p. 963-77.

35. Sadiq, M.A., et al., *Platelet derived growth factor inhibitors: A potential therapeutic approach for ocular neovascularization.* Saudi J Ophthalmol, 2015. **29**(4): p. 287-91.

36. Uutela, M., et al., *PDGF-D induces macrophage recruitment, increased interstitial pressure, and blood vessel maturation during angiogenesis.* Blood, 2004. **104**(10): p. 3198-204.

37. Rhee, S. and F. Grinnell, *P21-activated kinase 1: convergence point in PDGF- and LPA-stimulated collagen matrix contraction by human fibroblasts.* J Cell Biol, 2006. **172**(3): p. 423-32.

38. Dor, Y., et al., *Conditional switching of VEGF provides new insights into adult neovascularization and pro-angiogenic therapy.* EMBO J, 2002. **21**(8): p. 1939-47.

39. Lee, R.J., et al., *VEGF gene delivery to myocardium: deleterious effects of unregulated expression.* Circulation, 2000. **102**(8): p. 898-901.

40. Schwarz, E.R., et al., *Evaluation of the effects of intramyocardial injection of DNA expressing vascular endothelial growth factor (VEGF) in a myocardial infarction model in the rat--angiogenesis and angioma formation.* J Am Coll Cardiol, 2000. **35**(5): p. 1323-30.

41. Banfi, A., et al., *Therapeutic angiogenesis due to balanced single-vector delivery of VEGF and PDGF-BB.* FASEB J, 2012. **26**(6): p. 2486-97.

42. Talman, V. and H. Ruskoaho, *Cardiac fibrosis in myocardial infarction-from repair and remodeling to regeneration.* Cell and tissue research, 2016. **365**(3): p. 563-81.

43. Frangogiannis, N.G., *The inflammatory response in myocardial injury, repair, and remodelling.* Nat Rev Cardiol, 2014. **11**(5): p. 255-65.

44. Shinde, A.V. and N.G. Frangogiannis, *Fibroblasts in myocardial infarction: a role in inflammation and repair.* J Mol Cell Cardiol, 2014. **70**: p. 74-82.

45. van den Borne, S.W., et al., *Myocardial remodeling after infarction: the role of myofibroblasts.* Nat Rev Cardiol, 2010. **7**(1): p. 30-7.

46. Jaffer, F.A., et al., *Molecular imaging of myocardial infarction.* J Mol Cell Cardiol, 2006. **41**(6): p. 921-33.

47. Deb, A. and E. Ubil, *Cardiac fibroblast in development and wound healing.* J Mol Cell Cardiol, 2014. **70**: p. 47-55.

48. Willems, I.E., et al., *The alpha-smooth muscle actin-positive cells in healing human myocardial scars.* Am J Pathol, 1994. **145**(4): p. 868-75.

49. Heineke, J. and J.D. Molkentin, *Regulation of cardiac hypertrophy by intracellular signalling pathways.* Nat Rev Mol Cell Biol, 2006. **7**(8): p. 589-600.

50. Weber, K.T., et al., *Myofibroblast-mediated mechanisms of pathological remodelling of the heart.* Nat Rev Cardiol, 2013. **10**(1): p. 15-26.

51. Dai, Z., et al., *Coronary perivascular fibrosis is associated with impairment of coronary blood flow in patients with non-ischemic heart failure.* J Cardiol, 2012. **60**(5): p. 416-21.

52. Leask, A., *Potential therapeutic targets for cardiac fibrosis: TGFbeta, angiotensin, endothelin, CCN2, and PDGF, partners in fibroblast activation.* Circ Res, 2010. **106**(11): p. 1675-80.

53. Campbell, S.E. and L.C. Katwa, *Angiotensin II stimulated expression of transforming growth factor-beta1 in cardiac fibroblasts and myofibroblasts.* J Mol Cell Cardiol, 1997. **29**(7): p. 1947-58.

54. Frantz, S., et al., *Transforming growth factor beta inhibition increases mortality and left ventricular dilatation after myocardial infarction.* Basic Res Cardiol, 2008. **103**(5): p. 485-92.

55. De Mello, W.C. and P. Specht, *Chronic blockade of angiotensin II AT1-receptors increased cell-to-cell communication, reduced fibrosis and improved impulse propagation in the failing heart.* J Renin Angiotensin Aldosterone Syst, 2006. **7**(4): p. 201-5.

56. Shibasaki, Y., et al., *Impact of the angiotensin II receptor antagonist, losartan, on myocardial fibrosis in patients with end-stage renal disease: assessment by ultrasonic integrated backscatter and biochemical markers.* Hypertens Res, 2005. **28**(10): p. 787-95.

57. Leask, A., *Getting to the heart of the matter: new insights into cardiac fibrosis.* Circ Res, 2015. **116**(7): p. 1269-76.

58. Lijnen, P. and V. Petrov, *Induction of cardiac fibrosis by aldosterone.* J Mol Cell Cardiol, 2000. **32**(6): p. 865-79.

59. Campbell, S.E., A.A. Diaz-Arias, and K.T. Weber, *Fibrosis of the human heart and systemic organs in adrenal adenoma.* Blood Press, 1992. **1**(3): p. 149-56.

60. Ramires, F.J., et al., *Aldosterone antagonism in an inflammatory state: evidence for myocardial protection.* J Renin Angiotensin Aldosterone Syst, 2006. **7**(3): p. 162-7.

61. Ponikowski, P., et al., *2016 ESC Guidelines for the diagnosis and treatment of acute and chronic heart failure: The Task Force for the diagnosis and treatment of acute and chronic heart failure of the European Society of Cardiology (ESC). Developed with the special contribution of the Heart Failure Association (HFA) of the ESC.* Eur J Heart Fail, 2016. **18**(8): p. 891-975.

62. Ptaszek, L.M., et al., *Towards regenerative therapy for cardiac disease.* Lancet, 2012. **379**(9819): p. 933-942.

63. Cashman, T.J., V. Gouon-Evans, and K.D. Costa, *Mesenchymal stem cells for cardiac therapy: practical challenges and potential mechanisms.* Stem Cell Rev Rep, 2013. **9**(3): p. 254-65.

64. Bonaros, N., et al., *Combined transplantation of skeletal myoblasts and angiopoietic progenitor cells reduces infarct size and apoptosis and improves cardiac function in chronic ischemic heart failure.* J Thorac Cardiovasc Surg, 2006. **132**(6): p. 1321-8.

65. Botta, R., et al., *Heart infarct in NOD-SCID mice: therapeutic vasculogenesis by transplantation of human CD34+ cells and low dose CD34+KDR+ cells.* FASEB J, 2004. **18**(12): p. 1392-4.

66. Kocher, A.A., et al., *Neovascularization of ischemic myocardium by human bone-marrow-derived angioblasts prevents cardiomyocyte apoptosis, reduces remodeling and improves cardiac function.* Nature medicine, 2001. **7**(4): p. 430-6.

67. Bartunek, J., et al., *Intracoronary injection of CD133-positive enriched bone marrow progenitor cells promotes cardiac recovery after recent myocardial infarction: feasibility and safety.* Circulation, 2005. **112**(9 Suppl): p. I178-83.

68. Stamm, C., et al., *Autologous bone-marrow stem-cell transplantation for myocardial regeneration.* Lancet, 2003. **361**(9351): p. 45-6.

69. Choi, Y.H., A. Kurtz, and C. Stamm, *Mesenchymal stem cells for cardiac cell therapy.* Hum Gene Ther, 2011. **22**(1): p. 3-17.

70. Asahara, T., A. Kawamoto, and H. Masuda, *Concise review: Circulating endothelial progenitor cells for vascular medicine.* Stem Cells, 2011. **29**(11): p. 1650-5.

71. da Silva Meirelles, L., A.I. Caplan, and N.B. Nardi, *In search of the in vivo identity of mesenchymal stem cells.* Stem Cells, 2008. **26**(9): p. 2287-99.

72. Li, Z., et al., *Paracrine role for mesenchymal stem cells in acute myocardial infarction.* Biol Pharm Bull, 2009. **32**(8): p. 1343-6.

73. Poncelet, A.J., et al., *Intracardiac allogeneic mesenchymal stem cell transplantation elicits neo-angiogenesis in a fully immunocompetent ischaemic swine model.* Eur J Cardiothorac Surg, 2010. **38**(6): p. 781-7.

74. Bonaros, N., et al., *Neoangiogenesis after combined transplantation of skeletal myoblasts and angiopoietic progenitors leads to increased cell engraftment and lower apoptosis rates in ischemic heart failure.* Interact Cardiovasc Thorac Surg, 2008. **7**(2): p. 249-55.

75. Rissanen, T.T. and S. Yla-Herttuala, *Current status of cardiovascular gene therapy.* Mol Ther, 2007. **15**(7): p. 1233-47.

76. Omata, D., et al., *Nonviral gene delivery systems by the combination of bubble liposomes and ultrasound.* Adv Genet, 2015. **89**: p. 25-48.

77. Wu, Z., A. Asokan, and R.J. Samulski, *Adeno-associated virus serotypes: vector toolkit for human gene therapy.* Mol Ther, 2006. **14**(3): p. 316-27.

78. Pacak, C.A. and B.J. Byrne, *AAV vectors for cardiac gene transfer: experimental tools and clinical opportunities.* Mol Ther, 2011. **19**(9): p. 1582-90.

79. Korpisalo, P. and S. Yla-Herttuala, *Stimulation of functional vessel growth by gene therapy.* Integr Biol (Camb), 2010. **2**(2-3): p. 102-12.

80. Korpisalo, P., et al., *Vascular endothelial growth factor-A and platelet-derived growth factor-B combination gene therapy prolongs angiogenic effects via recruitment of interstitial mononuclear cells and paracrine effects rather than improved pericyte coverage of angiogenic vessels.* Circ Res, 2008. **103**(10): p. 1092-9.

81. Misteli, H., et al., *High-throughput flow cytometry purification of transduced progenitors expressing defined levels of vascular endothelial growth factor induces controlled angiogenesis in vivo.* Stem Cells, 2010. **28**(3): p. 611-9.

82. Wolff, T., et al., *FACS-purified myoblasts producing controlled VEGF levels induce safe and stable angiogenesis in chronic hind limb ischemia.* Journal of cellular and molecular medicine, 2012. **16**(1): p. 107-17.

83. Menasche, P., *Skeletal myoblasts and cardiac repair.* J Mol Cell Cardiol, 2008. **45**(4): p. 545-53.

84. Helmrich, U., et al., *Generation of human adult mesenchymal stromal/stem cells expressing defined xenogenic vascular endothelial growth factor levels by optimized transduction and flow cytometry purification.* Tissue engineering. Part C, Methods, 2012. **18**(4): p. 283-92.

85. Zuk, P.A., et al., *Human adipose tissue is a source of multipotent stem cells.* Mol Biol Cell, 2002. **13**(12): p. 4279-95.

86. Planat-Benard, V., et al., *Spontaneous cardiomyocyte differentiation from adipose tissue stroma cells.* Circ Res, 2004. **94**(2): p. 223-9.

87. Jumabay, M., et al., *Spontaneously beating cardiomyocytes derived from white mature adipocytes.* Cardiovasc Res, 2010. **85**(1): p. 17-27.

88. Sanchez, P.L., et al., *Cultured and freshly isolated adipose tissue-derived cells: fat years for cardiac stem cell therapy.* Eur Heart J, 2010. **31**(4): p. 394-7.

89. Melly, L.F., et al., *Controlled angiogenesis in the heart by cell-based expression of specific vascular endothelial growth factor levels.* Hum Gene Ther Methods, 2012. **23**(5): p. 346-56.

90. Bai, X. and E. Alt, *Myocardial regeneration potential of adipose tissue-derived stem cells.* Biochem Biophys Res Commun, 2010. **401**(3): p. 321-6.

91. Ozawa, C.R., et al., *Microenvironmental VEGF concentration, not total dose, determines a threshold between normal and aberrant angiogenesis.* J Clin Invest, 2004. **113**(4): p. 516-27.

92. Meirelles Lda, S., et al., *Mechanisms involved in the therapeutic properties of mesenchymal stem cells.* Cytokine & growth factor reviews, 2009. **20**(5-6): p. 419-27.

93. Martino, M.M., et al., *Extracellular matrix and growth factor engineering for controlled angiogenesis in regenerative medicine.* Front Bioeng Biotechnol, 2015. **3**: p. 45.

94. Awada, H.K., et al., *A single injection of protein-loaded coacervate-gel significantly improves cardiac function post infarction.* Biomaterials, 2017. **125**: p. 65-80.

95. Tang, J., et al., *A Regenerative Cardiac Patch Formed by Spray Painting of Biomaterials onto the Heart.* Tissue Eng Part C Methods, 2017. **23**(3): p. 146-155.

96. Boccardo, S., et al., *Engineered mesenchymal cell-based patches as controlled VEGF delivery systems to induce extrinsic angiogenesis.* Acta Biomater, 2016. **42**: p. 127-135.

97. Gaudiello, E., et al., *Scaffold Composition Determines the Angiogenic Outcome of Cell-Based Vascular Endothelial Growth Factor Expression by Modulating Its Microenvironmental Distribution.* Adv Healthc Mater, 2017. **6**(24).

98. Lee, K.Y., et al., *Controlled growth factor release from synthetic extracellular matrices.* Nature, 2000. **408**(6815): p. 998-1000.

99. Martino, M.M., et al., *Heparin-binding domain of fibrin(ogen) binds growth factors and promotes tissue repair when incorporated within a synthetic matrix.* Proc Natl Acad Sci U S A, 2013. **110**(12): p. 4563-8.

100. Johnson, T.D., R.L. Braden, and K.L. Christman, *Injectable ECM scaffolds for cardiac repair.* Methods Mol Biol, 2014. **1181**: p. 109-20.

101. Breen, A., T. O'Brien, and A. Pandit, *Fibrin as a delivery system for therapeutic drugs and biomolecules.* Tissue Eng Part B Rev, 2009. **15**(2): p. 201-14.

102. Bao, P., et al., *The role of vascular endothelial growth factor in wound healing.* J Surg Res, 2009. **153**(2): p. 347-58.

103. Zisch, A.H., et al., *Covalently conjugated VEGF--fibrin matrices for endothelialization.* J Control Release, 2001. **72**(1-3): p. 101-13.

104. Ehrbar, M., et al., *Cell-demanded liberation of VEGF121 from fibrin implants induces local and controlled blood vessel growth.* Circ Res, 2004. **94**(8): p. 1124-32.

105. Ehrbar, M., et al., *The role of actively released fibrin-conjugated VEGF for VEGF receptor 2 gene activation and the enhancement of angiogenesis.* Biomaterials, 2008. **29**(11): p. 1720-9.

106. Lorentz, K.M., et al., *Engineered aprotinin for improved stability of fibrin biomaterials.* Biomaterials, 2011. **32**(2): p. 430-8.

107. Sacchi, V., et al., *Long-lasting fibrin matrices ensure stable and functional angiogenesis by highly tunable, sustained delivery of recombinant VEGF164.* Proc Natl Acad Sci U S A, 2014. **111**(19): p. 6952-7.

108. Martino, M.M., et al., *Growth factors engineered for super-affinity to the extracellular matrix enhance tissue healing.* Science, 2014. **343**(6173): p. 885-8.

109. von Degenfeld, G., et al., *Microenvironmental VEGF distribution is critical for stable and functional vessel growth in ischemia.* FASEB J, 2006. **20**(14): p. 2657-9.

110. Greenberg, J.I., et al., *A role for VEGF as a negative regulator of pericyte function and vessel maturation.* Nature, 2008. **456**(7223): p. 809-13.

111. Zhang, H., et al., *Blood vessel repair and regeneration in the ischaemic heart.* Open heart, 2014. **1**(1): p. e000016.

112. Carmeliet, P. and R.K. Jain, *Molecular mechanisms and clinical applications of angiogenesis.* Nature, 2011. **473**(7347): p. 298-307.

113. Yla-Herttuala, S., et al., *Angiogenic gene therapy in cardiovascular diseases: dream or vision?* European heart journal, 2017. **38**(18): p. 1365-1371.

114. Banfi, A., G. von Degenfeld, and H.M. Blau, *Critical role of microenvironmental factors in angiogenesis.* Current atherosclerosis reports, 2005. **7**(3): p. 227-34.

115. Menasche, P., *Stem cell therapy for heart failure: are arrhythmias a real safety concern?* Circulation, 2009. **119**(20): p. 2735-40.

116. Hong, S.J., D.O. Traktuev, and K.L. March, *Therapeutic potential of adipose-derived stem cells in vascular growth and tissue repair.* Current opinion in organ transplantation, 2010. **15**(1): p. 86-91.

117. Choi, Y.S., et al., *Differentiation of human adipose-derived stem cells into beating cardiomyocytes.* Journal of cellular and molecular medicine, 2010. **14**(4): p. 878-89.

118. Rasmussen, J.G., et al., *Comparison of human adipose-derived stem cells and bone marrow-derived stem cells in a myocardial infarction model.* Cell transplantation, 2014. **23**(2): p. 195-206.

119. Ishida, O., et al., *Adipose-derived stem cell sheet transplantation therapy in a porcine model of chronic heart failure.* Translational research : the journal of laboratory and clinical medicine, 2015. **165**(5): p. 631-9.

120. Gautam, M., et al., *Transplantation of adipose tissue-derived stem cells improves cardiac contractile function and electrical stability in a rat myocardial infarction model.* Journal of molecular and cellular cardiology, 2015. **81**: p. 139-49.

121. Le, K.N., et al., *Vascular regeneration by local growth factor release is self-limited by microvascular clearance.* Circulation, 2009. **119**(22): p. 2928-35.

122. Ferrara, N., *VEGF-A: a critical regulator of blood vessel growth.* Eur Cytokine Netw, 2009. **20**(4): p. 158-63.

123. Schwarz, E.R., et al., *Evaluation of the effects of intramyocardial injection of DNA expressing vascular endothelial growth factor (VEGF) in a myocardial infarction model in the rat--angiogenesis and angioma formation.* Journal of the American College of Cardiology, 2000. **35**(5): p. 1323-30.

124. Melly, L.F., et al., *Controlled angiogenesis in the heart by cell-based expression of specific vascular endothelial growth factor levels.* Human gene therapy methods, 2012. **23**(5): p. 346-56.

125. Scherberich, A., et al., *Three-dimensional perfusion culture of human adipose tissue-derived endothelial and osteoblastic progenitors generates osteogenic constructs with intrinsic vascularization capacity.* Stem cells, 2007. **25**(7): p. 1823-9.

126. Frobert, A., et al., *Cell-based therapy for heart failure in rat: double thoracotomy for myocardial infarction and epicardial implantation of cells and biomatrix.* Journal of visualized experiments : JoVE, 2014(91): p. 51390.

127. Banfi, A., et al., *Therapeutic angiogenesis due to balanced single-vector delivery of VEGF and PDGF-BB.* FASEB journal : official publication of the Federation of American Societies for Experimental Biology, 2012. **26**(6): p. 2486-97.

128. Sepantafar, M., et al., *Stem cells and injectable hydrogels: Synergistic therapeutics in myocardial repair.* Biotechnology advances, 2016. **34**(4): p. 362-379.

129. Roger, V.L., et al., *Heart disease and stroke statistics--2011 update: a report from the American Heart Association.* Circulation, 2011. **123**(4): p. e18-e209.

130. Carmeliet, P., *Angiogenesis in health and disease.* Nature medicine, 2003. **9**(6): p. 653-60.

131. Gupta, R., J. Tongers, and D.W. Losordo, *Human studies of angiogenic gene therapy.* Circulation research, 2009. **105**(8): p. 724-36.

132. Scimia, M.C., A.M. Gumpert, and W.J. Koch, *Cardiovascular gene therapy for myocardial infarction.* Expert opinion on biological therapy, 2014. **14**(2): p. 183-95.

133. Boden, J., et al., *Vascular Regeneration in Ischemic Hindlimb by Adeno-Associated Virus Expressing Conditionally Silenced Vascular Endothelial Growth Factor.* Journal of the American Heart Association, 2016. **5**(6).

134. Johnson, K.E. and T.A. Wilgus, *Vascular Endothelial Growth Factor and Angiogenesis in the Regulation of Cutaneous Wound Repair.* Advances in wound care, 2014. **3**(10): p. 647-661.

135. Springer, M.L., et al., *VEGF gene delivery to muscle: potential role for vasculogenesis in adults.* Molecular cell, 1998. **2**(5): p. 549-58.

136. Park, J.E., G.A. Keller, and N. Ferrara, *The vascular endothelial growth factor (VEGF) isoforms: differential deposition into the subepithelial extracellular matrix and bioactivity of extracellular matrix-bound VEGF.* Molecular biology of the cell, 1993. **4**(12): p. 1317-26.

137. Zacchigna, S., et al., *In vivo imaging shows abnormal function of vascular endothelial growth factor-induced vasculature.* Human gene therapy, 2007. **18**(6): p. 515-24.

138. Gogiraju, R., et al., *Endothelial p53 deletion improves angiogenesis and prevents cardiac fibrosis and heart failure induced by pressure overload in mice.* Journal of the American Heart Association, 2015. **4**(2).

139. Giordano, F.J., et al., *A cardiac myocyte vascular endothelial growth factor paracrine pathway is required to maintain cardiac function.* Proceedings of the National Academy of Sciences of the United States of America, 2001. **98**(10): p. 5780-5.

140. Friehs, I., et al., *Vascular endothelial growth factor delays onset of failure in pressure-overload hypertrophy through matrix metalloproteinase activation and angiogenesis.* Basic research in cardiology, 2006. **101**(3): p. 204-13.

141. Tirziu, D., et al., *Myocardial hypertrophy in the absence of external stimuli is induced by angiogenesis in mice.* J Clin Invest, 2007. **117**(11): p. 3188-97.

142. Tang, J.M., et al., *VEGF/SDF-1 promotes cardiac stem cell mobilization and myocardial repair in the infarcted heart.* Cardiovascular research, 2011. **91**(3): p. 402-11.

143. Bry, M., et al., *Vascular endothelial growth factor-B acts as a coronary growth factor in transgenic rats without inducing angiogenesis, vascular leak, or inflammation.* Circulation, 2010. **122**(17): p. 1725-33.

144. Zacchigna, S., et al., *Bone marrow cells recruited through the neuropilin-1 receptor promote arterial formation at the sites of adult neoangiogenesis in mice.* J Clin Invest, 2008. **118**(6): p. 2062-75.

145. Menasche, P., *Cardiac cell therapy: lessons from clinical trials.* Journal of molecular and cellular cardiology, 2011. **50**(2): p. 258-65.

146. Dor, Y., et al., *Conditional switching of VEGF provides new insights into adult neovascularization and pro-angiogenic therapy.* The EMBO journal, 2002. **21**(8): p. 1939-47.

147. Groppa, E., et al., *VEGF dose regulates vascular stabilization through Semaphorin3A and the Neuropilin-1+ monocyte/TGF-beta1 paracrine axis.* EMBO molecular medicine, 2015. **7**(10): p. 1366-84.

148. Karantalis, V. and J.M. Hare, *Use of mesenchymal stem cells for therapy of cardiac disease.* Circulation research, 2015. **116**(8): p. 1413-30.

149. Kanelidis, A.J., et al., *Route of Delivery Modulates the Efficacy of Mesenchymal Stem Cell Therapy for Myocardial Infarction: A Meta-Analysis of Preclinical Studies and Clinical Trials.* Circulation research, 2017. **120**(7): p. 1139-1150.

150. Baum, C., et al., *Side effects of retroviral gene transfer into hematopoietic stem cells.* Blood, 2003. **101**(6): p. 2099-114.

151. De Ravin, S.S., et al., *Lentiviral hematopoietic stem cell gene therapy for X-linked severe combined immunodeficiency.* Science translational medicine, 2016. **8**(335): p. 335ra57.

152. Gianni-Barrera, R., et al., *Long-term safety and stability of angiogenesis induced by balanced single-vector co-expression of PDGF-BB and VEGF164 in skeletal muscle.* Sci Rep, 2016. **6**: p. 21546.

153. Melly, L., et al., *Myocardial infarction stabilization by cell-based expression of controlled Vascular Endothelial Growth Factor levels.* J Cell Mol Med, 2018. **22**(5): p. 2580-2591.

154. Talman, V. and H. Ruskoaho, *Cardiac fibrosis in myocardial infarction-from repair and remodeling to regeneration.* Cell Tissue Res, 2016. **365**(3): p. 563-81.

155. Kanisicak, O., et al., *Genetic lineage tracing defines myofibroblast origin and function in the injured heart.* Nat Commun, 2016. **7**: p. 12260.

156. Fu, X., et al., *Specialized fibroblast differentiated states underlie scar formation in the infarcted mouse heart.* J Clin Invest, 2018. **128**(5): p. 2127-2143.

157. Whelan, D., N.M. Caplice, and A.J. Clover, *Fibrin as a delivery system in wound healing tissue engineering applications.* J Control Release, 2014. **196**: p. 1-8.

158. Vardar, E., et al., *A bioactive injectable bulking material; a potential therapeutic approach for stress urinary incontinence.* Biomaterials, 2019. **206**: p. 41-48.

159. Kong, P., P. Christia, and N.G. Frangogiannis, *The pathogenesis of cardiac fibrosis.* Cell Mol Life Sci, 2014. **71**(4): p. 549-74.

160. Bale, M.D., M.F. Muller, and J.D. Ferry, *Rheological studies of creep and creep recovery of unligated fibrin clots: comparison of clots prepared with thrombin and ancrod.* Biopolymers, 1985. **24**(3): p. 461-82.

161. Zymek, P., et al., *The role of platelet-derived growth factor signaling in healing myocardial infarcts.* J Am Coll Cardiol, 2006. **48**(11): p. 2315-23.

162. Sano, H., et al., *Study on PDGF receptor beta pathway in glomerular formation in neonate mice.* Ann N Y Acad Sci, 2001. **947**: p. 303-5.

163. Hellstrom, M., et al., *Role of PDGF-B and PDGFR-beta in recruitment of vascular smooth muscle cells and pericytes during embryonic blood vessel formation in the mouse.* Development, 1999. **126**(14): p. 3047-55.

164. Tomasek, J.J., et al., *Myofibroblasts and mechano-regulation of connective tissue remodelling.* Nat Rev Mol Cell Biol, 2002. **3**(5): p. 349-63.

165. Shamhart, P.E. and J.G. Meszaros, *Non-fibrillar collagens: key mediators of post-infarction cardiac remodeling?* J Mol Cell Cardiol, 2010. **48**(3): p. 530-7.

166. Bujak, M. and N.G. Frangogiannis, *The role of TGF-beta signaling in myocardial infarction and cardiac remodeling.* Cardiovasc Res, 2007. **74**(2): p. 184-95.

167. Schachtrup, C., et al., *Fibrinogen triggers astrocyte scar formation by promoting the availability of active TGF-beta after vascular damage.* J Neurosci, 2010. **30**(17): p. 5843-54.

168. Petersen, M.A., J.K. Ryu, and K. Akassoglou, *Fibrinogen in neurological diseases: mechanisms, imaging and therapeutics.* Nat Rev Neurosci, 2018. **19**(5): p. 283-301.

169. Schnee, J.M. and W.A. Hsueh, *Angiotensin II, adhesion, and cardiac fibrosis.* Cardiovasc Res, 2000. **46**(2): p. 264-8.

170. Sun, Y., et al., *Cardiac angiotensin converting enzyme and myocardial fibrosis in the rat.* Cardiovasc Res, 1994. **28**(9): p. 1423-32.

171. Oliveira-Junior, S.A., et al., *AT1 receptor blockade attenuates insulin resistance and myocardial remodeling in rats with diet-induced obesity.* PLoS One, 2014. **9**(1): p. e86447.

172. Galie, P.A., et al., *Interstitial fluid flow and cyclic strain differentially regulate cardiac fibroblast activation via AT1R and TGF-beta1.* Exp Cell Res, 2012. **318**(1): p. 75-84.

173. Funck, R.C., et al., *Regulation and role of myocardial collagen matrix remodeling in hypertensive heart disease.* Adv Exp Med Biol, 1997. **432**: p. 35-44.

174. Pellicori, P., et al., *Effects of spironolactone on serum markers of fibrosis in people at high risk of developing heart failure: rationale, design and baseline characteristics of a proof-of-concept, randomised, precision-medicine, prevention trial. The Heart OMics in AGing (HOMAGE) trial.* Eur J Heart Fail, 2020.

175. Li, C., et al., *Pirfenidone controls the feedback loop of the AT1R/p38 MAPK/renin-angiotensin system axis by regulating liver X receptor-alpha in myocardial infarction-induced cardiac fibrosis.* Sci Rep, 2017. **7**: p. 40523.

176. Gonzalez-Santamaria, J., et al., *Matrix cross-linking lysyl oxidases are induced in response to myocardial infarction and promote cardiac dysfunction.* Cardiovasc Res, 2016. **109**(1): p. 67-78.

177. Mujagic, E., et al., *Induction of aberrant vascular growth, but not of normal angiogenesis, by cell-based expression of different doses of human and mouse VEGF is species-dependent.* Hum Gene Ther Methods, 2013. **24**(1): p. 28-37.

178. Gyongyosi, M., et al., *Meta-Analysis of Cell Therapy Studies in Heart Failure and Acute Myocardial Infarction.* Circ Res, 2018. **123**(2): p. 301-308.

179. Schaad, L., et al., *Correlative Imaging of the Murine Hind Limb Vasculature and Muscle Tissue by MicroCT and Light Microscopy.* Sci Rep, 2017. **7**: p. 41842.

180. Groppa, E., et al., *VEGF dose regulates vascular stabilization through Semaphorin3A and the Neuropilin-1+ monocyte/TGF-beta1 paracrine axis.* EMBO Mol Med, 2015. **7**(10): p. 1366-84.

181. Groppa, E., et al., *EphrinB2/EphB4 signaling regulates non-sprouting angiogenesis by VEGF.* EMBO Rep, 2018. **19**(5).

UCLouvain
Secteur des sciences de la santé

Institut de Recherche Expérimentale et Clinique (IREC), UCLouvain Bruxelles (B)
Department of Cardiac, Vascular and Thoracic Surgery, CHU UCL Namur (B)
Cell and Gene Therapy, Department of Biomedicine, University of Basel (CH)

Promoteur: Pr Benoît Rondelet

Ludovic Melly a suivi des études de médecine et une formation en chirurgie cardiaque et vasculaire thoracique en Suisse, son pays d'origine. Arrivé au CHU UCL Namur en 2016, l'opportunité de poursuivre sa recherche fondamentale dans une thèse de doctorat lui est proposée, travail qu'il mènera à bien entre les deux pays, parallèlement à son activité de chef de clinique adjoint. Avide de nouvelles technologies, il aspire à convertir son cheminement scientifique dans une application plus clinique.

Afin de stimuler la micro-vascularisation dans le cœur, il est possible d'injecter des facteurs de croissance qui permettent d'accroitre la quantité de capillaires autour des zones ischémiques. Nous avons ainsi pu démontrer qu'en introduisant le gène d'un facteur de croissance spécifique dans des cellules souches d'origine humaine et qu'en sélectionnant les cellules qui produisent un taux thérapeutique, nous pouvions obtenir la formation de nouveaux vaisseaux fonctionnels dans le cœur du rat ainsi que la stabilisation d'un infarctus en injectant ces cellules autour de la zone à risque. Dans un deuxième temps, nous avons étudié une méthode alternative, sans modification génétique, pour une applicabilité clinique plus directe. A cet effet, nous avons intégré les facteurs de croissance, sous forme de protéine, dans un gel de fibrine qui est injecté sous forme de dépôt dans le muscle cardiaque.

Ischemic heart disease is one of the most frequent causes of death worldwide. When an imbalance occurs between myocardial oxygen supply and demand, such as in angina or myocardial infarction, interventional and surgical revascularization strategies can restore blood flow in the ischemic region. However, many patients could benefit from an additional therapeutic stimulation of micro-vascular growth. First, we combined the cell and gene therapy approaches for a controlled and sustained expression of growth factors, showing the potential to stabilize an infarction in a rodent model. Then, we moved to an optimized fibrin-based delivery platform, which provides a convenient, clinically approved and off-the-shelf product to deliver the growth factors as recombinant proteins and investigated its feasibility in the heart.